

LONGITUDINAL TRENDS IN THE DOCKUM GROUP:  
VARIATIONS IN THE LATE TRIASSIC MEGAMONSOON

by

ANTHONY ROMAN SKALESKI

Bachelor of Science, 2018  
The University of Nebraska  
Lincoln, Nebraska

Submitted to the Graduate Faculty of the  
College of Science and Engineering  
Texas Christian University  
in partial fulfillment of the requirements  
for the degree of

Master of Science

May 2024

LONGITUDINAL TRENDS IN THE DOCKUM GROUP:  
VARIATIONS IN THE LATE TRIASSIC MEGAMONSOON

by

Anthony Roman Skaleski

Thesis approved:

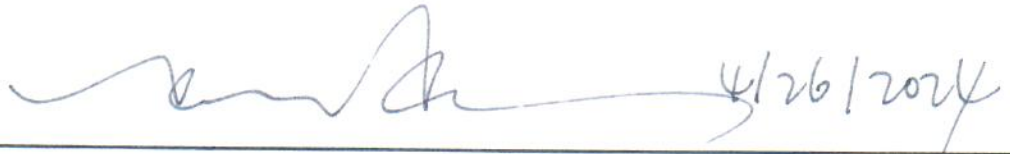


4/26/2023

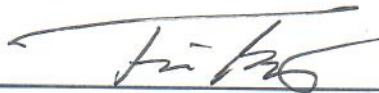
Major Professor



4/26/2024



4/26/2024



For The College of Science and Engineering



## ACKNOWLEDGEMENTS

I would like to thank Dr. John Holbrook, my advisor, for his guidance, wisdom, and patience. His advising was pivotal to the completion of this project. I would also like to thank Dr. Xiangyang Xie and Dr. Richard Denne for their roles as members on my thesis committee. Their insights and suggestions were greatly appreciated.

I would like to thank my TCU colleagues for their help both in and out of the field. Specifically, I would like to thank Clayton Freimuth, Blake Bezucha, and Shaun Prines. Their camaraderie and advice supported me more than they'll ever know. For similar reasons, I would like to thank my coworkers at the Utah DNR. Their patience and understanding provided a space in which I was able to complete this project. Specifically, I thank Amy Flowers, Maeghan White, and Aspen Johnston.

Finally, I'd like to thank my wife, Andrea Skaleski. She has been with me throughout this entire process and has helped me traverse the most difficult times. Her belief in my abilities never faltered, and she is truly my rock and better half.



## TABLE OF CONTENTS

ACKNOWLEDGMENTS .....	ii
TABLE OF CONTENTS.....	iii
LIST OF FIGURES .....	v
LIST OF TABLES .....	vi
1. INTRODUCTION .....	1
2. BACKGROUND .....	3
2.1 Exposure and extent.....	3
2.2 Stratigraphy, history, and naming conventions.....	5
2.3 Tectonics, deposition, and climate.....	8
2.4 Supercritical flows .....	11
3. METHODS .....	12
3.1 Field work and locations.....	12
3.2 Lithofacies analysis and lithosomes.....	15
4. RESULTS .....	16
4.1 Measured sections.....	16
4.2 Lithofacies.....	18
4.3 Upper-flow-regime channel-fill lithofacies .....	20
4.4 Lower-flow-regime channel-fill lithofacies.....	25
4.5 Lacustrine and non-channel lithofacies .....	28
4.6 Fluvial architecture .....	33
4.7 Lithosomes.....	35
4.8 Channel-fill lithosomes.....	36
4.9 Non-channel lithosomes.....	37
4.10 Paleocurrent data.....	40
4.11 Observed data not used in cross-section analysis .....	43
5. DISCUSSION.....	43
5.1 Dockum Group regional variability in lithosomes.....	43
5.2 Dockum Group regional depositional trends .....	48

5.3 Non-channel lithosomes.....	50
5.4 Dryland fluvial systems and climate.....	55
6. CONCLUSIONS.....	58
APPENDIX.....	60
REFERENCES .....	101
VITA	
ABSTRACT	

## LIST OF FIGURES

Figure 1: Exposure of Dockum Group.....	4
Figure 2: Map of field area .....	14
Figure 3: Cross-section of lithostratigraphic sections.....	17
Figure 4: Images of upper-flow-regime channels, Trujillo Sandstone, TX.....	23
Figure 5: Images of mixed-flow-regime channels, Trujillo Sandstone, TX.....	24
Figure 6: Image of mixed-flow-regime channel, Tecovas Formation, TX.....	26
Figure 7: Image of lower-flow-regime channel, Trujillo Sandstone, NM.....	27
Figure 8: Images of lacustrine lithofacies, Tecovas Formation, TX.....	31
Figure 9: Images of lacustrine lithofacies, Cooper Canyon Formation, NM.....	31
Figure 10: Cross-section with lithofacies shadings .....	32
Figure 11: Cross-section with lithosome shadings .....	39
Figure 12: Map of study area with rose diagrams showing paleocurrents .....	42
Figure 13: Depositional cartoon of Tecovas and Cooper Canyon Formations.....	54
Figure 14: Depositional cartoon of Trujillo Sandstone.....	55

## LIST OF TABLES

Table 1: Table of lithofacies .....	19
Table 2: Table of fluvial architectural elements .....	34
Table 3: Table of lithosomes.....	38

## 1. Introduction

The Late Triassic Dockum Group of West Texas and New Mexico is a dryland fluvial system which records abundant upper-flow-regime channel fills generated by supercritical flows fed by intense, cyclonic storms (Lamb, 2019; Walker, 2020; Bezucha, 2022). The Dockum Group historically has been studied not for its sedimentology and stratigraphy but rather for its significance to the paleontological record as it contains a diverse and rich record of Triassic vertebrate fossils (Green, 1954; Edler, 1978; Chatterjee 1983, 1984, 1985, 1986, 1991, 1993; Small, 1985, 1989a, b, 1997, 2002; Davidow-Henry, 1987, 1989; Hunt and Lucas, 1991a, b, 1992, 1993a, b, 1994, 1995, 1997; Long and Murry, 1995; Lehman et al., 1992; Lehman, 1994a, b; Simpson, 1998; McQuilkin, 1998; Edler, 1999; Bolt and Chatterjee, 2000; Atanassov 2002; Martz 2002, 2008; Weinbaum, 2002, 2007; Houle Mueller, 2004; Lehman and Chatterjee, 2005; Lehane, 2006; Mueller and Parker, 2006). With some noteworthy exceptions, the Dockum Group has received little attention regarding its depositional processes.

Recent work (Lamb, 2019; Walker, 2020) noted this lack of investigation and sought to rectify this by studying the sedimentology, paleohydraulics, and fluvial architecture of the Dockum Group. Lamb (2019) identified the presence of abundant upper-flow-regime channels and hypothesized that large, convective storms were the driver of the high discharge events that were common in the Dockum. Walker (2020) investigated further into this updated understanding of the strata and focused his research on detailed fluvial architectural analysis and the paleohydraulics of the system.

These studies, while presented in magnified detail, were localized to a few sections solely in West Texas. Since the discovery of these upper-flow-regime channels in the Dockum Group by Lamb (2019), no study has been done about how this updated understanding of flow

processes is exhibited in the larger, regional extent of the system. This study aims to assist in filling that void by integrating the data from these recent studies and applying it to an extensive outcrop analysis in New Mexico as well as additional sections in West Texas.

## **2. Background**

### **2.1 Exposure and extent**

The Dockum Group extends over approximately 246,050 km<sup>2</sup> (96,000 mi<sup>2</sup>) primarily from West Texas to eastern New Mexico with some extension into the panhandle of Oklahoma, eastern Colorado, and as far north as southwestern Kansas (McGowen et al., 1983). The Dockum Group ranges in thickness from tens of meters over local highs such as the Matador Arch of West Texas to thicknesses greater than 600 meters in the Midland Basin (McGowen et al., 1983; Lehman and Chatterjee, 2005; Lamb, 2019). It outcrops along the eastern escarpment of the Llano Estacado of West Texas, within the Canadian and Pecos River valleys of Texas and New Mexico, and along the eastern edge of the Rocky Mountains in New Mexico (Lehman and Chatterjee, 2005; Lamb, 2019) (Figure 1).

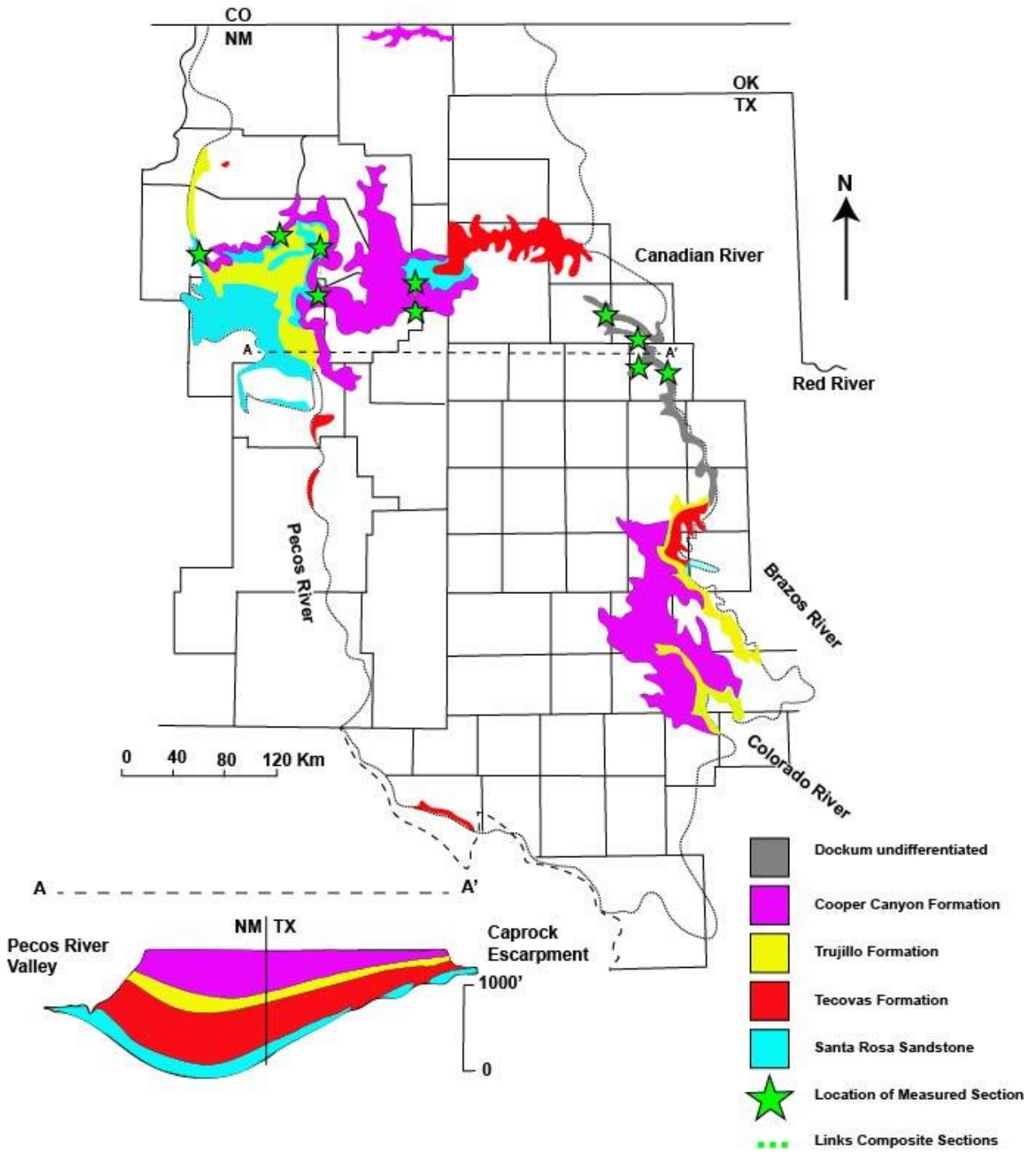


Figure 1. Approximate regional extent of exposed Dockum Group strata from West Texas to eastern New Mexico. Green stars indicate the location of a measured section within this study. A - A' is a basin-wide cross-section showing subsurface approximations of the thicknesses of the Formations within the Dockum Group. Figure modified from Lehman and Chatterjee



## 2.2 Stratigraphy, history, and naming conventions

The Dockum Group comprises four formations. In ascending stratigraphic order, they are: the Santa Rosa Formation, the Tecovas Formation, the Trujillo Sandstone, and the Cooper Canyon Formation. The Dockum Group is stratigraphically bound in its Texas extent by the Permian Quaternary Formation below and above by the Tertiary Ogallala Formation, as well as Cretaceous strata (May, 1988; Lamb, 2019). In New Mexico, the Dockum Group is bound by the Permian Artesia Group below and the Jurassic Entrada Sandstone above (Lucas et al., 2001). This study focuses on the Tecovas Formation, Trujillo Sandstone, and Cooper Canyon Formation.

The Triassic System in West Texas and eastern New Mexico has been investigated since the mid-1850s (Marcou, 1853, 1855, 1858) although it wasn't until 1890 that the Triassic strata in West Texas received the name 'Dockum' (Cummins, 1890). The Dockum Group strata were named thusly due to their proximity to the Dockum Creek in Dicken's County, TX (Cummins, 1890). Drake (1891) published work on the Dockum Group in which he identified three distinct, mappable units. Correlation of the Dockum Group into eastern New Mexico dates to Cummins (1892), where, at the time, no name had been given to the Triassic strata of the area.

Gould (1907) elevated the Dockum to group status and named two subunits. The lower unit was named the Tecovas Formation and was described as a variegated red, purple, yellow, and gray mudstone with interbedded quartzose sandstone and conglomerate. The upper unit was named the Trujillo Sandstone and was described as a basal series of cliff-forming sandstones with an upper-succession of slope-forming red mudstones and siltstones with lenses of sandstone (Gould, 1907; Lehman et al., 1992). Darton (1928) and Bullard (1928) conducted further correlation of Triassic beds into eastern New Mexico where the name 'Dockum' was also used.

Darton (1928) also identified and described the Santa Rosa Sandstone as the basal formation of the Dockum Group which appeared as a distinctive, thick sandstone beneath the Tecovas.

Chatterjee (1986) laid out historical evidence supporting restricting the Trujillo Sandstone of Gould (1907) to solely the basal cliff-forming sandstone. Further, Chatterjee (1986) proposed that the upper, slope-forming succession be named the Cooper member, identified a type section, and brought the Dockum Group down to formation rank. Lehman et al. (1992) updated the type section and demonstrated that the Cooper Member of Chatterjee (1986) exists in sufficient thickness (161.5 m) to warrant formation rank. Lehman et al. (1992) also addressed naming convention issues raised due to the existence of the Cooper Marl of South Carolina by adjusting the name to Cooper Canyon after the Cooper Creek from which the original name Cooper was derived. Thusly, Lehman et. al (1992), backed by historical precedence, named the rocks above the Trujillo Sandstone as the Cooper Canyon Formation.

The naming conventions of most of the Dockum Group are historically contested. It is a two-fold argument which is centered around formation-rank naming and group-rank naming. In 1985 Lucas et al. officially abandoned the name Dockum Group. Further, in 1989, Lucas and Hunt identified five formation rank units. In ascending order those five formations were named the Santa Rosa Sandstone, the Garita Creek Formation, the Trujillo Sandstone, the Bull Canyon Formation, and the Redonda Formation. In 1993 Lucas and Anderson placed these formations into the Chinle Group, extending this name for equivalent strata in the Four-Corners region to the West. Despite this, a review on nomenclature by Cather et al. (2013) maintains that the proper name for the collection should be Dockum Group at least to the eastern front of the Rocky Mountains of New Mexico due to the historical precedence and contiguous nature of exposure along the High Plains.

Formation-rank conventions are focused on the Tecovas and Cooper Canyon Formations while all parties agree on the names Santa Rosa Formation, Trujillo Sandstone, and the Redonda Formation (Lucas and Hunt, 1989; Lucas and Anderson, 1993; Lucas et al., 1994; Lehman, 1994). Lucas and Hunt (1989) claimed that the name Tecovas should be changed to Garita Creek in New Mexico, and that the Cooper Canyon should be abandoned entirely due to the name 'Cooper' being occupied elsewhere at the time the Cooper Canyon was first named. Lucas and Hunt (1989) proposed that the name Bull Canyon Formation be used in place of the Cooper Canyon Formation. Cather et al. (2013) reviews all arguments on both formations and decides that the name Tecovas Formation should remain and that the Bull Canyon Formation should be used in place of Cooper Canyon Formation. However, this study agrees with the arguments of Lehman (1994) which states that 'Cooper' had not yet been taken as all stratigraphic units also had a lithologic modifier attached to them (Cooper Limestone, Cooper Marl, Cooper Creek Limestone, Cooper Peak Dolomite, etc.). Furthermore, Lehman (1994) points out that stratigraphic code prefers redescription of a unit and revision of its boundaries over abandonment. As such, this study agrees with the naming conventions of Lehman and Chatterjee (2005), Lamb (2019), Walker (2020), and Bezucha (2022).

Furthermore, this study refers to all strata above the Trujillo Sandstone as the Cooper Canyon Formation including what has previously been named the Redonda Formation. The Redonda Member was first mapped in the Tucumcari, NM area by Dobrovolny et al. (1946), but a type section was never designated and the contact with the underlying strata was observed to be conformable. Griggs and Read (1959) raised the Redonda to formation rank. Then Lucas (1993) correlated the base of the Redonda Formation to the base of the Rock Point Formation of the Colorado Plateau based on a sharp, lithologic change. Lucas (1993) claimed this was proof of a

basin-wide expression of the Tr-5 unconformity. This study did not observe this basin-wide unconformity and continues the original assertion of the contact as conformable.

Although the Redonda Formation was previously interpreted as recording the deposition of a large, regional lake (Lucas et al., 2001), updated understanding revised the interpretation to a collection of smaller, more-shallow, localized ephemeral lakes (Hester and Lucas, 2001), which is consistent with how the Cooper Canyon Formation is interpreted in this study in Texas and New Mexico. Cather et al. (2013) says in reference to the entire Dockum Group “major lithostratigraphic units within the Dockum are generally considered to be formations, but their mappability has not been adequately assessed in some areas.” For these reasons and because this study did not observe the Tr-5 unconformity in a regional extent, this study will refer to all Dockum Group strata stratigraphically above the Trujillo Sandstone as the Cooper Canyon Formation rather than the Bull Canyon Formation and Redonda Formation of Lucas and Hunt (1989).

While not a focus of this study, due to being off-trend of other measured sections, the Travesser Formation of the Dry Cimarron Valley was measured (pp. 83 - 88). Lucas et al. (1987) named this formation in New Mexico, but it is not yet identified in Texas. Recent work by Bezucha (2022) found that it is temporally the same stratigraphic age as the Cooper Canyon Formation.

### **2.3 Tectonics, deposition, and climate**

The Dockum Group was deposited in the Late Triassic of the supercontinent Pangea which formed from the Late Paleozoic to the early Mesozoic as a result of the collision of Gondwana and Laurentia. This event formed major mountain ranges including the Ouachita Orogenic Belt which is thought to be a primary source of sediments for the Dockum Group

(Bezucha, 2022). The Matador Arch and Amarillo-Witchita Uplift were other, minor paleogeographic highs which formed at this time in the vicinity of Dockum Group deposition. Conversely, various basins formed concurrently. These include the Midland Basin, the Tucumcari Basin, and the Palo Duro Basin, in which the four Texas sections of this study are located, formed at this time as well and was a persistent low during the deposition of the Dockum Group (Walper, 1977; Kluth and Coney, 1981; Dickinson, 1981; Viele and Thomas, 1989).

The four formations of the Dockum Group are long interpreted to represent a succession of rocks recording fluvial, lacustrine, and deltaic environments; however, the relative magnitude that each of these environments is represented in the rock record has been debated over time (Green, 1954; McGowen et al., 1979; Lehman and Chatterjee, 2005; Lamb, 2019; Walker, 2020). Once the Dockum Group was interpreted to have been the product of dominantly, if not entirely, lacustrine and lacustrine deltaic deposition (Granata, 1981; McGowen et al., 1979, 1983). Interpretations also shifted to entirely fluvial deposits with arguments that lake sediments were misinterpreted floodplain deposits (McGowen et al., 1983; Frehler, 1987; May, 1988; Lehman and Chatterjee, 2005). However, recent work has concluded that indeed all depositional environments are recorded in the outcrops of the Dockum Group, and that no single one completely dominates over the others (Lehman and Chatterjee, 2005; Brown, 2016; Lamb, 2019; Walker, 2020).

The Dockum Group was described by Lehman and Chatterjee (2005) as two alluvial depositional sequences: the Santa Rosa-Tecovas, and Trujillo-Cooper Canyon intervals. This was due to both successions being broadly fining upwards sequences starting with a thick, sandstone body at their respective bases. The concept of large-scale sequences and the boundary between

the basal and upper sequence is explored in Walker's (2020) fluvial architectural analysis.

Walker concludes that this boundary between the Tecovas Formation and Trujillo Sandstone is unconformable, and the Trujillo Sandstone is a multivalley complex which was formed due to the fluctuation between intense megastorms during wetter periods scouring valleys and less-intense cyclonic storms during more arid period filling those valleys. In this way, the Dockum Group is a fluvial record of a monsoonal climate.

At the time of Dockum Group deposition, the climate of modern-day West Texas and northeast New Mexico was controlled by tropical, monsoonal storms. Parrish (1988) developed the idea that the size and global position of the supercontinent Pangea allowed for weather circulation conducive to generating massive, convective storms which Parrish named megamonsoons. She offered this as an explanation for deposits in the equivalent Chinle Group to the West. The depositional trends of the Dockum Group are consistent with this as stratigraphic units record varying arid and humid periods (Seni, 1977; May, 1988; Martz, 2008). Lamb (2019) argues that this variability is evidence that the flow of the Dockum Group was monsoon-controlled.

Another factor impacting climate during the extent of the deposition of the Dockum Group includes possible reactivation and uplift of the Ouachitas due to the opening of the Gulf of Mexico that would impact magnitude of rainfall from the megamonsoons and smaller, convective storms (McGowen et al., 1983). Parrish (1988) also notes that the climate of Pangea likely varied on time scales of higher magnitudes than seasons which likely meant that the alternating arid and humid periods apparent in the rock record were lengthy.

Recent sedimentology work from Lamb (2019) and paleohydraulics and fluvial architecture work from Walker (2020) concluded that megamonsoonal climate was indeed likely

the driving force for Dockum Group deposition in part due to the presence of abundant upper-flow-regime channels and sheets. Both in lithologic distribution and apparent magnitude of discharge, the strata of the Dockum Group record a climate which varied between large megastorms and smaller convective storms.

## **2.4 Supercritical flows**

Upper-flow-regime structures and bedforms are generated by supercritical and near-supercritical flows. Recent work argues that these structures and bedforms might be more abundant in the rock record than previously thought (Fielding et al., 2006, 2009, 2018; Yokokawa et al., 2010, 2016; Lang and Winsemann, 2013; Plink-Bjorklund, 2015; Slooman and Cartigny, 2018). This was true of the Dockum Group. Lamb (2019) was the first to identify upper-flow-regime channels and sheets in the Dockum Group. All five principle structures associated with supercritical flow were observed within the Dockum Group and in this study. These sedimentary structures in order ascending flow energy are: upper-plane-bed, symmetrical antidunes, breaking antidunes, chutes and pools, and cyclic steps.

Flow energy of these upper-flow-regime structures is calculated using the Froude number. The Froude number is a dimensionless number which divides the flow velocity (inertial/kinetic energy) by the square root of the acceleration of gravity times the flow depth (gravitational of potential energy). The transition from subcritical to supercritical flow is when the Froude number is 1.0, and the first supercritical flow structures, symmetrical antidunes, start to form at 0.84-1.0 (Kennedy, 1961, 1963, 1969; Van den Berg and Van Gelder, 1993; Carling and Shvidchenko, 2002; Fielding et al., 2006, 2009; Kostic et al., 2010; Cartigny, 2012; Cartigny et al., 2011, 2013; Lang and Winsemann, 2013; Yokokawa et al., 2010, 2016; Froude et al., 2017; Slooman and Cartigny, 2018).

Fluvial systems that record supercritical flows are commonly fueled by flashy, extreme flows caused by convective storms such as monsoons (Latrubesse et al., 2005; Syvitsky et al., 2014; Plink-Bjorkund, 2015). These types of flashy flows often are associated with rapid onset of flow and rapid waning of flow. Walker (2020) found these types of hydrographs to be consistent with quantitative measurements of the paleohydraulics of the Dockum Group. Walker (2020) also concluded that the Dockum Group's flow parameters are consistent with high to very high discharge variance river systems.  $CVQ_p$  is a measure of the standard deviation of the annual peak flood discharge divided by the mean annual peak flood discharge.  $CVQ_p$  is a value used to define the inter-annual variability of fluvial systems (Fielding et al., 2018; Hansford et al., 2020; Walker, 2020). Walker (2020) found that the  $CVQ_p$  value for Dockum Group channels were consistent with upper-flow-regime channels controlled by megamonsoonal climates ( $CVQ_p > 0.60 - 0.90$ ) (Fielding et al., 2018; Hansford et al., 2020).

### **3. Methods**

#### **3.1 Field work and locations**

This project uses lithology, sedimentary structures, and fluvial architecture collected from field observations of outcrops to analyze facies relationships of the Dockum Group on a regional scale. Data collected from twelve field locations were used to build nine composite lithologic sections. These locations span from the panhandle of Texas to the eastern front of the Rocky Mountains in New Mexico. Although twelve locations were observed, this study will focus on ten locations. These ten locations are from east to west: TX Hwy 256, Tule Canyon, TX Hwy 207, Palo Duro Canyon SP, NM Hwy 469, Route 66, NM Hwy 156, NM Hwy 104, Trujillo Hill, and US Hwy 84 (Figure 2). The two locations that are not being used are a location in the Dry Cimmaron Valley of New Mexico and a location along U.S. Interstate 25 by Romeroville, New



Mexico. These locations are denominated Red Rock Ranch and I-25 respectively. The section measured at the Red Rock Ranch (RRR) location is not used because it is off-trend from the rest of the locations, and the section measured at the I-25 (RG-B) location is not used because it lacks stratigraphic context due structural complexity of the area (Figure 2).

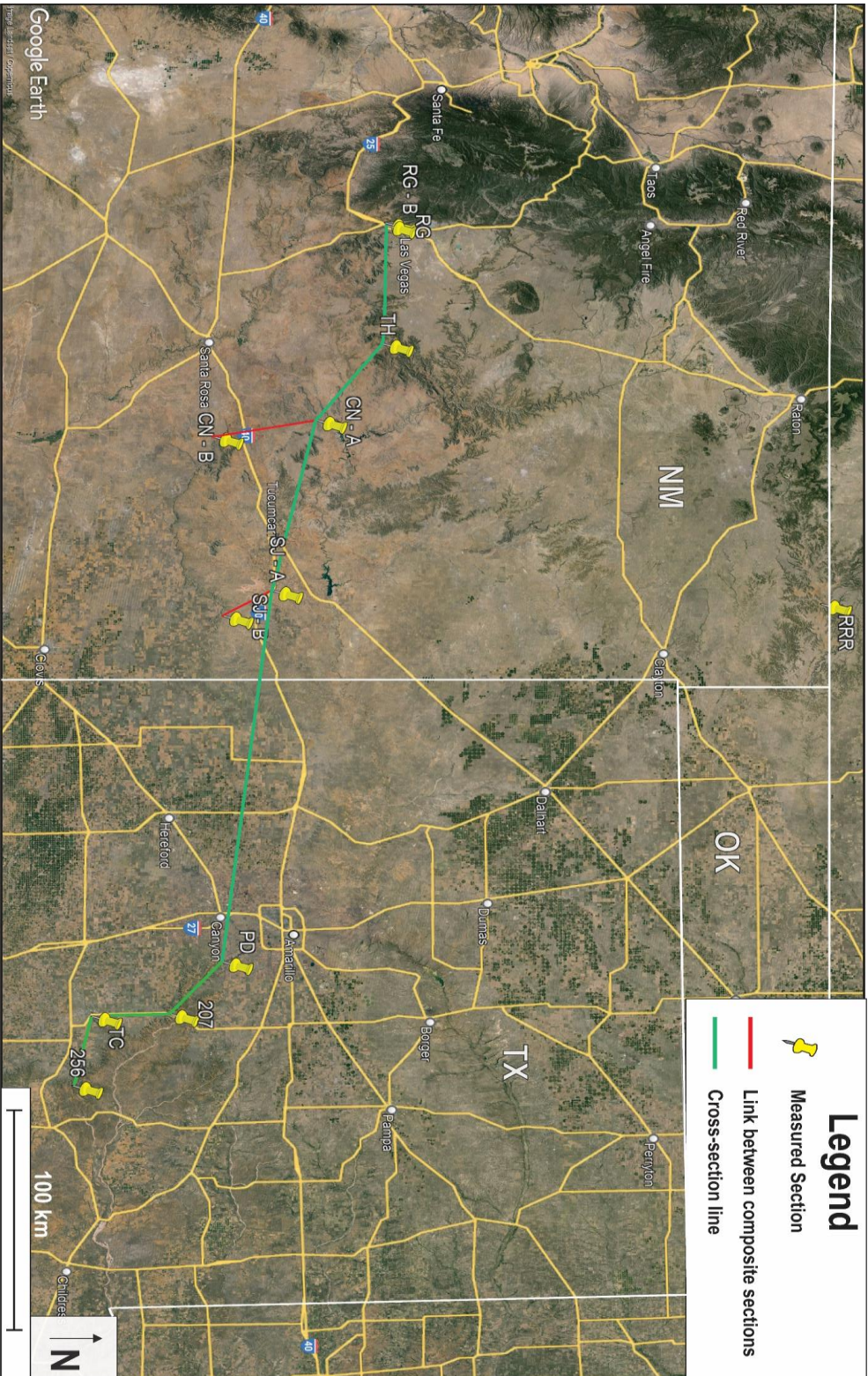


Figure 2 Map showing location of all ten sections measured. From east to west locations are Texas Highway 256 (256) 34° 28' 16" N 101° 5' 37" W, Tule Canyon (TC) 34° 32' 31" N 101° 25' 41" W, Texas Highway 207 (207) 34° 47' 56" N 101° 26' 12" W, Palo Duro Canyon State Park (PD) 34° 58' 55" N 101° 41' 6" W, San Jon (SJ-A & SJ-B) 35° 9' 27" N 103° 28' 11" W & 34° 59' 40" N 103° 20' 54" W, Conchas and Newkirk (CN-A & CN-B) 35° 17' 52" N 104° 17' 30" W & 34° 57' 22" N 104° 12' 32" W, Trujillo Hill (TH) 35° 30' 50" N 104° 39' 56" W, and Romeroville Gap (RG) 35° 30' 55" N 105° 14' 39" W. Also shown are two sections not used in analysis in this study. They are Red Rock Ranch (RRR) 36° 58' 22" N 103° 24' 37" W and I-25 near Romeroville Gap (RG-B) 35° 30' 44" N 105° 15' 22" W (Image from Google Earth)

Some of the sections are composite stratigraphic sections. Because outcrop exposure in eastern New Mexico was limited and rarely captured the entirety of the Dockum Group, the composites built from the New Mexico locations sometimes span a distance. The longest of these distances is thirty-eight kilometers which is between the Conchas and Newkirk locations used to build the Conchas/Newkirk composite section. In cases where one location is not visually correlatable to another location, this study uses the regionally correlated marker beds of the Trujillo Sandstone and Exeter Sandstone to ensure stratigraphic context. The composite sections from Texas locations share the name of the location because they are composites within one general location, but a couple of the names of the New Mexico composite sections are named differently than their corresponding locations due to the component sections of the composite not being measured in the same, singular location. The names are given to these composites based on the proximity of the component section's location to a town. These sections are, from east to west, San Jon and Conchas/Newkirk. The San Jon composite comprises NM Hwy 469 and Route 66 and is named thusly due to both location's proximity to San Jon, and the Conchas/Newkirk composite comprises NM Hwy 104 and NM Hwy 156 (Figure 2).

Data was collected in measured sections from field observations of grain size, sedimentary structures, and biota. Photos were captured in the field using a Cannon EOS Rebel T3i camera with either an 18-55 mm or 55-250 mm lens. Thicknesses were measured using a Trimble Geo7x. Paleocurrents were measured using a Brunton compass. Graphics were generated using Adobe Illustrator

### **3.2 Lithofacies analysis and lithosomes**

An updated interpretation of the lithofacies present in the Dockum Group was introduced by Lamb (2019) and was further refined by the work of Walker (2020). This research agrees with

the works of Lamb and Walker, and this project's study area comprises the study areas of those respective projects as a part; therefore, this work utilizes the lithofacies analysis of Walker to inform the descriptions of the lithologic patterns present in the outcrops analyzed for this project.

The aim of this project is to take the well-defined sedimentologic and stratigraphic information from Lamb (2019) and Walker (2020) from the localized grouping of sections in Texas and compare it with the data from the Dockum Group system on a much larger, regional scale. Therefore, lithosomes were generated from Lamb's (2019) and Walker's (2020) lithofacies (Table 1) to show regionalized trends of deposition.

## **4. Results**

### **4.1 Measured sections**

Ten measured sections were analyzed in this study, two of which were used to form composite sections, amounting ultimately to four sections in Texas and four sections in New Mexico. Measured sections vary in terms of formation exposure (Figure 3). In Texas the Ogallala Formation scours into the Cooper Canyon Formation, which dramatically decreased the preserved thickness in some locations. In New Mexico the Tecovas Formation is not exposed in its entirety either. As a result, most correlation and subsequent analysis on a regional scale is limited to the data available, of which the most complete are from the Trujillo Sandstone and Cooper Canyon Formation. Still, despite only recording the uppermost of the Tecovas in New Mexico, some observations can be made from what information is available.

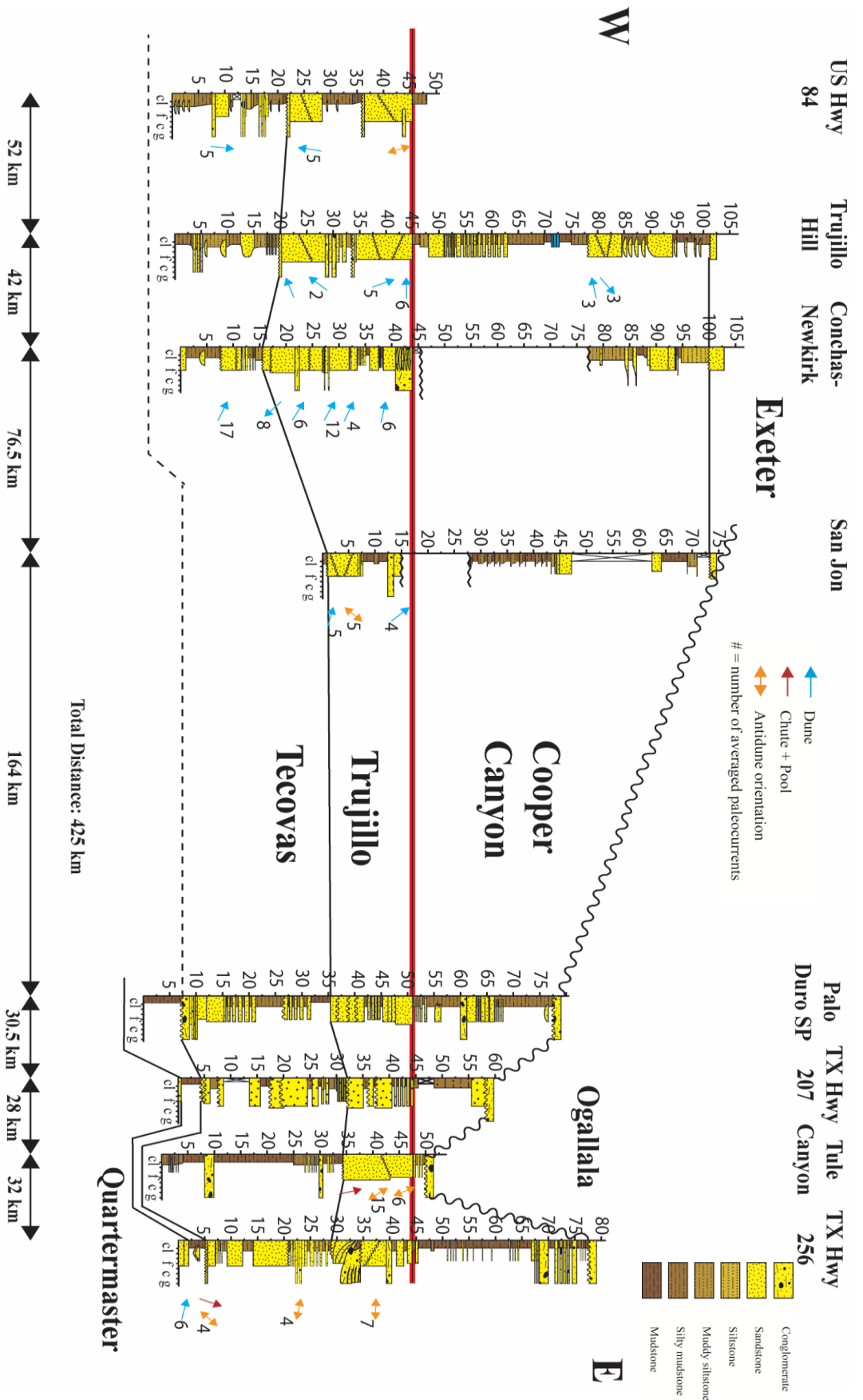


Figure 3. Cross-section showing all eight lithostratigraphic sections. The red line is the top of the Trujillo Sandstone which was used for regional correlation. Cross-section line shown on map in Figure 2.

## **4.2 Lithofacies**

Twelve unique lithofacies were observed within the Tecovas Formation, Trujillo Sandstone, and Cooper Canyon Formation throughout the extent of the study area. These assemblages are distinguished based on their lithology, sedimentary structures, and biogenic influences (bioturbation/trace fossils or lack thereof). Clast sizes range from clay to gravel, and sedimentary structures include ripples, dunes, trough cross-bedding, upper-plane beds and requisite laminae, symmetrical antidunes, breaking antidunes, chutes and pools, and cyclic steps.

This study includes the sections measured and analyzed in Walker (2020), and this research identified all the same lithofacies identified in that work. However, this project encompasses a greater field area which contains deviations from the parameters laid out in Walker (2020). The lithofacies descriptions have been modified to accurately capture these differences (Table 1) but the naming convention for lithofacies code has been maintained for continuity.



Code	Lithofacies	Lithology	Sedimentary Structures	Characteristics	Interpretation
Gac	Sandstone to gravel with upper-flow-regime structures	Light red to white, poorly sorted, coarse-grained quartz sandstone to gravel clasts	Unstable antidunes, chutes and pools, and cyclic steps	Bed are 0.1 – 0.2 m thick, minor component of observed fluvial deposits, forms sheet or lens geometries	Local hydraulic jump in upper-flow-regime channel fill
Gp	Sandstone with gravel and minor silt, inclined	Red to white, moderately sorted, silt to gravel sediments	Massive, to local minor antidune structures on distal end of inclined gravel deposits	Beds range from 0.1 – 0.5 m with thick interbedded silty sections, distinctive coarser grained progradational lenses, encased in Fcf	Prograding delta foresets in lacustrine fill
Sac	Sandstone with upper-flow-regime structures	Red to gray, moderately sorted, upper-fine to medium grained quartz sandstone	Antidunes and less common chutes and pools and cyclic steps bedforms	Beds are 0.2 – 2 m thick, moderately preserved upper-flow-regime lithofacies, forms lensoid beds	Upper-flow-regime channel fill
Sh	Planar laminated sandstone	Red to gray, moderately sorted, upper-fine to medium grained quartz sandstone	Upper plane bed laminations	Beds are 0.05 – 0.3 m thick, dominate preserved upper-flow-regime lithofacies	Upper-flow-regime channel fill
Sl	Sandstone with transitional-flow-regime structures	Red to white, well sorted, upper-fine quartz sandstone	Sigmoidal cross-bedding to washed out dunes	Beds are 0.4 – 2 m thick, rare preservation in study area, distinct gradual slopping on cross-beds	Transitional flow at Froude numbers close to 0.84 within channel fill
Stb	Sandstone with inclined lower-flow-regime structures	Red to white, well sorted, upper-fine quartz sandstone	Tabular cross-bedding and ripples	Beds are 0.2 – 0.8 m thick, distinguished by lateral accretion sets with lower-flow-regime structures parallel to accretion surfaces, fines into floodplain muds, forms wedge or lobe geometries	Lower-flow-regime bar or channel fill
Sr	Sandstone with lower-flow-regime structures	Red to white, well sorted, upper-fine quartz sandstone	Asymmetric ripples, dunes and tabular to trough cross-stratification	Beds are 0.4 – 2 m thick, rare preservation in study area, transitions into fine muds, forms lens or concave up geometries	Lower-flow-regime channel fill
Scvh	Sandstone with convoluted bedding, parallel laminations	Buff to white, well sorted, upper-fine quartz sandstone	Convoluted bedding, Parallel laminations	Beds are 0.5 – 1 m thick, rare preservation in study area, found in close association with Fmh and Fcf in, found immediately beneath planar laminated and ripple laminated sandstone	Deltaic slope sands
Fmh	Sandstone, laminated	Red to light red, very well sorted, silt to fine grained sediments	Dominated by planar laminations with minor ripples to local antidunes	Beds are thin ranging from 0.05 to 0.5 m, with interbedded muds, local fluid escape structures, encased in Fcf	Sandy lacustrine base
Fl	Massive mudstone	Reddish orange to white, very well sorted, mud grain sizes	No sedimentary structures to minor local ripples and planar laminations	Beds are 1 – 3.5 m thick, separates coarse sandstone packages, forms blanket geometries	Floodplain mudflat
Fcf	Claystone to mudstone	Red to light orange, very well sorted, clay to mud sediments	Weakly to strongly developed parallel, wavy and ripple laminations	Beds range from 0.5 – 15 m with alternating thin and thick sections, distinguished by preserved development of laminations, limited to no bioturbation	Lacustrine fill
P	Mudstone with soil profiles	Red orange and white to yellow, silt to mud sediments	No sedimentary structures	Beds are 0.2 – 0.4 m thick, alternating calcrete and silcrete horizons, some bioturbation, root halos and blocky-platy pedologic structures observed, distinctive color profile	Paleosols

Table 1. Lithofacies table for the Dockum Group. Modified from Walker (2020)

### **4.3 Upper-flow-regime channel-fill lithofacies**

The most commonly identified lithofacies in this study in both Texas and New Mexico is Sh (Figures 4, 5, 6). Sh is characterized as a very fine-grained to medium-grained sandstone, red to white in color, with dominance of planar lamination interpreted as upper-plane-bed forms. This lithofacies is present in channel-filling sandstones predominantly within the Tecovas Formation and Trujillo Sandstone. Sh is found in conjunction with other lithofacies as a portion of a stack of channel-fill sandstones although it can be the sole lithofacies in a single channel-filling sandstone.

When the Sh lithofacies is found in association with other channel-forming lithofacies it is usually within a relatively thicker stack of channel-fill sandstones, and it is interpreted as recording transitional to either waxing or waning flows. In the locations researched in Texas, these stacks of channel-fill sandstones can be thick, wide, large-scale sand bodies that record storm-driven flooding events. However, when Sh is the highest energy lithofacies in a channel-fill sandstone, the sandstone unit is usually relatively thinner and is interpreted to be recording independent floodplain channels, chute channels, or splays tied to the larger channels (Walker 2020).

This is generally not true in New Mexico. The majority of the channel-fill sandstones that comprise the Sh lithofacies do not contain a lithofacies that captures an event of higher energy. Furthermore, in New Mexico the thinner channel-fill sandstones interpreted as floodplain channels, which in Texas comprise Sh, comprise lithofacies characterized by lower-flow-regime sedimentary structures from dunes and ripples (Figure 10).

Common to locations in Texas, the two facies that record upper-flow-regime structures in channel-fill sandstones are Sac and Gac which are both characterized by having abundant



antidunes with local chutes-and-pools and cyclic steps (Figure 4). Sac is a fine to medium-grained, channel-fill sandstone that ranges in color from red to white. Gac is otherwise the same as Sac but has predominantly gravel sized grains with limited very-coarse sandstone. Similarly to Sac, Gac records intense upper-flow-regime flow rates that are recorded by the same sedimentary structures as Sac. Gac is less common than Sac in Texas, but both lithofacies are much less common in the measured sections of New Mexico (Figure 10).

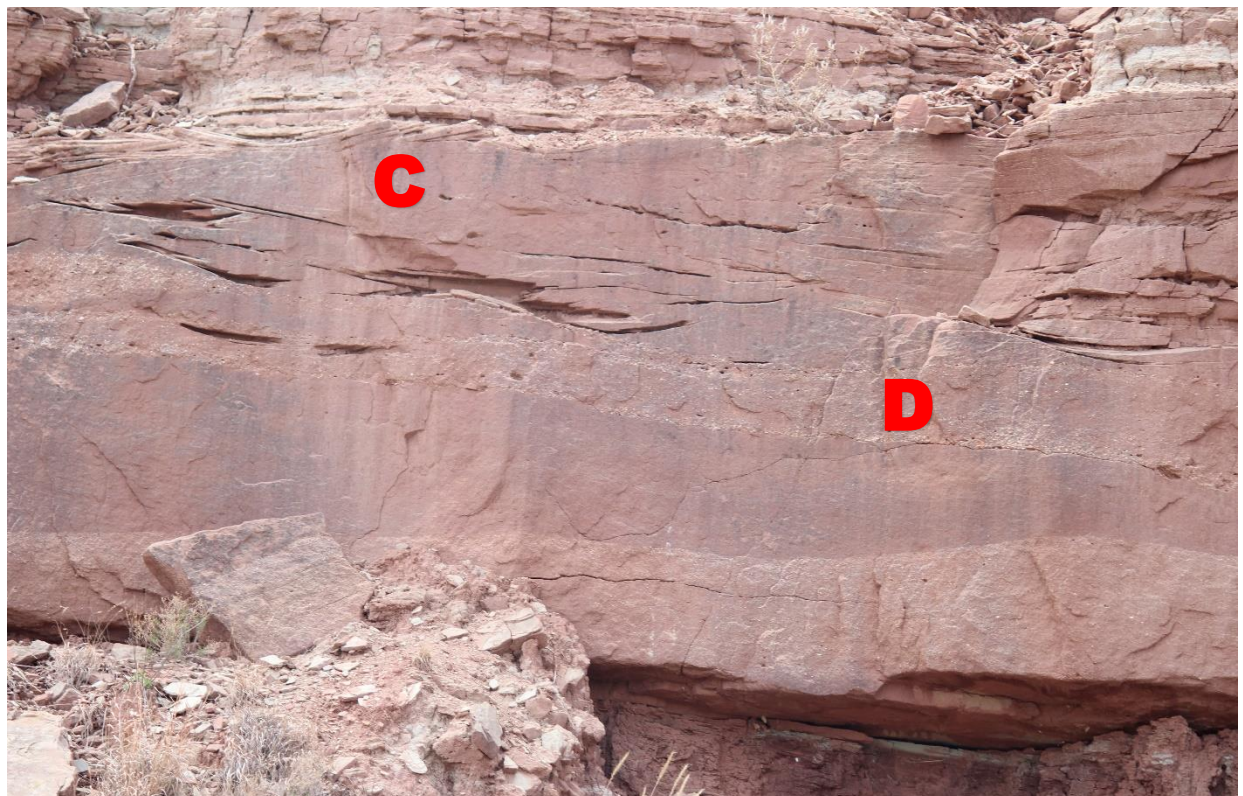
Gac is associated with Sac as this study has not identified Gac without Sac being present within the same channel-fill sandstone unit. However, the same is not true of Sac. Sac is observed independent of the presence of Gac. In fact, most of the sections containing Sac lithofacies observed in New Mexico locations contained no Gac. The most common sedimentary structure in Sac is symmetrical antidunes whereas chutes-and-pools and cyclic steps are less common. This is true of the entire study area where Sac was observed, but it is noteworthy that chutes-and-pools and cyclic steps were not observed in any of the New Mexico sections, and were only observed in some of the Texas sections.

In Texas, Sac and Gac are prevalent in channel-fill sandstones of the Tecovas, Trujillo and Cooper Canyon, but in New Mexico Sac was only observed as a component of some large channel-fill sandstones in the Trujillo Sandstone. Sac in the Trujillo Sandstone of New Mexico, if present at all, represents much smaller parts of channel-fill sandstone units than in measured sections in Texas. The thickest units of Sac and the only presence of Gac in New Mexico is exhibited in the uppermost Trujillo Sandstone at the Conchas location of the Conchas-Newkirk composite section. The Conchas location included the only example of Sac within the Tecovas Formation, and the lithofacies was observed in thin, discrete, channel-fill sandstones encased in

floodplain mudstones. Sac is common in the Tecovas sections of Texas. Sac was not observed in any of the Cooper Canyon sections observed in New Mexico.



Figure 4: (Above) A - abundant Sac overlying minor Sh (B)—Trujillo Sandstone, Texas Hwy 256 location. (Below) Sac (C) and Gac (D)—Tecovas Formation, Texas Hwy 256 location.





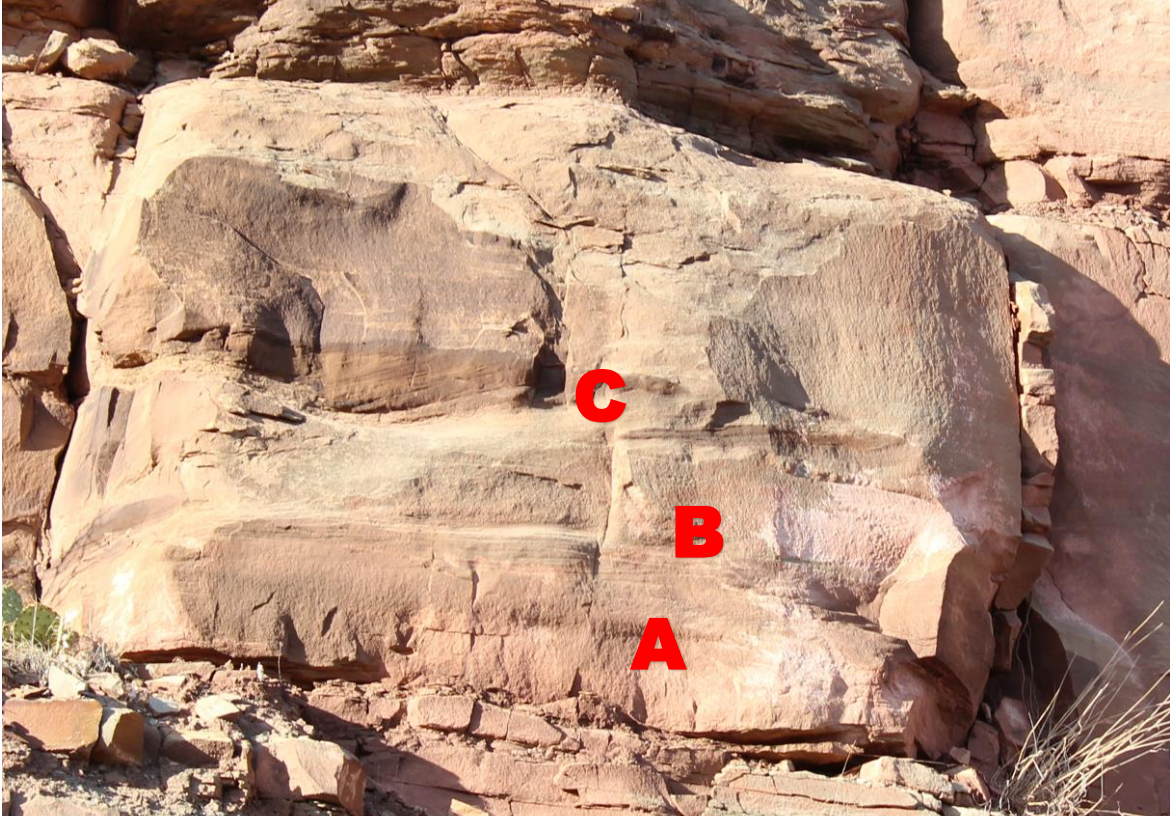
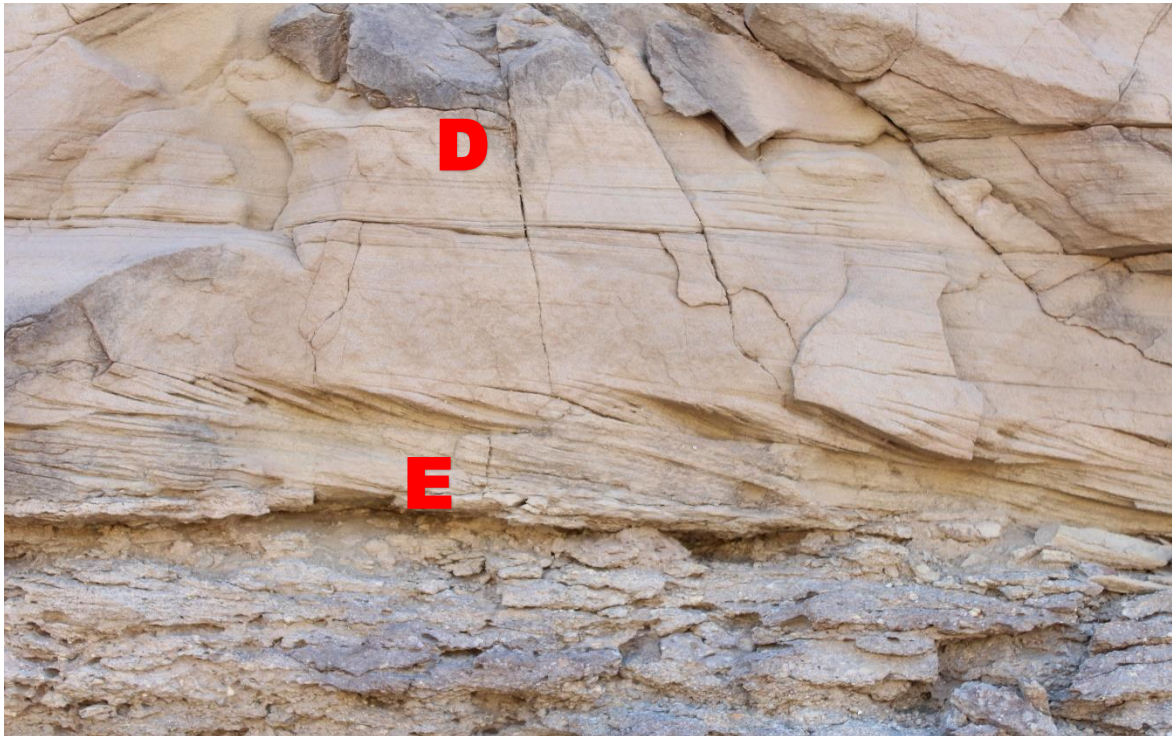


Figure 5: (Above) Mixed Sh (A), Sl (B), and Sr (C) lithofacies—Trujillo Sandstone, Trujillo Hill location. (Below) Sh (D) and Sl (E) lithofacies—Trujillo Sandstone, Conchas portion of Conchas/Newkirk measured section (CN-A, Figure 2).



#### **4.4 Lower-flow-regime channel-fill lithofacies**

The S1 lithofacies is defined as a very-fine grained to fine-grained channel-fill sandstone which contains sigmoidal cross-lamination that are interpreted to be washed-out dunes (e.g., Saunderson and Lockett, 1983; Chakraborty and Bose, 1992; Fielding and Webb, 1996; Fielding, 2006; Lang and Winsemann, 2013; Walker, 2020). Washed-out dunes are indicative of a waxing transitional flow as the Froude number approaches one when sediments would begin to form upper-plane beds.

The S1 lithofacies is rare in Texas locations, but it is more prevalent in New Mexico (Figure 5). Regionally it is almost exclusively found within the Trujillo Sandstone, but thin units of this lithofacies are also found in the Cooper Canyon Formation at the Trujillo Hill location (Figure 10). S1 is typically observed as a thin unit directly at the base of Sh sandstones. It is found within larger-scale channel-fill sandstones, and not associated with floodplain channels of smaller width and thickness.

The remaining lower-flow-regime channel-fill lithofacies identified in this study are Sr and Stb. These lithofacies are similar. Both lithofacies are composed of red to white, very fine grained to fine-grained sand, and contain similar sedimentary structures: ripples, dunes, and tabular to trough crossbedding (Figure 7). However, Walker 2020 distinguished the two based on the presence of accretion sets and the higher abundance of trough-cross lamination in the Stb facies. Another difference between the two lithofacies is that Sr is commonly a component of larger-scale channel-fill sandstones that otherwise contain upper-flow-regime channel-fill lithofacies whereas Stb is interpreted to be indicative of traditional lower-flow-regime channel fill and bar deposits that do not contain higher energy lithofacies.



Sr and Stb are rare in the measured sections in Texas. They are found within the Tecovas and Cooper Canyon Formations and there exists only one example of a thick unit of Sr present at the Hwy 256 location within the Tecovas Formation. The rest of Sr and Stb in Texas is expressed as either thin, minor components of thick upper-flow-regime channel-fill sandstones or thin, discrete floodplain channels. In New Mexico, however, the Sr and Stb lithofacies are both more common and also represent thicker portions of the sandstone units in which they are present. These lithofacies are present in various proportions throughout the extent of the measured sections, but the Trujillo Sandstone is where they are the least common. Within the Tecovas and Cooper Canyon Formations of New Mexico, Sr and Stb are dominant lithofacies (Figure 10).

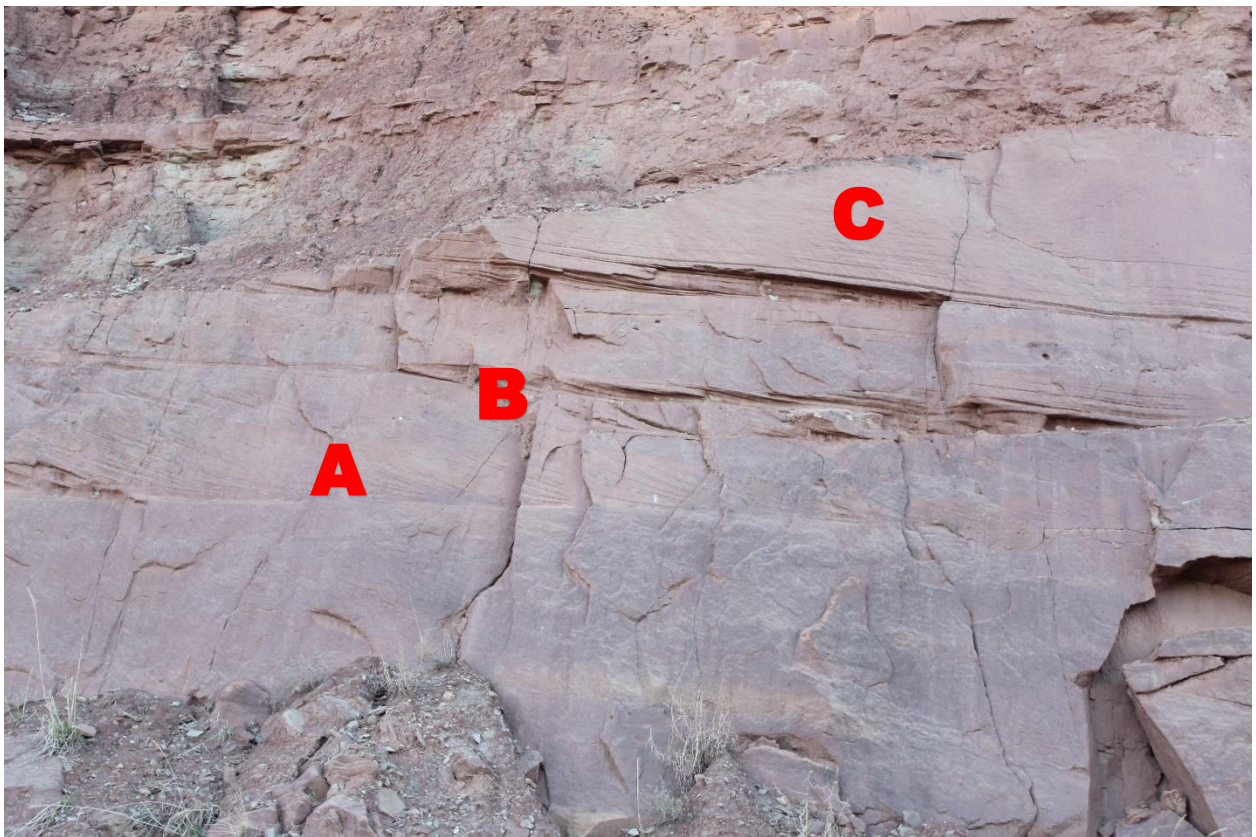


Figure 6: Sr (A), Sl (B), and Sh (C) in a thick (6.81 m) stack of channel sands—Tecovas Formation, Texas Hwy 256 location.



Figure 7: Stb (A) in channel sands—Trujillo Sandstone, Conchas location of Conchas/Newkirk composite section.

#### **4.5 Lacustrine and non-channel lithofacies**

Interpreted as a floodplain mudflat, the Fl lithofacies is characterized by its clay to silt sized sediments in varying proportions. It is described as massive with localized ripples or parallel lamination. Heavily bioturbated, this lithofacies may contain root traces and other traces of biogenic activity. Fl can exhibit soil-like characteristics as well. In some units, Fl exhibits a blocky, pedogenic weathering style as well as slickensides. The Fl lithofacies is interpreted as a record of overbank mud-sized sediments settling out of suspension during channel aggradation.

The Fl lithofacies is of varying thicknesses through all formations although the thickest successions are found in the Tecovas and Cooper Canyon Formations. There is not a drastic difference in the abundance of Fl between sections of these formations in Texas and sections in New Mexico. Fl encases channel-fill sandstones. It locally has a gradational contact with lacustrine facies, preserving a package of ‘wetting upwards’ lithofacies.

The P lithofacies, mudstone with soil profiles, is similar to Fl. P is characterized by clay to silt sized sediments with colors that range from red, orange, white, and purple. P exhibits pedogenic weathering, cutans, slickensides, manganese staining, phosphate nodules, calcrete nodules, and bioturbation such as root traces and oxidation halos. The P lithofacies is interpreted as paleosols.

The characteristics of P are variable based on location. Some are very well-developed paleosols while others are less defined. In Texas a thick, correlatable unit of P is found beneath the Tecovas Formation commonly referred to as the Palo Duro Geosol or informally the ‘Spanish Skirts’ (McGowen et al., 1979; Lamb, 2019). This geosol exhibits well-defined color banding with alternating calcrete and silcrete horizons which reflect fluctuations from dry to humid climates (Lamb 2019) (c.f., Retallack, 1992; Kanhalangsy, 1997). In New Mexico this unit of P



is not observed. In New Mexico P is generally found in thinner packages and is usually found in conjunction with the Fl lithofacies. Within the Cooper Canyon Formation in at the Trujillo Hill location, a thick, well-developed P unit exhibits calcrete beds up to 1 meter in thickness.

The channel-fill sandstones of the Dockum Group are not just encased by the Fl and P lithofacies. The Fcf lithofacies is another example of a fine-grained lithofacies present in the measured sections. It is a red to light orange or grey colored claystone to mudstone that contains little to no bioturbation, parallel laminations that vary in strength, and minor local ripples. It is interpreted as lacustrine fill (Walker, 2020). Prior research from Walker which focused solely on the Tecovas Formation and Trujillo Sandstone claimed that this lithofacies was confined to the Tecovas, but the addition of the Cooper Canyon Formation in this study shows that thick successions of this lithofacies are present in both the Tecovas and Cooper Canyon Formations. However, the distribution of these packages varies between the two formations. One thick stack of the Fcf lithofacies is found within the Tecovas Formation at the Tule Canyon location (Figure 8), but otherwise the lithofacies is observed in relatively thin packages that are interpreted as shallow, local depressions rather than a lake of substantial size. This differs from the Cooper Canyon Formation in which stacks up to 10 meters are common across the field area.

Interbedded within the Fcf lithofacies at some locations is the Fmh lithofacies. This is defined as a silt to fine grained sandstone that ranges in color from red to buff. It is characterized by planar laminations, local antidunes, and soft sediment deformation in the form of flame structures and ball and pillow structures (Figure 9). This lithofacies is interpreted as sandy, density-flow deposits that spread out across lake bottoms (Walker 2020). This lithofacies is identified within both the Tecovas and Cooper Canyon Formations in Texas, and in the Cooper Canyon Formation in New Mexico. This lithofacies is not associated with the shallow, localized

Fcf units but rather with larger stacks of Fcf. A minor lithofacies that is associated with lacustrine deposits is Gp. The Gp lithofacies is defined as inclined accretion sets of sandstone with gravel and minor silt encased within the Fcf lithofacies (Walker 2020). Gp is massive with local antidunes and is interpreted as prograding delta foresets.

One of the changes to the lithofacies of Walker (2020) is the addition of Scvh, which is another lithofacies associated with lacustrine deposits and similar to the previous two lithofacies yet distinct in grain size and interpretation of depositional environment. Scvh is defined as a well-sorted, fine grained sandstone buff to white in color with parallel lamination and bedding and convoluted bedding with recumbent folds. While Fmh is interpreted to be along the bottom of lakes and the prodelta, Scvh is interpreted as being more proximal to the shoreline and associated with the delta front.



Figure 8: (Left) Close-up of Fcf lithofacies—Tecovas Formation, Tule Canyon location. (Right) A hoodoo composed almost entirely of a thick (>25 m) Fcf lithofacies—Tecovas Formation, Tule Canyon location. While the Fcf lithofacies is typically observed as thin and discrete in both the Tecovas Formation and Trujillo Sandstone, this is the major exception to that rule.



Figure 9: (Left) Stack of repeating Fcf and Fmh lithofacies (0.5 – 2 m packages)—Cooper Canyon Formation, Hwy 469 location of San Jon composite section. (Right) Fluid escape structures, Fmh lithofacies—Cooper Canyon Formation, same location as left picture.

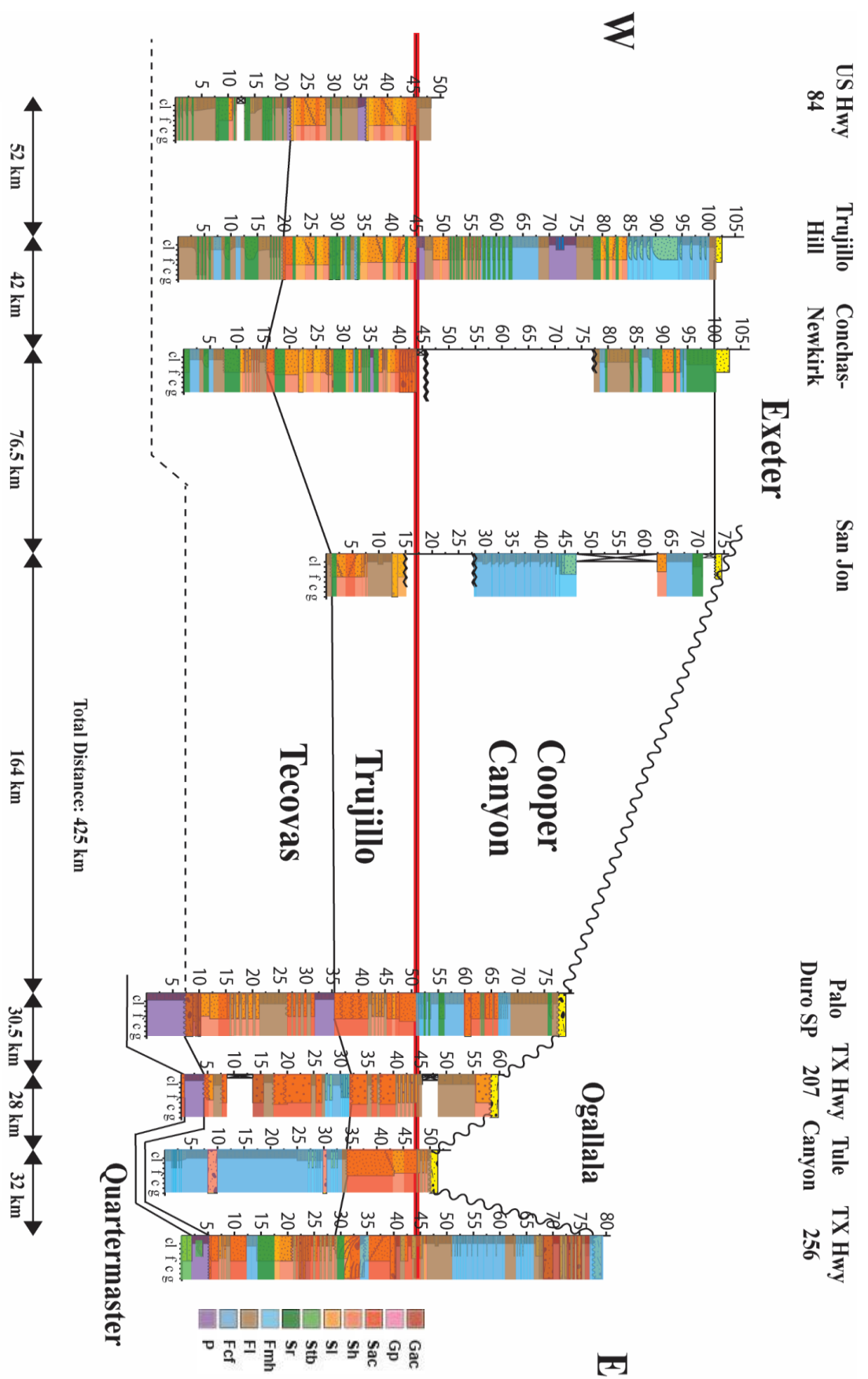


Figure 10: Cross-section of measured sections with lithofacies interpretations shading. Geographic context of sections used in cross-section from Figure 2

## 4.6 Fluvial Architecture

The architectural elements of the Dockum Group identified in Walker (2020) are consistent with field observations throughout the field area of this study. Established in the aforementioned research, are seven channel-scale elements, two valley-scale elements, and one sequence-level element (Table 2). The channel-scale architectural elements are named UCHI, UCHs, USB, CH, MCH, FF, and LF. Respectively, these codes represent large-scale upper-flow-regime channel fill, small-scale upper-flow-regime channel fill, upper-flow-regime side-attached bar, lower-flow-regime channel fill, mixed-flow-regime channel fill, floodplain mudflat, and open lake fill. These architectural elements are characterized by geometry, dimensions, bounding surfaces, and lithofacies that are found within them. The valley-scale elements are named VF and FTD which are, respectively, valley fill and fluvial terrace deposits. MVC is the final architectural element code and is representative of a multivalley complex.

<b>Channel-Scale Architectural Elements</b>	<b>Code</b>	<b>Geometry</b>	<b>Characteristics</b>	<b>Interpretation</b>
Large-Scale Upper-Flow-Regime Channel Fill	UCHI	Geometry: Narrow to broad sheets Width: 48 – 118 m Thickness: 1.7 – 4.3 m Aspect Ratio (W/T): 35	Thick fluvial sandstone body, dominated by Sac and minor Gac transitioning into Sl, Sh and Sr lithofacies, bound by 3 <sup>rd</sup> or 4 <sup>th</sup> order surfaces.	Records cut and fill of wide channels under supercritical flow conditions. Generally recording waning flow with channel filling.
Small-Scale Upper-Flow-Regime Channel Fill	UCHs	Geometry: Broad ribbons to thin sheets Width: 5 – 20 m Thickness: 0.1 – 0.5 m Aspect Ratio (W/T): 41	Thin fluvial sandstone body dominated by Sh and Sr with minor Stb lithofacies, bound by 2 <sup>nd</sup> or 3 <sup>rd</sup> order surfaces. Identified by the distinct lack of Sac lithofacies	Records rapid pulse of upper-flow-regime waning flow energy. Localized to floodplains and minor incisions into large-scale upper-flow-regime channel bodies. May record independent flow events, splays, or chutes from larger channels.
Upper-Flow-Regime Side-Attached Bar	USB	Geometry: Wedge or lobe Width: 10 – 35 m Thickness: 1 – 12 m	Lateral accretion surfaces building out into channel body. Limited identification within study area. Contains Sac and minor Gac transitioning into Sh alternating with 2 <sup>nd</sup> order accretion sets bound by 4 <sup>th</sup> or 5 <sup>th</sup> order basal surface.	Records consistent duration of supercritical waning flow energy allowing for the formation and growth of an upper-flow-regime lateral accretion sets as side-attached bar and cut bank moved laterally. Uncommon due to lack of consistent flow energy and preservation.
Lower-Flow-Regime Channel Fill	CH	Geometry: Lens to concave-up narrow ribbons Width: 5 – 20 m Thickness: 1 – 5 m Aspect Ratio (W/T): 4	Lens or concave-up ribbon, well sorted sandstone dominated Stb and Sr lithofacies, uncommon in study area, bound by 4 <sup>th</sup> or 5 <sup>th</sup> order surfaces.	Records hiatus in supercritical flow deposition and a return to lower-flow-regime channel architecture.
Mixed Flow-Regime Channel Fill	MCH	Geometry: Narrow sheet Width: 40 – 50 m Thickness: 1.5 – 3 m Aspect Ratio (W/T): 20	Thick fluvial sandstone body, with Sac, Sh, Sl with intermixed Sr lithofacies, bound by 3 <sup>rd</sup> order surfaces. Full preservation is uncommon within study area.	Records fluctuation and transition in waning flow energy from supercritical to subcritical flow or vice versa. Commonly partly to completely eroded by overlying channels.
Floodplain Mudflat	FF	Geometry: Blankets Width: 3 – 40 m Thickness: 0.2 – 4 m	Blankets commonly interbedded with channel deposits, dominated by Fl and P lithofacies, bound by 2 <sup>nd</sup> or 3 <sup>rd</sup> order surfaces.	Records overbank fines settling out of suspension as flow energy further decreases with intermittent status characterized development of soil horizons.
Open Lake Fill	LF	Width: 5 – 25 m Thickness: 3 – 17 m	Vary in size from few meters to tens of meters. Dominated by Gp, Fmh, Fcf and some interbedded Gac, Sac, Sh and Sr lithofacies, adjacent to channel bodies, bound by 2 <sup>nd</sup> or 3 <sup>rd</sup> order surfaces.	Records large and small bodies of standing water, commonly with deltaic development.
<b>Valley-Scale Architectural Elements</b>	<b>Code</b>	<b>Geometry</b>	<b>Characteristics</b>	<b>Interpretation</b>
Fluvial Terrace Deposit	FTD	Geometry: Down-step pinch-outs Width: 2 – 4 m Thickness: 1 – 3 m	Small pinch-out section of a fluvial body on outer or inner bank of valley scour. Contains channel-scale architectural elements such as UCHI, UCHs, SBu, FF and or CH, bound by 4 <sup>th</sup> or 5 <sup>th</sup> order surfaces.	Preserved section of channel fill or floodplain before following incision, within the confines of a larger valley.
Valley Fill	VF	Geometry: V or U shape Width: 20 – 90 m Thickness: 5 – 15 m Aspect Ratio (W/T): 4.3	Large confining architecture containing all channel-scale architectural elements and FTD major architectural element. Bound by 5 <sup>th</sup> or 6 <sup>th</sup> order surfaces.	Records multiple channel cut and fill episodes confined within one cumulative higher order surface.
<b>Sequence-Scale Architectural Elements</b>	<b>Code</b>	<b>Geometry</b>	<b>Characteristics</b>	<b>Interpretation</b>
Multivalley Complex	MVC	Geometry: Extensive shallow, smooth elongated U shape Width: 220 m Thickness: 25 m	Largest confining architecture containing all channel-scale and valley-scale architectural elements. Bound by 7 <sup>th</sup> or 8 <sup>th</sup> order surfaces.	Records multiple laterally amalgamated valley fills confined within a higher order surface or sequence boundary.

Table 2: Architectural elements identified within the Dockum Group (Walker 2020)

## 4.7 Lithosomes

To demonstrate large-scale, regional trends in the distribution of channel-fill sandstones across the field area, this study grouped lithofacies and fluvial architectural elements into lithosomes in a similar fashion to the research of Lamb (2019). These lithosomes serve as a relative scale of the recorded strength of flow of channel-fill sandstones and general distribution of non-channel sediments. Lithosomes comprise two categories: channel lithosomes and non-channel lithosomes.

A lithosome comprises channel-scale architectural elements in varying proportions. The lithosomes are defined in this research in part by the channel-scale architectural elements that compose them. Lithosomes also are defined by the presence and relative abundance of lithofacies and the proportions of sedimentary structures within. Channel-fill lithosomes are used as a proxy in this case for the strength of flow of the fluvial system as it flowed or didn't flow through a specific area at a specific time. The thickness of individual lithosomes is variable inasmuch as a section of valley fill can only be as large as the paleogeography allowed.

This study identified six unique lithosomes; four channel lithosomes and two non-channel lithosomes (Table 3). The channel lithosomes are defined based on the presence of the lithofacies that corresponds with the highest energy sedimentary structures. Lower-energy-representative lithofacies and the corresponding sedimentary structures are common within higher energy-representative lithosomes. Non-channel lithofacies such as Fl are sometimes contained within a valley fill and therefore a lithosome, but they are minor, thin components that interfinger with channel sands when they are not amalgamated.

#### **4.8 Channel-fill lithosomes**

The LCP lithosome records high-upper-flow-regime deposits, and is defined by the presence of chute-and-pool structures, cyclic steps, or antidunes in greater than 50% abundance throughout the extent of the unit. This lithosome comprises architectural elements UCHI, UCHs, and USB with high abundance of these high-froude-number upper-flow-regime structures. Although the corresponding architectural elements are all defined as upper flow regime with dominant Sac, Gac and Sh lithofacies, lower-flow-regime lithofacies such as Sl and Sr are present and preserved in waning and waxing flow stages. Also, not every UCHI contains abundant chute-and-pool structures, cyclic steps, or has antidunes in >50% abundance, so only those which do would qualify as part of lithosome LCP. This lithosome represents periods when channels had sustained flow that reached or exceeded a Froude number of 1.

The LA lithosome is defined by upper-flow-regime channel fills with Sac or Gac up to antidunes only, and in abundance less than 50%. This lithosome comprises varying proportions of the architectural elements UCHI, UCHs, MCH. The Sac lithofacies is present, but below the threshold of 50% abundance. Most of the antidunes identified are discrete and contained within the MCH architectural element. The dominant lithofacies in this lithosome is Sh, but Sl and Sr are preserved as waxing and waning flow. This lithosome represents valley fill of channels that commonly had sustained rates of flow approaching supercritical and intermittently exceeded a Froude number of 1.

The LUPB lithosome is defined by the presence of upper-plane-bed. This lithosome comprises the architectural elements UCHs and MCH. The lithofacies that marks the highest recorded sedimentary structure in this lithosome is Sh; no Sac was observed in this lithosome. Sh, Stb, and Sr are found in higher abundance within LUPB than within LA, and some channel-



scale architectural elements such as CH contain only lower-flow-regime lithofacies. However, upper-flow-regime channel-scale architectural elements such as UCHs are still common and can comprise almost entirely upper-plane bed and laminations. This lithosome represents valley fill of channels that fluctuate between subcritical flow rates to flow rates near or approaching supercritical.

The LD lithosome is defined by the presence of dunes and trough crossbedding. This lithosome is exclusively composed of the architectural element CH. The lithofacies which contains the highest-energy sedimentary structure in this lithosome is Stb which is defined by trough cross-bedding. Sr is also common. Every channel-scale architectural element found in this lithosome exclusively contains lower-flow-regime sedimentary structures representative of subcritical flow. This lithosome represents valley fill of channels with flow exclusively at subcritical rates.

#### **4.9 Non-channel lithosomes**

The LF lithosome is defined by the presence of any non-channel floodplain lithofacies which include Fl and P. This is most like the architectural element FF of Walker (2020). The lithofacies that compose this lithosome do not demonstrate channelized flow or associated sedimentary structures. This lithosome represents sections of valley fill where channel sands are not present.

The LL lithosome is defined by the presence of any lacustrine lithofacies. This lithosome comprises the LF architectural element which includes the lithofacies Fcf, Fmh, Gp, and Scvh. While not channel-fill sandstones, these lithofacies can locally indicate the strength of flow of the corresponding channel sands which flow into them. For example: Gp and some Fmh

lithofacies observed in measured sections contain discrete antidunes. This lithosome represents sections of fill where channel sands terminate into a lake or local depression.

<b>Lithosome Code</b>	<b>Sedimentary Structures</b>	<b>Lithofacies</b>	<b>Channel-Scale Architectural Elements (Walker, 2020)</b>
<b>LCP</b>	Cyclic steps, chutes and pools, antidunes >50% relative abundance, upper-plane bed, transitional dunes	Sac, Gac, Sh, Sl	UCHI, UCHs, USB
<b>LA</b>	Antidunes – discrete or in >50% relative abundance, upper-plane bed, transitional dunes	Sac, Sl, Sh, occasional Sr	UCHI, UCHs, MCH
<b>LUPB</b>	Upper-plane bed, transitional dunes, ripples, dunes	Sl, Sh, Sr	UCHs, MCH, CH (if other channels in valley scour contain supercritical bedforms)
<b>LD</b>	Dunes, ripples, trough cross-bedding, tabular beds	Sr, Stb	CH
<b>LL</b>	Horizontal laminations, wavy to ripple laminated, mud-cracks, fluid-escape structures	Fcf, Fmh, Gp, Scvh	LF
<b>LF</b>	Massively bedded, heavily bioturbated, horizonated	Fl, P	FF

Table 3: Table of lithosomes. Lithofacies in column 3 from Table 1. Channel-scale architectural elements in column 4 from Table 2 (Walker, 2020).

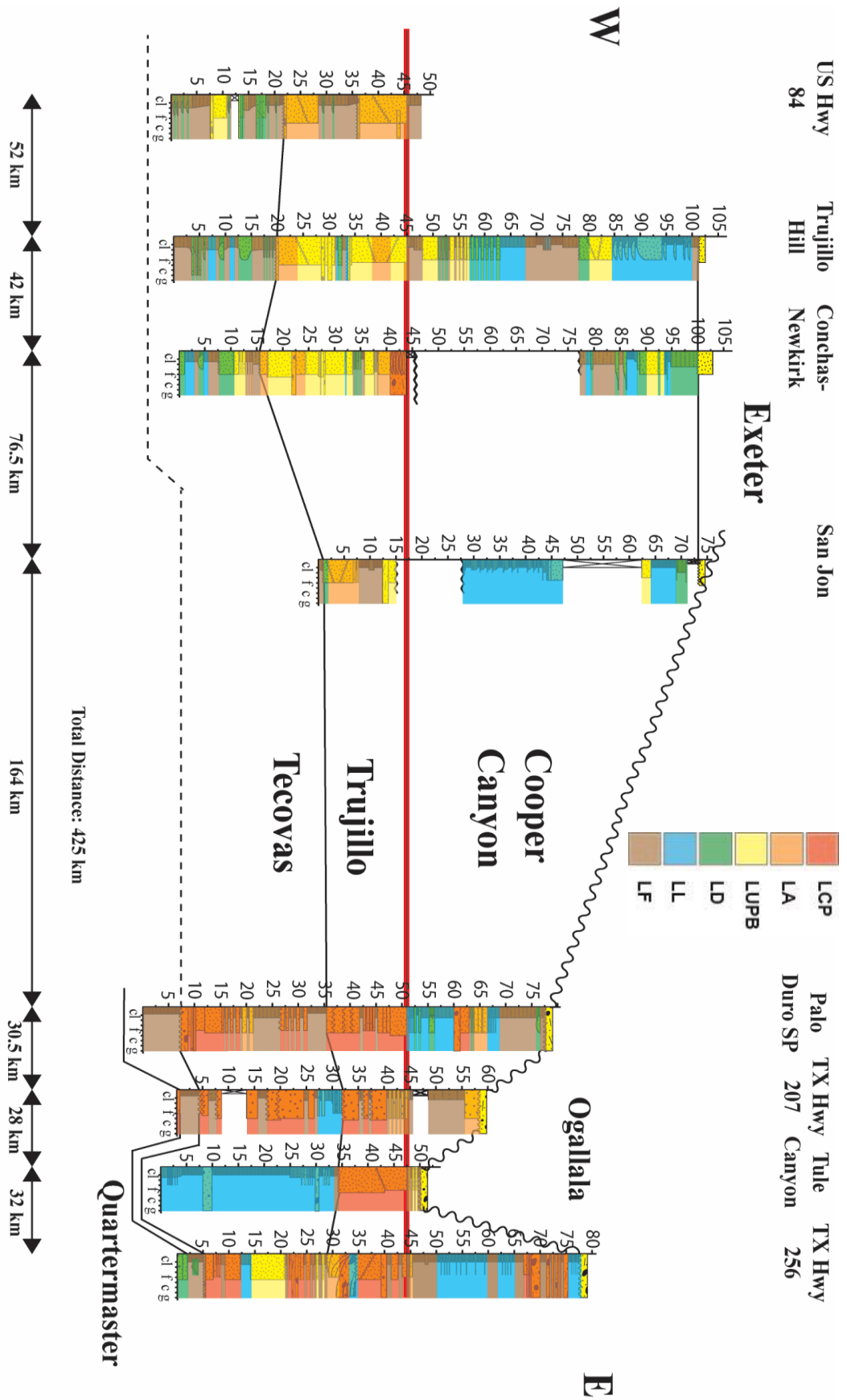


Figure 11: Cross-section of measured sections with lithosome interpretations shading.

#### 4.10 Paleocurrent data

Paleocurrents of the Dockum Group have been previously and recently researched (Lehman and Chatterjee, 2005, Bezucha, 2022). However, Lehman and Chatterjee (2005) lacked the knowledge that the Dockum Group was rife with upper-flow-regime structures which gives the possibility that antidune cross-sets may have been misinterpreted as dune cross-sets. This is significant because antidune cross-sets dip upstream whereas dune cross-sets dip downstream. Bezucha (2022) focused primarily on the Santa Rosa Formation. No study has analyzed paleocurrents in the Tecovas Formation, Trujillo Sandstone, or Cooper Canyon Formation since antidunes and other upper-flow-regime sedimentary structures have been identified. Therefore, this study took paleocurrents at six of the eight measured sections to compare with previously published paleocurrents.

Paleocurrents were taken using both lower-flow-regime and upper-flow-regime structures. In Texas the majority of paleocurrents were taken using the crest of symmetrical antidunes. In these cases, the paleocurrent recorded is  $\pm 90^\circ$  to the bearing shot along the crest of the antidune. This method suggests that paleoflow could be in either one bearing or in  $180^\circ$  to that bearing. In New Mexico most paleocurrents were taken using dune cross-sets, but some paleocurrents were taken from antidunes when applicable.

Paleocurrents, regardless of whether they were measured from upper-flow-regime structures or lower-flow-regime structures, showed that channels of all three formations were broadly flowing to the west-northwest (Figure 12). Bezucha (2022) found that this is true of the Santa Rosa Formation as well. Furthermore, the paleocurrents measured in this study are consistent with findings from Bezucha's detrital zircon study (2022) which confirms the source

for the Dockum Group is the Ouachita front to the east and southeast of this study's field area and sediment dispersed to the west across the Dockum basin.



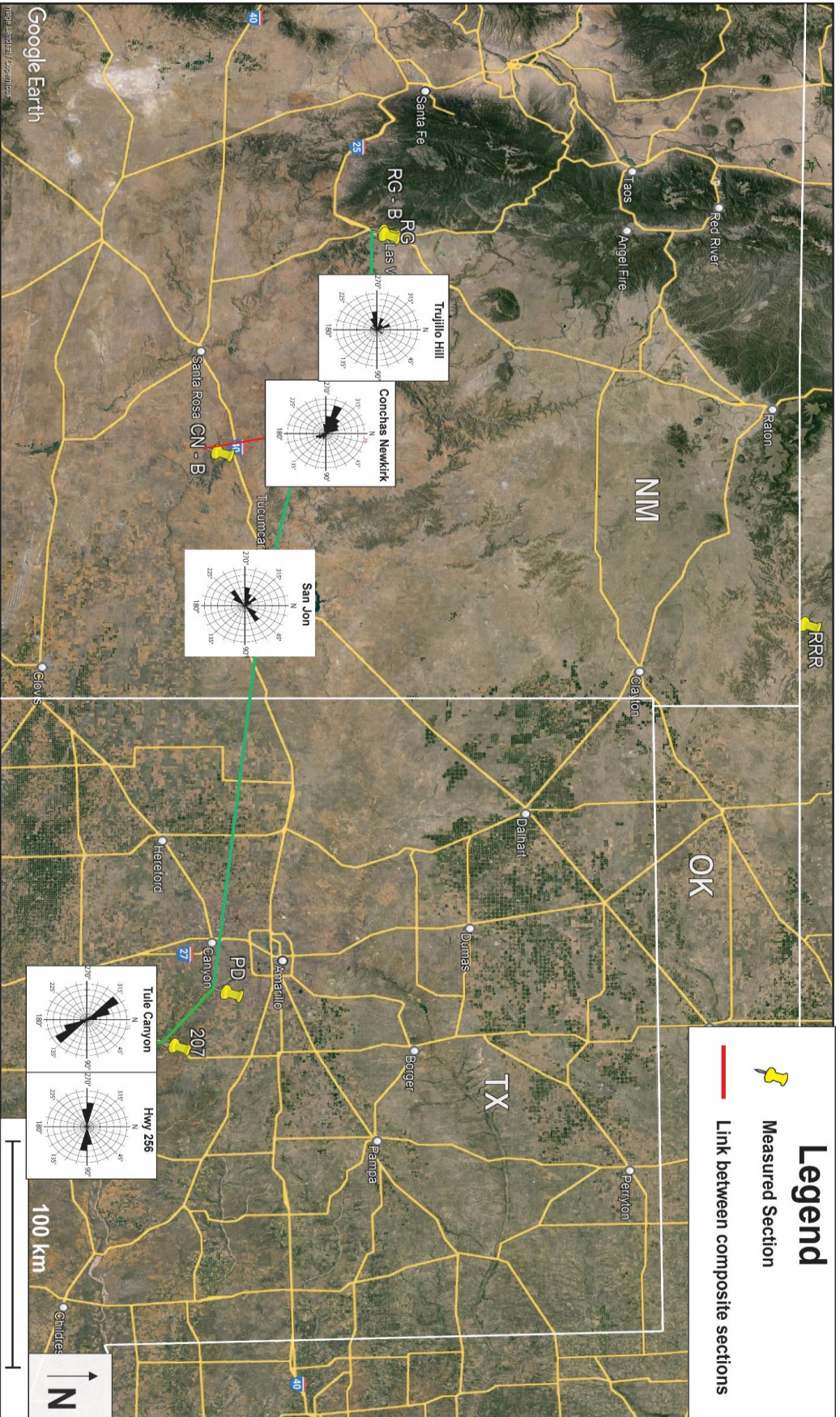


Figure (12) Rose Diagrams showing paleocurrents from Trujillo Sandstone at the following locations from east to west: TX Hwy 256, Tule Canyon, San Jon, Conchas-Newkirk, Trujillo Hill. All paleocurrent measurements are available in the appendix but shown are rose diagrams made from paleocurrents taken from the Trujillo Sandstone. As the most sand-rich formation of the Dockum Group, the Trujillo Sandstone is the best for high populations of paleocurrents. While the Tecovas and Cooper Canyon Formations show similar trends, fewer paleocurrents were measured due to lack of reliable examples.

#### **4.11 Observed data not used in cross-section analysis**

Two sections in this study were observed and recorded but were not used for cross-section analysis due to one, Red Rock Ranch (appendix cc), being off-trend and another, Romeroville Gap (appendix aa), lacking correlatability in a structurally complex region.

They both exhibited similar characteristics to other Dockum Group sections with prevalent upper-flow-regime structures but lacked enough evidence to be fully included in this study. However, A recent zircon study by Bezucha (2022) suggests that the uppermost strata of the Red Rock Ranch section, the Travesser Formation, are likely temporally at the same stratigraphic age as the Cooper Canyon Formation. Further research would be needed to correlate stratigraphically lower formations of the Dockum Group into the Dry Cimarron Valley where the Red Rock Ranch section was measured.

### **5. Discussion**

#### **5.1 Dockum Group regional variability in lithosomes**

The Dockum Group of West Texas and northeast New Mexico is a succession of fluvial sandstone, floodplain mudstone, and isolated lacustrine mudstone characterized by the presence of abundant upper-flow-regime structures. Lithosomes, which are groupings of lithofacies, were generated for analysis of the distribution of these structures. The relative abundance of these lithosomes varies both longitudinally through the system as well as vertically (Figure 11).

Discharge estimations for upper-flow-regime channels of the Dockum Group were made by Walker (2020). In that work he noted that the antidunes preserved in channel-fill sandstones are forming past the peak discharge and during the waning stages of flow, as is consistent with modern observations (Langford and Bracken, 1987; Alexander and Fielding, 1997; Alexander et

al., 1999, 2001; Russell and Arnott, 2003; Fielding et al., 2009, 2018; Alexander, 2008; Kostic et al., 2010; Froude et al., 2017; Izumi et al., 2017; Baines et al., 2018). Still, despite peak discharge for Dockum Group channels being an indeterminate value greater than the preserved sedimentary structures might suggest, these do record associations in relative strength of flow for channels based upon what sedimentary structures are preserved. Such is the aim of categorizing these stratigraphic units into lithosomes.

The defining characteristic of the LCP lithosome is the presence of either any amount of chutes and pools or cyclic steps or the presence of antidunes in relative abundance of 50% or more throughout entire channel fills. Chutes and pools form when the Froude number is between 1.6 and 2.1, and cyclic steps form when the Froude number is greater than 2.2 (Alexander et al., 2001; Cartigny et al., 2011, 2013, 2014; Cartigny, 2012; Muto et al., 2012). Stable antidunes form when the Froude number is approximately 1 (Gilbert, 1914; Lighthill, 1978; Kennedy, 1961, 1963, 1969; Allen, 1984; Cartigny et al., 2011, 2013; Cartigny, 2012). Therefore, units of measured sections that are labeled LCP are representative of periods of deposition when discharge was at the highest magnitude of any channel building events in the Dockum Group.

The strongly upper-flow-regime LCP lithosome is almost exclusively identified in Texas with only one exception in New Mexico. LCP is associated with thick, amalgamated channel-fill sandstone lenses to sheets in the Texas locations and is less frequently observed in thinner, discrete sandstone beds. The entirety of the Dockum Group in Texas is largely composed of the LCP lithosome.

The Trujillo Sandstone contains the highest relative abundance of the LCP lithosome compared to other lithosomes. In fact, the only example of the LCP lithosome in the more western exposures of New Mexico is within the uppermost Trujillo Sandstone at the Conchas



portion of the Conchas-Newkirk composite section. No chutes-and-pools nor cyclic steps were observed in New Mexico, and while antidunes were observed they were in lower relative abundance in than in Texas.

The LCP lithosome is also dominant within the Tecovas Formation of Texas, however, there is a higher abundance of lower-energy lithosomes than in the Trujillo Sandstone (Figure 11). The Cooper Canyon Formation in Texas is unique in that its expression is more variable than the other two formations. Every lithosome is present within the Cooper Canyon Formation of Texas. The LCP lithosome composes approximately 50% of the channel sands across all Texas locations, but other lower-energy lithosomes are present in relatively higher proportions than the other two formations of the Dockum Group. The LCP lithosome was not observed within the Tecovas and Cooper Canyon Formations of New Mexico (Figure 11).

The LA lithosome is defined by the presence of antidunes in relative abundance of less than 50% across the unit. Commonly associated with lower-energy-representative structures, the LA lithosome represents periods of Dockum Group channel deposition when flow only barely reached supercritical conditions.

The less intensive medial-upper-flow-regime channel-fill deposits of the LA lithosome were observed across the entire extent of the study area. In Texas, it can be found in every formation, but it is associated with thinner sections of valley fill than LCP. Typically in Texas sections, if antidunes are present within a channel-fill sandstone they are present in large abundance, and; therefore, would be categorized as the LCP lithosome. This differs from the distribution of LA in New Mexico which is only present in the Trujillo Sandstone. In fact, the LA lithosome is a dominant component of the Trujillo Sandstone in New Mexico sections. The LA lithosome does not occur in either the Tecovas Formation or the Cooper Canyon Formation

in New Mexico. When the LA lithosome is observed in the Trujillo Sandstone in New Mexico sections, it is found in thick, channel-fill sandstones whereas when the LA lithosome is observed in the Trujillo Sandstone in Texas sections it is found in thinner sandstone units. This is due to large channel-fill sandstones of the Trujillo Sandstone in Texas being of high enough flow energy to be classified as the LCP lithosome.

The LUPB lithosome is defined by upper-plane bed being the highest energy-representative structure present in a unit. Upper-plane-bed laminations form when the Froude number is less than 0.84 (Gilbert, 1914; Lighthill, 1978; Kennedy, 1961, 1963, 1969; Allen, 1984; Cartigny et al., 2011, 2013; Cartigny, 2012). In this case, the channel only achieved the lower levels of upper flow regime for brief intermittent periods during filling, and may locally for brief episodes reached supercritical conditions if at all.

The mixed weak-upper-flow-regime to lower-flow-regime LUPB lithosome is observed across the entire extent of the study area, but it is most prevalent within the New Mexico locations where it is present in all sections and formations. In Texas the LUPB lithosome was only observed within the Tecovas and Cooper Canyon Formations. There were no measured sections in Texas in which the LUPB lithosome was not observed in the Tecovas and Cooper Canyon Formations. This differs from the Trujillo Sandstone in which none of the Texas sections included the LUPB lithosome. The LUPB lithosome in Texas is expressed as thin, discrete channel sandstones with the exception of one thick, local unit found in the Tecovas Formation at the Hwy 256 location.

In New Mexico, the LUPB lithosome comprises thick, amalgamated sandstones in every formation across all sections. Differing from the Trujillo Sandstone in Texas sections, the LUPB lithosome is the dominant component of the Trujillo Sandstone in New Mexico. The LUPB

lithosome is associated with the LA lithosome when observed in the Trujillo Sandstone.

However, in the Tecovas and Cooper Canyon Formations of New Mexico, the LUPB lithosome is associated with the LD lithosome.

The LD lithosome is defined by the presence of only lower-flow-regime structures in a unit. Units labeled LD are representative of the smallest magnitude of discharge recorded in the Dockum Group. The LD lithosome is observed throughout the study area, however, in Texas it is only found within the Tecovas Formation and within the Cooper Canyon Formation. In Texas it is expressed as thin, discrete sandstones, and it is associated with either the floodplain sediments or small-scale lakes forming in local depressions. There are no sections in Texas in which the LD lithosome was observed in the Trujillo Sandstone.

In New Mexico, the lower-flow-regime LD lithosome is found in all formations, but the expression of the lithosome varies depending on the formation. Within the Trujillo Sandstone, LD is composed of thin, discrete sandstones associated with the floodplain. Within the Tecovas and Cooper Canyon Formations; however, the LD lithosome is observed as both small-scale floodplain channels as well as thick, large-scale units of channel-fill sandstone. There is a higher frequency and relative abundance of the LD lithosome within the Tecovas Formation compared to the Cooper Canyon Formation.

The LL lithosome is observed throughout the extent of the study area. The Tecovas Formation in Texas contains one, thick unit of the LL lithosome, however, the LL lithosome in the Tecovas Formation is also expressed as thin, local packages of lacustrine sediments in both Texas and New Mexico. This is very similar to the distribution of the LL lithosome within the Cooper Canyon Formation. The LL lithosome identified within the Cooper Canyon Formation is expressed both as thick successions of lacustrine mudstones as well as thin, non-laterally

extensive units. Both thick and thin packages of this lithosome are found in Texas and New Mexico within the Cooper Canyon Formation. In the Trujillo Sandstone all units of the LL lithosome across the field area were observed to be thin and not laterally extensive.

The LF lithosome is observed throughout the extent of the study area. Within the Tecovas and Cooper Canyon Formations, the LF lithosome is expressed in a similar character in both Texas and New Mexico. In both formations the LF lithosome was observed as both thin units separating channel-fill sandstones as well as thick, slope-forming units. The Trujillo Sandstone, however, contains a different distribution of the LF lithosome from Texas to New Mexico. In Texas, very little LF is present at all because the majority of the formation is composed of amalgamated channel-fill sandstones. In New Mexico not only is LF more common in the Trujillo Sandstone, but also there is a common trend of a thick, slope-forming LF lithosome separating two major Trujillo sandstones. While this bimodal distribution is observed in the Trujillo Sandstone in Texas (Walker 2020), the common presence of a thick LF unit separating them is unique to New Mexico.

## **5.2 Dockum Group regional depositional trends**

The Dockum Group is a dryland fluvial system characterized by the presence of upper-flow-regime channels fed by intermittent, intense rainfall from storms in the system's headwaters of the Ouachita Orogenic Belt (Lamb, 2019; Walker, 2020; Bezucha, 2022). However, the expression of the rocks both stratigraphically and longitudinally within the same formation indicate that conditions during deposition varied through time as well as downstream. Flashy discharge related to the megamonsoon is interpreted to be the cause of upper-flow-regime deposition (Walker and Holbrook, 2022). The distribution of upper-flow-regime channel fills

argues that this condition dissipated downstream and was most intensive in the middle of the Dockum Group during Trujillo time.

The units of LCP lithosome, the lithosome that records the highest upper-flow-regime discharge, are almost exclusively in the four Texas measured sections to the east. Texas records the most updip of the Dockum Group sections, nearest to the Ouachita source area, and the New Mexico sections are more distal. This is backed by paleocurrent data (Figure 12), and by detrital zircons (Bezucha, 2022). The LCP lithosome is also present in all three formations in Texas albeit in different proportions. Still, this indicates that throughout the entire Dockum Group in the up-dip direction flows frequently exceeded a Froude number of 1.0. The Trujillo Sandstone stands out in Texas as the formation with the most LCP relative to other lithosomes and, therefore, represents the period of Dockum Group deposition when the magnitude variation of discharge was highest and channels filled under intensive upper-flow-regime conditions more often. All channel lithosomes observed in Texas are representative of high discharge variation, with the only low energy lithosome LD being observed in small, discrete floodplain channels of the Cooper Canyon and Tecovas Formations. The Cooper Canyon Formation is the most diverse of the 3 formations in terms of flow strength, although this is a relative statement as all formations in all the sections in Texas still dominantly record high-intensity flows.

To the west in the four New Mexico measured sections there is a drop-off in flow strength. In terms of the LCP lithosome, there is only one isolated unit observed at the Conchas-Newkirk composite section. The highest energy-representative lithosome of significant abundance otherwise is the LA lithosome which was only observed within the Trujillo Sandstone. The Tecovas and Cooper Canyon Formations generally only had strength of flow at high enough values to produce upper-plane bed in these more distal locations. The starkest

change is within the Tecovas Formation. In Texas it is mostly the LCP lithosome with minor LA and LUPB, but the Tecovas in New Mexico is dominantly the LD lithosome with minor LUPB. Whereas the channel sandstones within the Cooper Canyon Formation in New Mexico are closer to 50 percent LUPB and 50 percent LD. Regardless, both the Tecovas and Cooper Canyon Formations were observed to have major drop-offs of flow strength distally toward the New Mexico outcrops. Furthermore, the channel sands of both formations more typically exhibit channel-form lensoid geometries in New Mexico, in contrast to the typical wide and flood-out appearance of the time-equivalent sections in Texas.

This change to more channelized sandstone bodies was not seen in the Trujillo Sandstone in New Mexico. Rather, the Trujillo Sandstone was observed to still outcrop as large sheets as it does in Texas. It is the only of the three formations where the LD lithosome is not a major component. Depending on location it is either dominated by the LA lithosome or it is a mix between the LA and LUPB lithosomes in these distal areas.

The discharge of the flows during the time of deposition of the Trujillo Sandstone were still powerful enough to generate upper-flow-regime fills with antidunes and upper-plane bed across a longitudinal reach of over 400 kilometers. Whereas the flows during the deposition of both the Tecovas and Cooper Canyon Formations were not conducive to preserving much upper-flow-regime structures beyond 120 – 160 km down dip of the furthest east of the Llano Estacado caprock sections in Texas.

### **5.3 Non-channel lithosomes**

The deposition of non-channel lithosomes and their distribution is similar to the channel lithosomes inasmuch as the Tecovas and Cooper Canyon Formations follow similar trends to each other from east to west, whereas the Trujillo Sandstone varies more in its longitudinal

expression. The LF lithosome is present in the Tecovas Formation in similar proportions both in up-dip sections and down-dip sections. There is not a noteworthy increase or decrease in its presence. The same is true of the LF lithosome in the Cooper Canyon Formation. The distribution of the LL lithosome from east to west in both formations is similar to the LF lithosome in that there is not a noteworthy increase or decrease in proportion. The one exception is a thick unit of LL in the Tecovas at the Tule Canyon location in Texas otherwise the LL lithosome comprises thin units throughout the Tecovas both up-dip and down-dip. The LL lithosome in the Cooper Canyon is observed as both thick and thin units regardless of whether in an up-dip section or down-dip section. This study found no evidence to suggest that either formation loses flow regionally to large, terminal lakes in either Texas or New Mexico.

Because there is no noticeable longitudinal difference in the abundance of the LL or LF lithosome in the Tecovas and Cooper Canyon Formations, it is likely that these formations were primarily driven by a system that provided a sufficient sediment supply to continue providing coarse sediment both upstream and downstream, but not sufficient overall to keep up with accommodation. The degree to which channel belts tend to amalgamate vs disperse and preserve floodbasin deposits has long been tied to the rate of accommodation (Leeder, 1978; Allen, 1978; Bridge and Leeder, 1979). More recent work shows that the rate of coarse sediment supply has a similar impact of channel amalgamation, whereby higher supply translates to greater amalgamation (Bryant et al., 1995; Heller and Paola, 1996). This effect is so strong, that Colombera et al. (2015) were able to show that accommodation rate alone rarely correlates to degree of channel amalgamation in actual rock sections. The presence of similar relative abundance of lacustrine sediments up-dip versus down-dip suggests that sediment supply was low enough to fail to fill these local depressions. Furthermore, the lack of meaningful longitudinal difference in floodplain sediments shows that regional aggradation was higher than

the rate of channel-sand deposition. However, sediment transport and, therefore, channel-sand deposition is positively correlated with discharge magnitude (Tooth, 2013; Fielding et al., 2018). The flow strength in channels of these formations had dissipated, and yet there exists no noticeable change in the proportion of either lacustrine or floodplain sediments between when channel sands record supercritical flows (up-dip) versus when they record subcritical flows (down-dip). Since the units are not appreciably thinner down dip, it is unlikely that the maintenance of sand to mud ratio can be explained by a proportional drop in accommodation rate down dip. Supply of coarse sediment apparently maintained and did not dramatically dissipate down dip, maintaining ratios of mud and sand with accommodation variation as a lesser factor.

The Trujillo Sandstone in Texas comprises very little LF lithosome or LL lithosome. In New Mexico that is still true of the LL lithosome; however, there is an increase in the LF lithosome comparatively. The Trujillo Sandstone has commonly been described as exhibiting a bimodal distribution of two amalgamated sandstones. In both the San Jon and Hwy 84 locations the LF lithosome is observed separating these two thick sandstone bodies to a greater extent than is observed in sections further up-dip. These two locations are also where the Trujillo Sandstone contain the highest proportion of LA lithosome compared to other Trujillo Sandstone sections in New Mexico, so the increase in LF lithosome is likely not related to any weakening of flow in these locations.

The absence of lacustrine sediments in the Trujillo Sandstone suggests that sediment supply was high, and channels were effective in filling local depressions channel-fill sediment. This trend does not vary substantially up-dip versus down-dip, nor does the thickness of the unit dramatically change. This argues for an increased rate of sediment supply during the Trujillo deposition compared to the proportion found in the Tecovas and Cooper Canyon Formations.



The well-fed Trujillo Sandstone channels had more opportunities to rework the floodplain muds and replace them with coarser sands and gravels. This is generally true for the entire longitudinal profile. However, the down-dip increase in floodplain sediments caused the Trujillo Sandstone to separate into two thick sandstone units with some LF lithosome between. Some loss of coarse sediment to upstream storage is likely the reason for this slight increase in floodbasin mud preservation (c.f. Leeder, 1978; Allen, 1978; Bridge and Leeder, 1979). Sediment supply is linked to flow strength (Tooth, 2013; Fielding, 2018). Loss of flow strength down dip in the Trujillo, though minor compared to the Tecovas and Copper Canyon formations, likely did have some impact on rate of filling of accommodation by channel fills. The Trujillo Sandstone is a series of two fluvial sequences which merge updip in Texas sections into one sequence (c.f. Holbrook, 2001).

The higher relative abundance of LF and LL in the Tecovas and Cooper Canyon Formations compared to the Trujillo Sandstone indicates that conditions during the deposition of the Trujillo Sandstone were more conducive to larger magnitude, more-sustained, and more frequent flows that extended farther down dip. Larger storms bring higher magnitude of discharge and move more coarse sediment downstream. While all formations dissipate in flow strength down dip, the Trujillo Sandstone persists upper-flow-regime conditions farther down dip than the Tecovas or Cooper Canyon formations. This is evidenced by the proportionally more abundant higher-energy-representative lithosomes in New Mexico sections of Trujillo Sandstone versus the Tecovas and Cooper Canyon Formations. Both sediment supply and scour depth are positively correlated with flow strength (Powell et al., 2007; Tooth, 2013; Fielding et al., 2018). Not only does the Trujillo Sandstone record a period in the Late Triassic in which the storms that fed this system were larger in magnitude, but also it suggests that the storms were more frequent. The amalgamation of the of the Trujillo Sandstone is likely heavily controlled by an increased

sedimentation rate caused by larger, more-frequent storms rather than a decrease in aggradation rate.

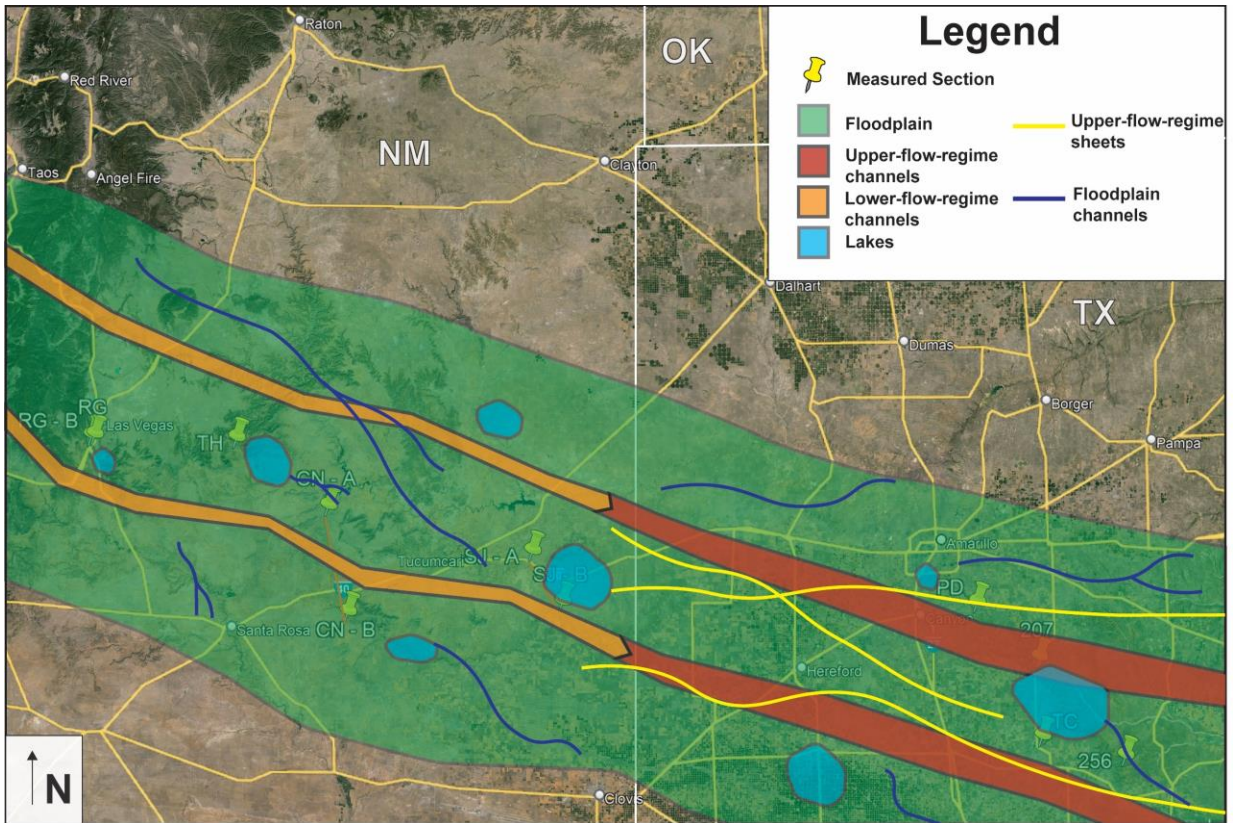


Figure (13) Depositional cartoon depicting the depositional environments for both the Tecovas and Cooper Canyon Formations. Flow is to the north-northwest from the source area of the Ouachitas. Lakes of various size are present up dip and down dip. Upper-flow-regime sheets terminate down dip, and upper-flow-regime channels transition into lower-flow-regime channels down dip. Channels narrow down dip. Figure not to scale.

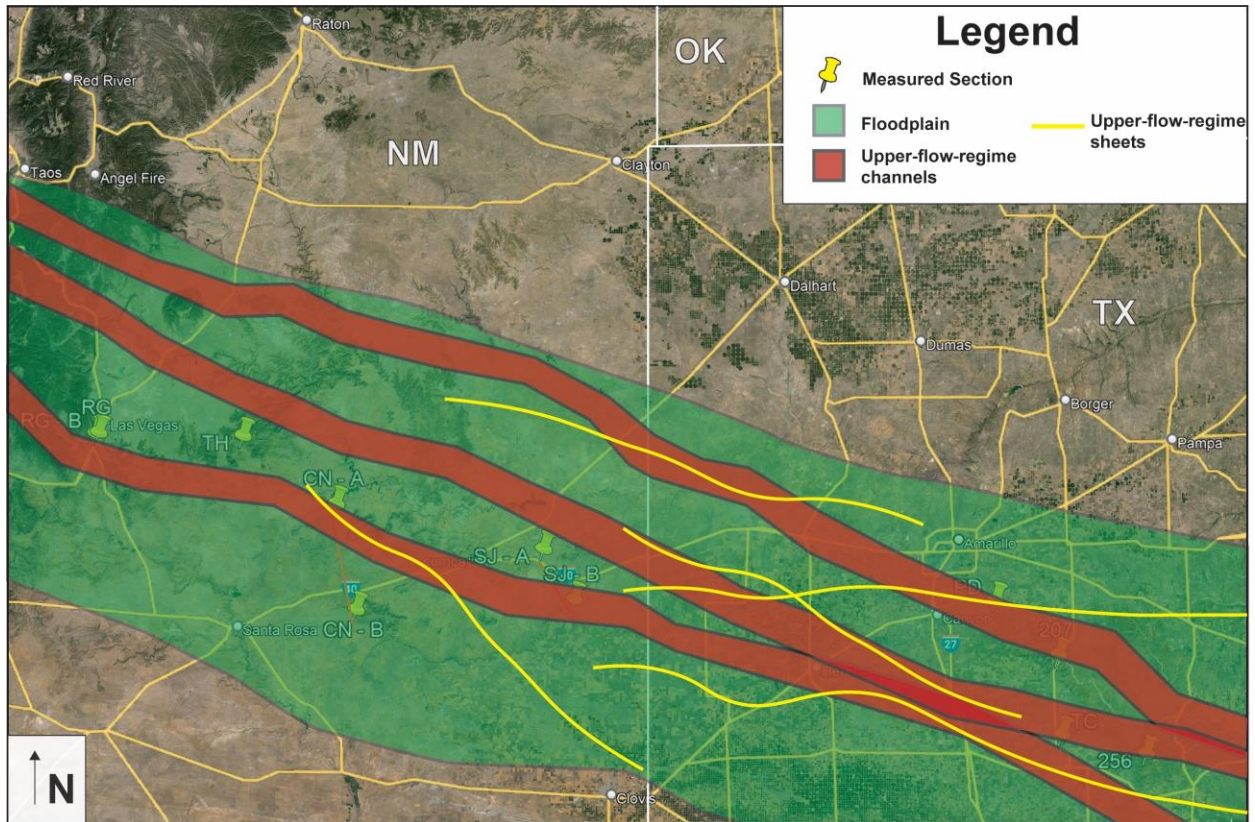


Figure (14) Depositional cartoon depicting the depositional environment for the Trujillo Sandstone. Flow is to the north-northwest from the source area of the Ouachitas. Wide upper-flow-regime channels persist down dip, and upper-flow-regime sheets are found further down dip compared to the Tecovas and Cooper Canyon Formations (Figure 13). Figure not to scale.

#### 5.4 Dryland fluvial systems and climate

Dryland fluvial systems are susceptible to many variable environmental factors but are particularly controlled by runoff and sediment supply (Tooth, 2013). Parrish (1993) proposed that during the late Triassic the climate of the modern-day southwest of the United States was controlled by megamonsoons. Work from Lamb (2019) hypothesized that the upper-flow-regime channels in the Dockum Group are evidence of these violent, convective storms. Further work by Walker (2020) on the flow parameters of the Tecovas Formation and Trujillo Sandstone strengthened the megamonsoon hypothesis by calculating that both formations record river systems with high to very high discharge variance consistent with systems controlled by a

megamonsoonal climate. Bezucha (2022) showed that these strata originate from the Ouachita Mountains, bolstering the claims by both Lamb (2019) and Walker and Holbrook (2022) that these flashy discharge channels originate where these large convective megamonsoonal storms orographically lifted as they collided with the high Ouachita topography. The channels then flowed downstream toward the west and flow dissipated in strength.

This study shows that all formations of the Dockum Group lose flow strength and volume downstream, but it also shows that the magnitude of that loss is not uniform across all formations (Figure 11). The Tecovas and Cooper Canyon Formations are observed to have a dramatic drop in flow intensity and volume while the Trujillo Sandstone records less of a drop in upper-flow-regime discharge (Figures 13 & 14). This is likely, in part, the result of shifts in climate which impacted the magnitude, duration, and frequency of the storms which fueled the flow of rivers of the Dockum Group.

Ephemeral and intermittent dryland fluvial systems are similar and often grouped together in the literature, yet the two have some important differences which impact how they behave. Ephemeral channels are fed by highly localized storms which produce flash floods. The hydrographs associated with these events are characterized by steep rising and receding limbs with short time bases (Walters, 1989; Rhoads, 1990; Hassan, 1990; Reid et al., 1994; Dick et al., 1997; Belmonte and Beltran, 2001; Cigizoglu et al., 2002; Tooth, 2013). Other common characteristics of ephemeral channels are the presence of a poorly connected drainage network and an output with high variability (Tooth, 2013). Walker (2020) states “The Tecovas Formation comprises a diverse range of architectural elements recording a wide range of depositional environments”. Walker and Holbrook’s (2022) findings and analysis of lithofacies distribution in both the Tecovas and Cooper Canyon Formations suggest that these two formations are

characterized by thin channels recording ephemeral flow conditions. These smaller, flashy events produced by localized convective storms likely were the primary source of water for Tecovas and Cooper Canyon channels. Ephemeral to intermittent exists on a spectrum, however, so it is important to note that, while not the norm, occasional storms of greater intensity or duration likely contributed to deposition as well.

Intermittent channels, on the other hand, are fed by storms with longer-lived single peaks, multiple peaks, or produced by seasonality. These storms tend to be subtropical in origin or frontal systems that exhibit a hydrograph with a less steep rising limb and a broader time base (Jacobson et al. 1995; Knighton and Nanson, 1997; Tooth, 2013). These larger storms with greater duration and frequency likely fed the Trujillo Sandstone. The amalgamation of the sandstones in Trujillo channels, the smaller magnitude drop-off in discharge down-dip, and the lack of LF and LL lithosomes suggest this to be the case.

The Trujillo Sandstone records an intensification of the megamonsoon on a timescale of millions of years, which is indicative of a climate shift on at least a continental scale. Megamonsoons were the controlling variable during deposition of all three formations, but the magnitude, duration, and frequency varied from formation to formation. This is evidenced by all formations in the up-dip sections of Texas being dominated by LCP and LA but only the Trujillo Sandstone having significant upper-flow-regime lithosomes in down-dip sections of New Mexico. These larger and more frequent storms during the Trujillo time also influenced the amalgamation and contiguous nature of the unit, and the expression of this higher flow strength is to the increased channel-fill deposition in this interval related to the monsoonally increased sediment supply. The same correlation is seen in the Tecovas and Cooper Canyon Formations where both lacustrine sediments and floodplain muds are present without significant longitudinal

trends. This, paired with the less steep drop-off of upper-flow-regime structures in channel sands down dip, is evidence that the Trujillo Sandstone records a long period of a more intensified megamonsoonal climate compared to the Tecovas and Cooper Canyon Formations.

The Trujillo Sandstone also records shorter timescale cyclicality of the megamonsoon cycle. Walker (2020) found that the Trujillo Sandstone is a multivalley complex. Periods of higher water to sediment ratio in wetter times cut these valleys, and the subsequent drier periods with a lower water to sediment ratio filled them. This argues the Trujillo Sandstone was dominated by shorter cycles of monsoon intensification on top of the longer cycle that controlled its deposition on the formational scale. This small timescale cyclicality on sediment supply is also likely at the root of the separation of two distinct Trujillo Sandstone sequences in down-dip sections of New Mexico.

## **6. Conclusions**

The Dockum Group of West Texas and northeast New Mexico is a dryland fluvial system fed by megamonsoons of temporally varying strength, recorded by supercritical flow in Dockum rivers. Six lithosomes—four channel lithosomes and 2 non-channel lithosomes—were defined from outcrop data to characterize measured sections based on relative flow strength in a regional context.


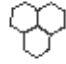




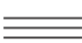

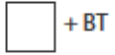





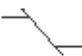









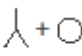













1. The channels of the Dockum Group generally flowed to the northwest from the headwaters in the Ouachitas
2. Flow strength in Dockum Group channels dissipates to the west across all formations, but supercritical flow during Trujillo Sandstone time persists farther down dip than in the Tecovas Formation or the Cooper Canyon Formation. The only evidence of supercritical flows in New Mexico is within the Trujillo Sandstone.



3. There is no longitudinal increase or decrease in floodplain muds and lacustrine sediments in the Tecovas Formation and Cooper Canyon Formation; both formations comprise varying but comparable thicknesses of floodplain and lacustrine sediments across the study area. The Trujillo Sandstone comprises almost no lacustrine sediments both in up-dip and down-dip sections, but there is a slight increase in floodplain muds which separates two fluvial sequences of the Trujillo Sandstone down dip in New Mexico.
4. Deposition was controlled by megamonsoons which controlled the sediment supply for the Dockum Group and influenced the amalgamation of channel sands. Sediment supply was low relative to aggradation in the Tecovas Formation and Cooper Canyon Formation, and it was high relative to aggradation in the Trujillo Sandstone.
5. An intensification of the megamonsoon during deposition of the Trujillo Sandstone caused an increase in sediment supply which caused the amalgamation of channel fills that distinguishes this formation. This represents climate changes on a timescale of millions of years. The multivalley complex identified in the Trujillo Sandstone also suggests smaller-scale cyclicity in the climate during deposition of this formation.

# Appendix

## Graphic Section Key

	Ripple cross-lamination		Mud cracks
	Dune cross-sets		Flame structures
	Planar bedding		Mud chips
	Planar lamination		Vertical burrows
	Blocky weathering texture and Bioturbation		Horizontal burrows
	Peds		Network of burrows
	Concretions		Bed thickness increases upwards
	Slickensides		Bed thickness decreases upwards
	Cutans		Normal grading
	Weak lamination		Weak ripple cross-lamination
	Antidunes		Fossilized wood
	Sigmoidal dune cross-sets		
	Rooting traces	<b>Lithologies</b>	
	Rooting halos		Conglomerate
	Chute and pool		Sandstone
	Cyclic Steps		Siltstone
	Convolute beds		Muddy siltstone
	Overturned blocks		Silty mudstone
			Mudstone
		<b>Paleocurrents</b>	
			Dune cross-sets
			Chute + Pool
			Antidune orientation



## **TX Hwy 256**

**34° 28' 16" N**

**101° 5' 37" W**

**Base of section:** Contact between Triassic strata and underlying Permian Quartermaster

**1.9 m** Sandstone, fine to medium-grained, red, dunes cross-sets, bottom half of unit contains extra-formational chert pebbles

**Paleocurrent measurements:**

Dunes: 288°, 295°, 287°, 278°, 280°, 272°

**3.37 m** Paleosol, purple/white/yellow, mottled, root traces, discrete sandstone bodies encased within paleosol – up to 3.4 m thick, at top of paleosol – fragipan surface

**2 m** Sandstone, fine to medium-grained, red external and gray internal, scours into underlying paleosol, antidunes, overturned blocks, chute and pool, planar bedding

**Paleocurrent measurements:**

Antidune crests: 235°/55°, 211°/31°, 242°/62°, 208°/28°

Chute and pool: 20°

**1.37 m** Sandstone, fine-grained, interbedded with silty mudstone, sandstone – planar bedding, beds on 10's cm scale, thickness of sandstone beds decreases upwards

**0.86 m** Silty mudstone

**2.99 m** Sandstone, fine to medium-grained, red external and gray internal, long wavelength antidunes, antidunal hummocks, planar bedding

**1.99 m** Silty mudstone, red and gray, laminated

**6.81 m** Sandstone, fine to medium-grained, red external and gray internal, transverse bar and dune cross-sets in the bottom half, top half – sigmoidal dunes, planar bedding

The next **8.94 m** of the section is lateral—to the E—of previously measured section and is situated within an intraformational scour.

**0.87 m** Silty mudstone

**3.17 m** Sandstone, fine to medium-grained, red and gray, sandstone is thin sheets which occasionally interbed with silty mudstone—cm scale—or conglomerate, sheets also amalgamate, antidunes

**Paleocurrent measurements:**

Antidune crests: 95°/275°, 108°/288°, 103°/283°, 97°/277°

**4.9 m** Silty mudstone, red and gray, discrete sand sheets—thickest at 0.7 m—sandstone bed thickness decreases upwards, planar bedding

**3.2 m** Sandstone, a stack of amalgamated and truncating sandstones – 4 total sandstone bodies, very fine-grained at base, grain size increases to fine-grained upwards, basal sandstone – ripple cross-lamination and planar lamination, sandstones above – antidunes, and planar bedding

**2.9 m** Conglomerate, 5 distinct lateral accretion surfaces which truncate previous sandstone units, dipping into subsurface

Lateral to the conglomerate, mudstone, well-laminated, red and white, mud chips, overturned blocks

**Contact** – sharp, erosional with the Trujillo Ss.

**5.1 m** Sandstone, fine to medium-grained, white with red and gray staining, abundant antidunes, low angle dipping strata, entire unit is amalgamated sandstones

**Paleocurrent measurements:**

Antidune crests: 91°/271°, 99°/279°, 261°/81°, 92°/272°, 101°/281°, 269°/89°, 265°/85°

**1 m** Conglomerate, antidunes, accretion surfaces, not laterally continuous

**0.9 m** Silty mudstone, gray and red

**1.36 m** Sandstone, fine to medium-grained, gray with red staining, antidunes

**0.71 m** Silty mudstone, gray and red

**0.89 m** Sandstone, fine-grained, gray with red staining, antidunes

**Contact** – gradational with the Cooper Canyon Fm.

**0.61 m** Silty mudstone, gray and red

**0.5 m** Sandstone, fine-grained, gray with red staining, sigmoidal dunes, planar bedding

**21.42 m** Mudstone, high content of clay, well laminated, periodic siltier sections with developed peds

Sandstone sheets, fine-grained, cm-scale dipping to the E, discrete within the mudstone—approx. thirteen individual sandstone sheets

**1.48 m** Sandstone, fine-grained, gray with red staining, conglomerate lenses, fossilized wood, antidunes

**1.73 m** Conglomerate, fossilized wood, antidunes

**8.15 m** Mudstone, white and red, with conglomerate beds, 5 discrete conglomerate beds – dipping to the west, antidunes, mudstone at the top has high clay content, develops lamination

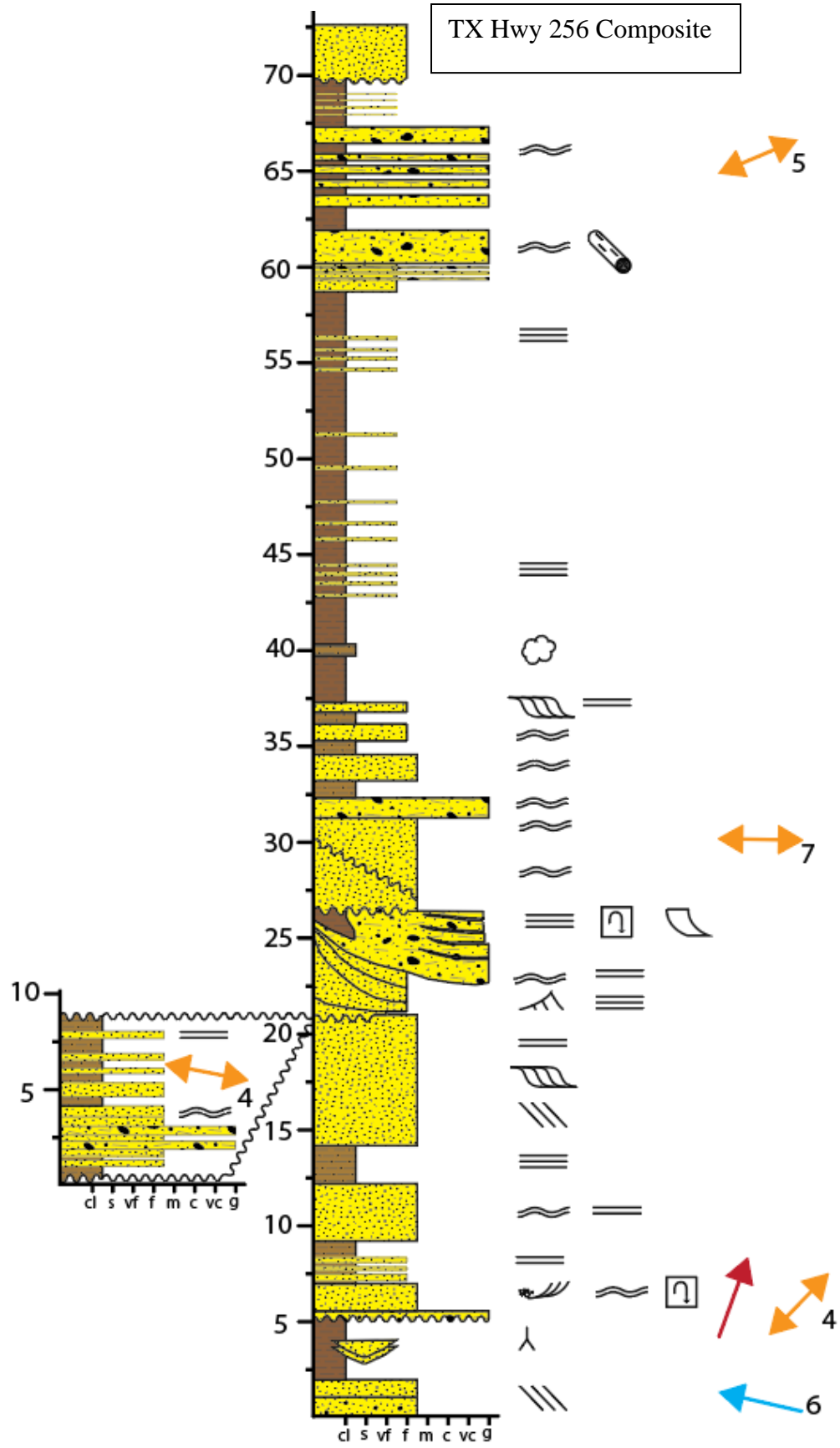
**Paleocurrent measurements:**

Antidune crests: 255°/75°, 235°/55°, 247°/67°, 243°/63°, 254°/74°

**Contact** – sharp, erosional with overlying Ogallala Fm.

**Top of section**

TX Hwy 256 Composite





Tecovas Fm (bottom), Trujillo SS (middle), Cooper Canyon Fm (top)

## **Tule Canyon**

**34° 32' 31" N**

**101° 25' 41" W**

The notes from the Tule Canyon location are in 3 parts. These parts are labeled as Section A, B, and C respectively. These three parts were used to build the composite graphic section.

### **SECTION A**

**Base of section:** Lower Tecovas Fm.

**2.13 m** Siltstone, clay, very fine-grained sand, laminated  
cm scale medium to fine-grained sandstone sheets, antidunes. Sandstone sheets laterally amalgamate at top of unit to form a 0.3 m thick sandstone bed.

**2.93 m** Similar facies as prior: higher clay content than prior unit, cm scale sandstone lenses are entirely discrete

**3.14 m** Claystone, mostly red and grey stripes, well-laminated

**1.34 m** Conglomerate – gravel-sized clasts—up to 2.5 cm in width—encased in the middle of claystone. Rip-up clasts and blocks, overturned blocks on meter scale, antidunes

**20.1 m** of inaccessible section, observed from distance – dominantly claystone from underlying units, exhibits same character as bottom-most 3 m.

Top 5 m of the section – channel-form sandstone body

**Top of section A**

### **SECTION B**

**Base of section:** Upper Tecovas Fm.

**2.44 m** Mudstone, blocky weathering texture, root halos, slickensides, peds

**0.76 m** Conglomerate, bedding surfaces shallowly dip to the NW, laterally thins/pinches out to the NW

**0.91 m** Sand and silt, unconsolidated sediment, lacks internal structure

**0.67 m** Claystone, well-laminated

**Contact** – sharp, erosional with the overlying Trujillo Ss.

\*Trujillo Ss. not measured here due to poor quality of exposure and availability of better-quality exposure at Section C.

**Top of section B**

## SECTION C

**Base of section:** Upper Tecovas Fm.

**4.88 m** Mudstone, clay, minor silt, weakly laminated, cm scale sandstone lenses/sheets encased in the mudstone, antidunes

**0.61 m** Conglomerate

**2.13 m** Similar facies to the basal unit of this section—sandstone sheets are thicker, mudstone has higher silt content.

**1.52 m** Mudstone, well-laminated

Mudstone beds immediately beneath the contact with Trujillo Ss. are contorted and have rip-up clasts

**Contact** - Sharp, erosional with the overlying Trujillo Ss.

The Trujillo Ss is **13.7 m** thick and comprises stacked, amalgamated channel sandstones, white/buff to grey in color. These notes split the Trujillo Ss. into two distinct units based on differences in grain size and sedimentary structures relative abundance.

**7.6 m** Sandstone, medium to fine-grained, high abundance of antidunes – both regular and long wavelength, low amplitude, chute and pool, cyclic steps

**Paleocurrent measurements:**

Antidune crests: 330°/150°, 318°/138°, 324°/144°, 318°/138°, 314°/134°, 338°/158°, 322°/142°, 328°/148°, 327°/147°, 323°/143°, 327°/147°, 318°/138°, 325°/145°, 333°/153°, 330°/150°

Chute and pool: 346°

**6.1 m** Sandstone, fine-grained, antidunes, antidunes preserved as hummocks, planar bedding

**Paleocurrent measurements:**

Antidune crests: 345°/165°, 345°/165°, 332°/152°, 334°/154°, 324°/144°, 332°/152°

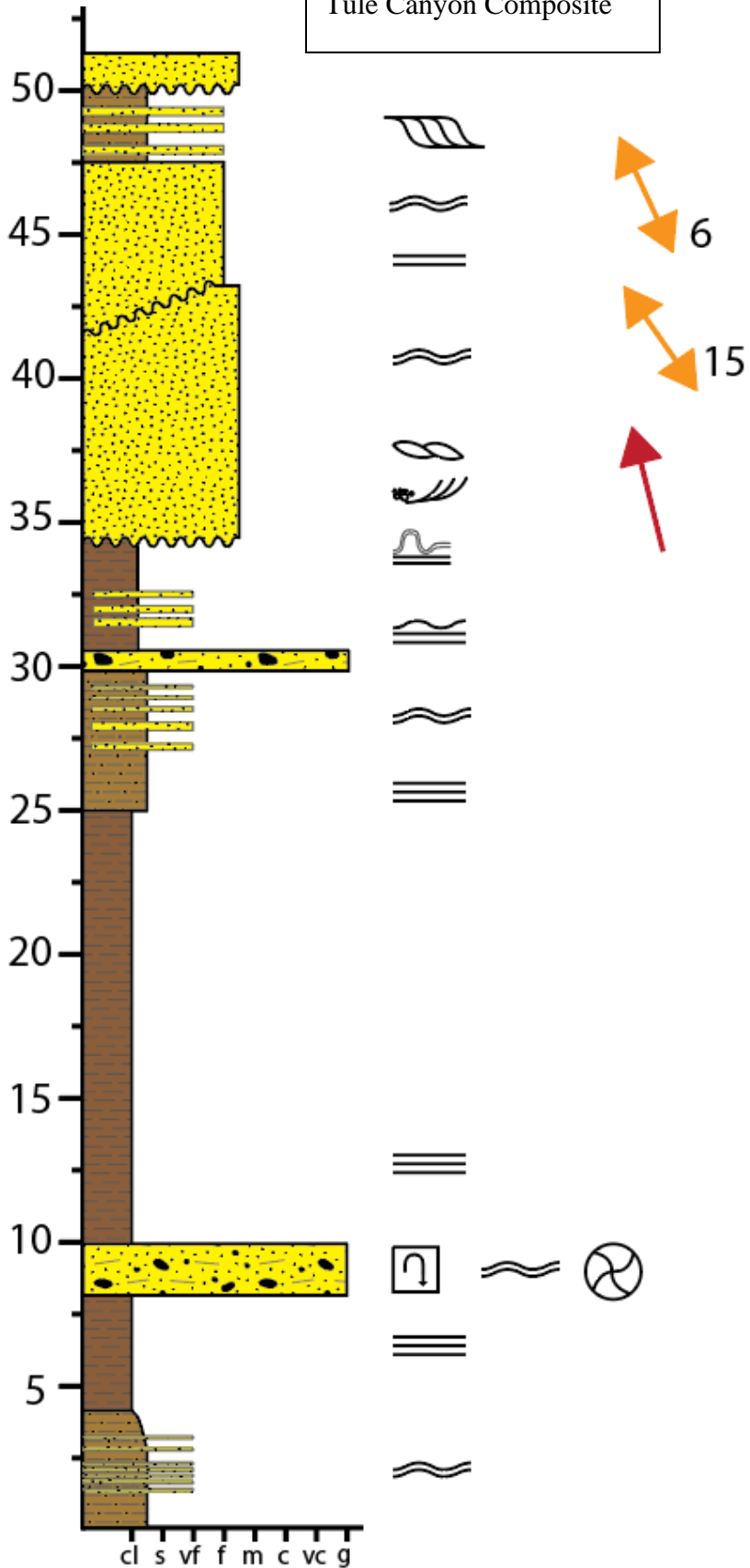
**Contact** – gradational with overlying Cooper Canyon Fm.

**2.74 m** Mudstone, red, interbedded with 10's of cm scale sandstone sheets, fine-grained, sigmoidal dune cross-sets

**Contact** - sharp, erosional contact with overlying Tule/Ogallala Fm.

**Top of section C and entire Tule Canyon composite section**

Tule Canyon Composite







Tecovas Fm (below), Trujillo SS (above)



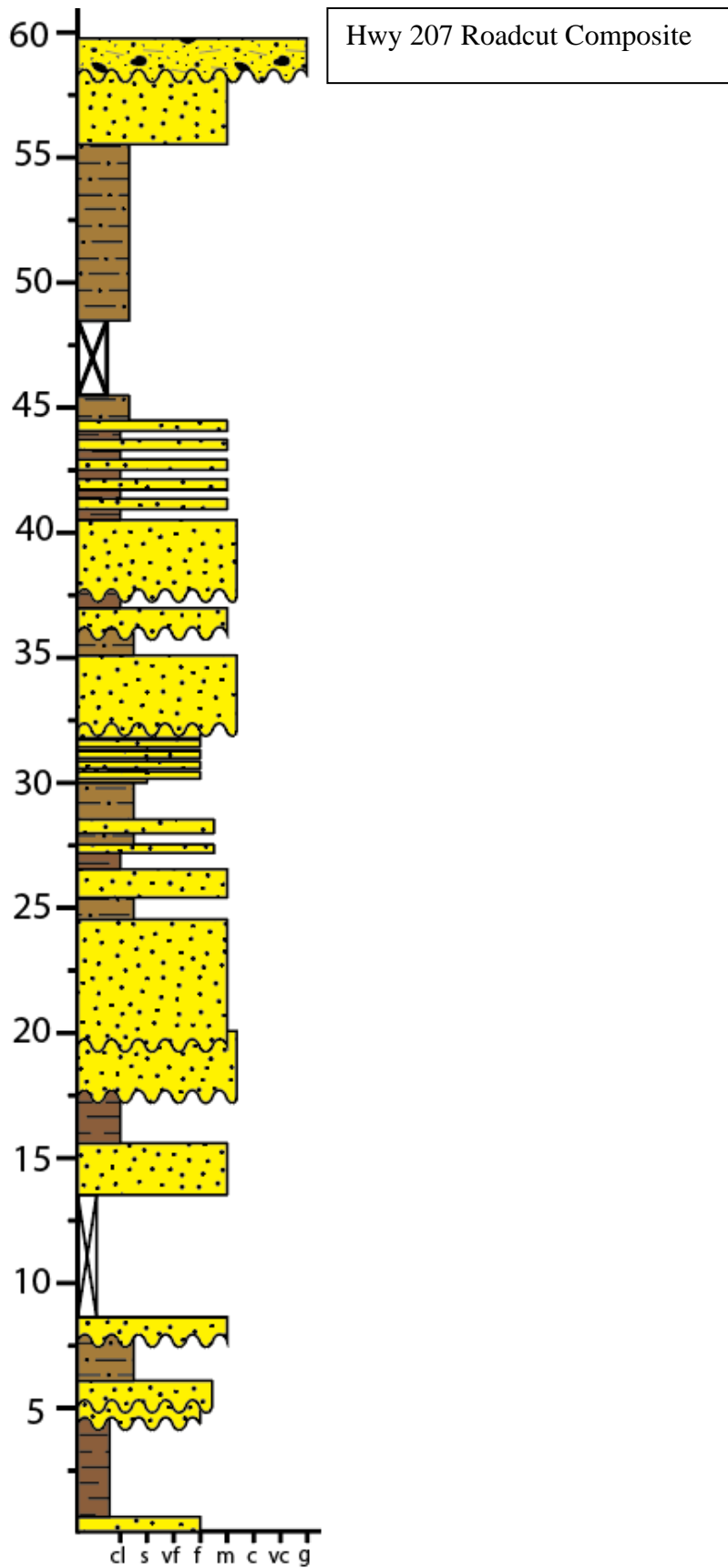


## **TX Hwy 207**

**34° 47' 56" N**

**101° 26' 12" W**

Graphic section was built from prior research (Lamb 2019, Walker 2020).  
Walker (2020) and Lamb (2019) for pictures.



## **Palo Duro Canyon SP**

**34° 58' 55" N**

**101° 41' 6" W**

The notes taken at this section are portions of measured section which were previously unrecorded in recent research. These are the bottom-most Tecovas Fm. and the entirety of the Cooper Canyon Fm. until the contact with the overlying Ogallala.

The portions of the section without notes expressly written here were previously studied and demonstrated in prior research (Lamb 2019 and Walker 2020).

**Base of section:** Previously studied and measured (Lamb 2019) paleosols

**Start of newly introduced data:** Base of Tecovas Fm.

**1.22 m** Conglomerate

**1.83 m** Conglomerate interbedded with medium-grained sandstone, antidunes

**1.83 m** Sandstone, fine-grained, red and white striping, recessive with a heavily weathered appearance, poorly consolidated, planar bedding

**3.96 m** Sandstone, fine to medium-grained, resistant/ledge forming, antidunes: long wavelength and low amplitude, 1 channel story

**6.1 m** Sandstone interbedded with silty mudstone, meter scale sandstone sheets, planar bedding

**5.49 m** mudstone/siltstone

**Continuation of previously studied strata** (Lamb 2019 & Walker 2020)

Facies designations and field observations are taken from the aforementioned research.

**Resumption of newly introduced data:** Base of Cooper Canyon Fm.

**Contact** – gradational with underlying Trujillo Ss.

**1.43 m** Mudstone, minor sand and silt, thinly laminated, wavy lamination; Sandstone, fine-grained, cm scale lenses encased in the mudstone

**0.61 m** Sandstone, fine-grained, ripple cross-lamination

**40 cm** Mudstone, minor silt, laminated

**0.76 m** Sandstone, fine-grained, ripple cross-lamination

**1.83 m** Mudstone/siltstone, laminated, varies in thickness - laterally pinches out

**1.22 m** Sandstone, fine-grained, ripple cross-lamination, dune cross-sets in the middle of sandstone body

Laterally – up the road – sandstone body breaks into at least 3 distinct smaller sandstone sheets encased in laminated mudstone

**4.27 m** Mudstone/siltstone, laminated, cm scale fine-grained sandstone sheets

Laterally – up the road – sandstone sheets amalgamate into 1 m of sandstone, ripple cross-lamination, dune cross-sets, planar lamination.

**1.52 m** Conglomerate, bedded

**1.83 m** Fine-grained sandstone, white, planar bedding, antidunes preserved as hummocks

Laterally – thins and pinches out into silty mudstone

**1.22 m** Mudstone/siltstone, cm scale sandstone sheets

**0.98 m** Sandstone, fine-grained, white, antidunes preserved as hummocks

**2.13 m** Sandstone (same facies as prior), 2 bodies each about 1 m thick, 0.3 m of mudstone in between them

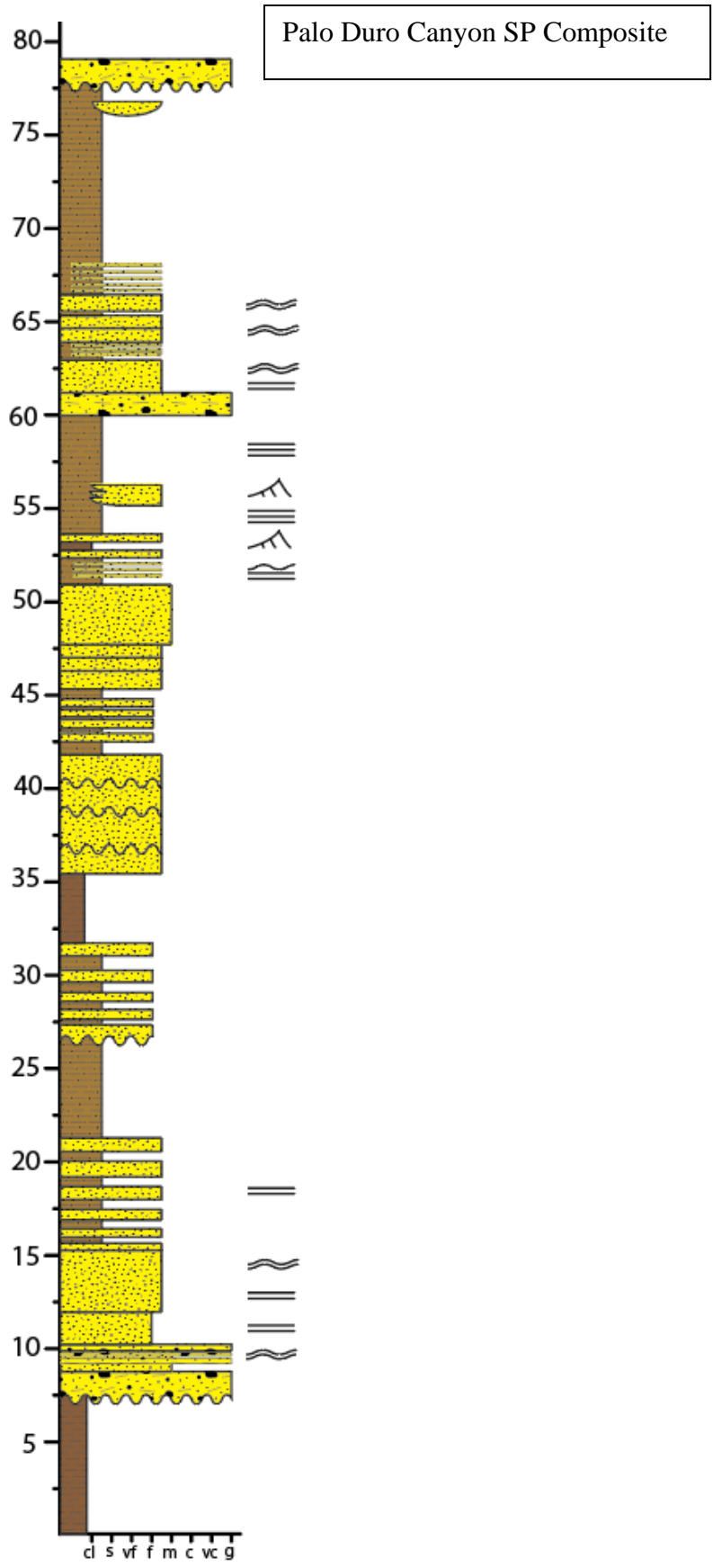
**2.13 m** Mudstone, laminated, cm scale sandstone sheets

**10.97 m** Mudstone, minor silt, slope forming, soil/cover.

Laterally – 0.61 m thick sandstone and conglomerate interbeds within the top 2 m of the unit

**Contact** – sharp, erosional with the overlying Ogallala Fm.

**Top of section**





Cooper Canyon Fm

## **Route 66**

(San Jon Composite 1 of 2)

**35° 9' 27" N**

**103° 28' 11" W**

This section and Hwy 469 near San Jon were combined to build the composite San Jon section.

**Base of section:** Uppermost Tecovas Fm.

**0.91 m** Silty mudstone

**Contact** – sharp, erosional with overlying Trujillo Ss.

The Trujillo Ss. here is a **7.1 m** stack of amalgamated channel sandstones buff to white in color. It is broken into units by differences in internal sedimentary structures

**2.44 m** Sandstone, fine-grained, planar bedding, dune cross-sets

**Paleocurrent measurements:**

Dunes: 282°, 287°, 279°, 282°, 290°

**2.44 m** Sandstone, fine-grained, antidunes preserved as hummocks, low angle dipping strata, planar bedding

**Paleocurrent measurements:**

Antidune crests: 210°/30°, 226°/46°, 231°/51°, 227°/47°, 217°/37°

**1.22 m** Sandstone, fine-grained, ripple cross-lamination

**1 m** Sandstone, fine-grained, 10's of cm scale beds, interbedded with silty mudstone, ripple cross-lamination

**Contact** – gradational with overlying Cooper Canyon Fm.

**4.33 m** Mudstone, minor silt, red, blocky weathering texture, peds, slickensides, bioturbated

**2.71 m** Bottom ½ is conglomerate, red and gray; Top ½ is sandstone, fine-grained, red, dune cross-sets

**Paleocurrent measurements:**

Dunes: 336°, 315°, 309°, 317°

Cover – modern soil

**Top of section**

## **NM Hwy 469**

(San Jon Composite 2 of 2)

**34° 59' 40" N**

**103° 20' 54" W**

**Base of section:** Redonda Fm.

**0.52 m** Muddy siltstone, red, fissile with occasional indurated beds, weakly laminated

at top – nodular, cm scale bed

**1.07 m** Claystone, weakly laminated, weakly effervescent

at top – Siltstone, gray, well-indurated, calcareous, mudcracks on bedding surfaces.

**1.83 m** Mudstone, minor silt and sand, fines upwards into claystone

at base – weakly laminated

top ½ – Mud chips/balls encased, flame structures

at top – Siltstone, gray, well-indurated, calcareous

**1.43 m** Same fining-upwards sequence as previous unit, which includes the top siltstone bed, lamination in mudstone improves upwards

**1.1 m** Same fining-upwards sequence – calcareous siltstone bed at top is interbedded with mudstone

**2.41 m** Same fining-upwards sequence – calcareous siltstone is thicker than prior sequences, 10's of cm thick, planar lamination and ripple cross-lamination, pinches and thickens laterally

**1.52 m** Same fining-upwards sequence – mudstone is remains weakly laminated further up in sequence than in prior sequences

**1.25 m** Same fining-upwards sequence – all mudstone is well-laminated throughout sequence

**1.74 m** Same fining-upwards sequence – sequence starts with less silt content than prior sequences, mudstone is well-laminated throughout sequence

**1.28 m** Same fining-upwards sequence

**0.91 m** Same fining-upwards sequence – topmost calcareous siltstone is 10's of cm thick

**0.82 m** Claystone, laminated to weakly laminated, glossy appearance, mud balls – green and gray.

At top – sandstone, very fine-grained, planar lamination

**43 cm** Siltstone, gray, 5 amalgamated beds, effervescent

**7.6 cm** Mudstone with minor silt, laminated

**18 cm** Sandstone, fine-grained, pale red, planar lamination



**15 cm** Sandstone fine-grained, planar lamination, interbedded with cm-scale silty mudstone

**30 cm** Sandstone, fine-grained, pale red, ripple cross-lamination, well-indurated

**.61 m** Sandstone, fine-grained, red, convolute beds, laterally the convolute beds become planar lamination

**5.1 cm** Mudstone with minor silt

**1.92 m** Sandstone, fine-grained, red, tabular beds, beds pinch and swell from cm scale to 10's of cm scale, planar lamination, ripple cross-lamination

**15 m** cover – modern soil, vegetation

**1.95 m** Sandstone, very fine-grained, red/brown externally, yellow/brown internally, planar bedding

**4.51 m** Claystone, purple, well-laminated, slickensides, glossy appearance, peds

**15.2 cm** Sandstone, fine-grained, gray/white, ripple cross-lamination

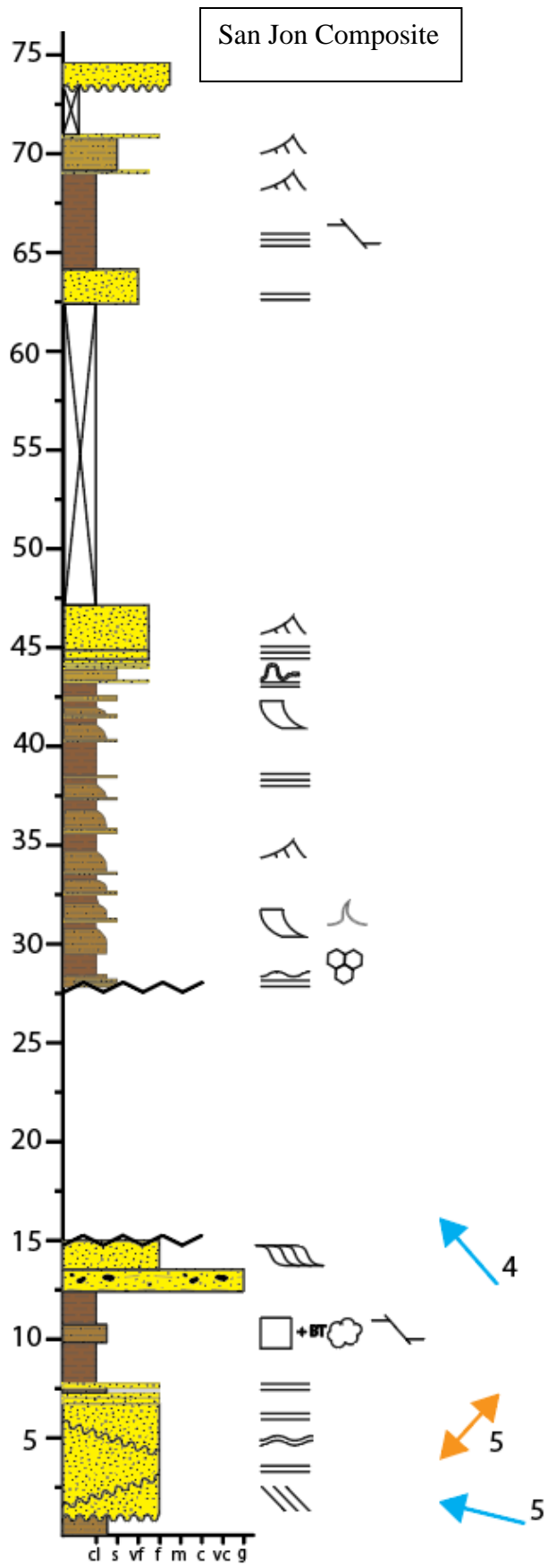
**1.86 m** Siltstone with minor mud sediments, gray/white, laminated

**15.2 cm** Sandstone, fine-grained, gray/white, ripple cross-lamination

**2.8 m** Cover – modern soil, vegetation

**Contact** - sharp and erosional with the overlying Jurassic Exeter

**Top of section**





Cooper Canyon Fm

## **NM Hwy 104**

(Conchas/Newkirk 1 of 2)

**35° 17' 52" N**

**104° 17' 30" W**

Due to the nature of the exposure at this location, this section is logged in several sections from either side of the road cut. The composite section for this location was assembled using the following sections (A-H) that were logged on either the north wall (N wall) or south wall (S wall) of the exposure. Many of these sections start with a note to contextualize stratigraphic location by describing any repeat strata from the prior section.

**Base of section:** Tecovas Fm.

### **Section A – N wall**

**0.91 m** Sandstone, fine-grained, red, micaceous, ripple cross-lamination and planar lamination

**2.26 m** Silty mudstone, red, proportion of silt varies throughout unit, planar lamination – varies from well-laminated to weakly-laminated.

Top **0.5 m** coarsens into sandy siltstone directly beneath the overlying sandstone body

**1.24 m** Sandstone, very fine-grained, red, well-indurated, ripple cross-lamination, tool marks on bedding surfaces, laterally continuous on meter scale. Present on both N and S walls of roadcut

**3.08 m** Muddy siltstone, red

Bottom **1 m**, planar lamination that varies in strength.

Top **2 m** fractured, contorted bedding, intraformational rip-up clasts and mud balls

Top **1 m** rooting traces

**38 cm** Conglomerate, scour surface at base of sandstone

**3.17 m** Sandstone, fine-grained, yellow-gray-buff, dune cross-sets, bars, no distinct channel-form geometries.

#### **Paleocurrent measurements:**

Dunes: 258° 315° 311° 251° 248° 260° 316° 304° 307° 293° 303° 308° 288° 276° 323°  
332° 299°

**6.04 m** Sandstone, fine-grained, yellow-gray-buff, 8 thin sheets each up to 1 meter in thickness, low angle dipping, planar bedding in the bottom half of the sheets, antidunes preserved as hummocks in the upper half of the sheets, sheets are interbedded muddy siltstone—cm scale, sandstone sheets occasionally amalgamate laterally

**1.95 m** Sandstone, fine-grained, yellow-gray-buff

**1.37 m** Conglomerate, lateral accretion surfaces, not laterally continuous

**1.13 m** Sandstone, fine-grained, yellow-gray-buff

### **Section B – N wall**

This section starts with the topmost **2.04 m** of the **3.17 m** ‘dune cross-set sandstone’ from **Section A**

**0.78 m** Sandstone, fine-grained, yellow-gray-buff, dune cross-sets (see Section A)

**1.26 m** Sandstone, fine-grained, yellow-gray-buff, sigmoidal dunes at base, planar bedding and lamination at top

**2.87 m** Sandstone, fine-grained, yellow-gray-buff, 8 sheets up to 1 meter thick, antidunes preserved as hummocks, sheets/beds thin upwards from m scale to cm scale

**1.49 m** Siltstone, yellow-gray, no obvious bedding or structure, poorly consolidated

**0.67 m** Sandstone, fine-grained, gray-yellow-buff

### **Section C – N wall**

This section starts directly on top of the **1.49 m** silt from **Section B**

**Contact** – sharp, erosional with the overlying Trujillo Ss.

**1.1 m** Sandstone, fine-grained, minor gravel lenses, not laterally continuous, antidunes preserved as hummocks

**5.33 m** Sandstone, fine to medium-grained, yellow-buff, micacious, dune cross-sets, lateral accretion surfaces, planar bedding at top

#### **Paleocurrent measurements:**

Dunes: 134° 108° 164° 112° 142° 127° 143° 154°

### **Section D – N wall**

This section starts at the planar bedding from the top **1.5 m** of the top part of **Section C**

**1.16 m** Sandstone, fine to medium-grained, yellow-buff, micacious, planar bedding

**0.73 m** Conglomerate

**1.89 m** Sandstone, fine-grained, micacious, yellow-gray-buff, sigmoidal dune cross-sets, planar bedding on top, scoured by overlying sandstone

#### **Paleocurrent measurements:**

Bottom ½ of this unit – sigmoidal dunes: 288° 302° 296° 297° 321° 297°

**2.23 m** Sandstone, fine-grained, micacious, gray-yellow-buff, sigmoidal dune cross-sets, planar bedding on top

### **Section E1&E2 – S wall**

This section is broken into 2 parts rather than 2 separate sections because of their close proximity to each other. **E1** starts at the planar laminations from the top of **Section D**

- **E1**

**1.4 m** Sandstone, fine-grained, yellow-gray-buff, micacious, planar bedding

**1.25 m** Sandstone, fine to medium-grained, interbedded with conglomerate, sandstone contains mud clasts, sandstone beds are up to 0.3 m, conglomerate beds are thinner than sandstone beds

- **E2**

This part of the section is directly lateral to the top of **E1**

**3.66 m** Sandstone, fine-grained, yellow-gray-buff, ripple cross-lamination, dune cross-sets (bottom 2.5 m of section), sigmoidal dunes and planar bedding at top

**Paleocurrent measurements:**

Dunes: 315° 282° 342° 306° 276° 331° 288° 257° 293° 270° 292° 311°

**Section F – S wall**

This section starts above the sandstone at the top of Section **E2**

**42 cm** Silty mudstone, gray, well-laminated, fissile

**1.22 m** Sandstone, fine-grained, channel-form, dune cross-sets, planar bedding

**Paleocurrent measurements:**

Dunes: 286° 284° 299° 302°

**1.55 m** Sandstone, very fine-grained, interbedded with silty mudstone, sandstone beds are up to 0.5 m in thickness, the 4 mudstone beds are cm scale

**Section G – S wall**

This section starts above the interbeds from **Section F**

**0.88 m** Mudstone, red, heavily bioturbated, slicken sides, rooting traces, peds, paleosol horizon developments

**1.62 m** Sandstone, fine-grained, yellow-gray-buff, dune cross-sets, planar bedding

**Section H – S wall**

**0.88 m** Silty mudstone, gray, blocky weathering texture, thin cm-scale discrete sand lenses within the mudstone. Sand lenses—planar bedding

**2.35 m** Sandstone, fine-grained, yellow-gray-buff, antidunes preserved as hummocks, sigmoidal dunes, planar bedding

**Paleocurrent measurements:**

Sigmoidal dunes: 273° 283° 290° 279° 294° 279° 266°

**Section I – S wall**

**45 cm** Sandstone, same unit as the top of **Section H**

**3.2 m** Sandstone sheets, fine to medium-grained, not laterally continuous, encased in conglomerate and gravels, antidunes, planar bedding

Cover – modern soil and vegetation

**Top of section**

## **NM Hwy 156**

(Conchas/Newkirk 2 of 2)

**34° 57' 22" N**

**104° 12' 32" W**

**Base of section:** Redonda Fm.

**1.19 m** Siltstone, red, well-indurated, blocky weathering texture

Top 10 cm of siltstone is white to gray with mottled appearance, reactive to HCl, bioturbated

**1.22 m** Siltstone, red, weakly laminated, blocky weathering texture, poorly consolidated

**39 cm** Sandstone, very fine-grained, red, well-indurated, no organized internal structure

**4.85 m** Siltstone, red, blocky weathering texture, no organized internal structure

**0.73 m** Sandstone, very fine-grained, white and red, sandstone bed coarsens upwards to very coarse-grained at the top, infilled trace fossils/burrows – fill reacts to HCl

**1.89 m** Siltstone, red, blocky weathering texture, no organized internal structure

At top – 0.5 m thick sandstone, coarse-grained, purple to orange, abundant bioturbation and burrows, reactive to HCl

**2.23 m** Claystone, purple, gray mud balls, friable, weakly laminated, coarsens to a silty mudstone by the top of the unit

**0.64 m** Sandstone, very fine-grained, red, top ½ of unit is interbedded with purple mudstone beds on cm scale

**5.35 m** Sandstone, fine-grained, red, this unit is traceable on a valley scale, planar bedding and lamination, not channel-form

**45 cm** Mudstone, purple, weakly laminated, occasional sandstone lenses, fine-grained

**21 cm** Sandstone, medium-grained, gray, dune cross-sets

**0.88 m** Silty mudstone, dark red, weakly laminated

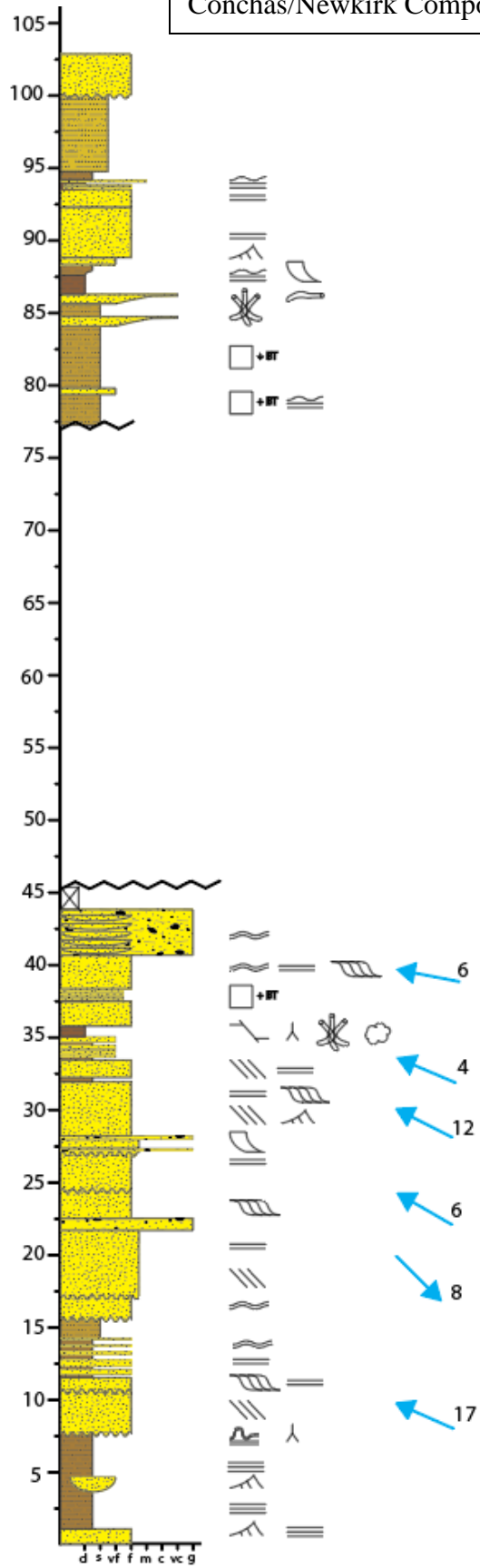
**5.64 m** Sandstone, very fine-grained, minor silt, gray, poorly consolidated, no organized internal structure, faintly reactive to HCl

**Contact** – sharp, erosional with Jurassic Exeter – contact is traceable on valley scale

**3.05 m** Sandstone, fine-grained, buff, iron staining

**Top of section**

Conchas/Newkirk Composite







Tecovas Fm (bottom), Trujillo SS (middle), Cooper Canyon Fm (top)

## Trujillo Hill

35° 30' 50" N  
104° 39' 56" W

The graphic section built from these field notes is a composite which aims to depict the overall character of the section. The notes may contain extraneous information that, while present at the outcrop, failed to fit into a single, representative graphic section.

Base of the section: Tecovas Fm.

### **5.18 m** Muddy siltstone, peds, cutans, blocky weathering texture

Topmost 2.75 m – ½ meter scale coarsening upward sequences – silty mudstone to very coarse-grained sandstone, 3 sequences

### **4.42 m** Siltstone, wavy lamination to planar lamination

First **61 cm** sandstone, fine-grained, ripple cross-lamination, cm scale, continuous and thickens and thins laterally.

Topmost **2.59 m** sandstone, fine-grained, ripple cross-lamination, meter-scale

### **7.62 m** Silty mudstone, blocky weathering texture, no organized internal structure

Near bottom of section approx. 1 meter thick section is weakly laminated

Middle of section – **3 m** discrete sandstone body, fine-grained, weakly ripple cross-lamination

Above sandstone – silty mudstone becomes siltstone

### **2.44 m** Interbedded siltstone and sandstone, sandstones thicken laterally into channel-form bodies

Laterally where the sandstones thicken they amalgamate into a **4.6 m** thick stack of sandstone

**Contact** – sharp, erosional with overlying Trujillo Ss.

### **8.84 m** Sandstone, medium-grained, buff, stack of amalgamated channels, sigmoidal dune cross-sets, planar bedding, dune cross-sets, discrete antidunes preserved as hummocks

#### **Paleocurrent measurements:**

Sigmoidal dunes: 250°

Dunes: 205°

### **9.1 m** Paleosol, minor sand and silt, purple and gray striped

Lateral to **8.8 m** stack of amalgamated sandstones

### **5.79 m** Sandstone, fine to medium-grained, buff, amalgamated stack of sandstones, dune cross-sets, planar bedding, scours the underlying paleosol – stratigraphically equivalent with the **8.8 m** sandstone unit,

**Paleocurrent measurements:**

Dunes: 234°

**4.88 m** Sandstone, medium-grained, ripple cross-lamination, conglomerate interbeds, interbedded with siltstone at the top of unit, friable, weakly planar lamination in mudstones, beds up to 2 meters thick

**7.62 m** Sandstone, fine to medium-grained, stack of amalgamated sandstones, dune cross-sets, transitional dunes, planar bedding and lamination. Discrete antidunes preserved as hummocks

**Paleocurrent measurements:**

Dunes and sigmoidal dunes: 342° 31° 337° 317° 307°

**2.74 m** Sandstone, fine to medium-grained, planar lamination, dunes and transitional dunes

**Paleocurrent measurements:**

Dunes and sigmoidal dunes: 256° 259° 262° 254° 286° 279°

**Contact** – gradational with the overlying Cooper Canyon Fm.

**3 m** Silty mudstone, peds, slickensides, rooting traces, blocky weathering texture

**5.88 m** Sandstone sheets, fine-grained, planar lamination, bottom ½ of unit is amalgamated and the top ½ is interbedded with siltstone. Top ½ ripples and dunes

**9.17 m** Sandstone sheets, fine-grained, interbedded with muddy siltstone, sandstone sheets are on cm scale. Sand sheets contain ripple cross-lamination. Muddy siltstone interbeds are laminated, sometimes weakly

**7.13 m** Silty mudstone, bottom 2/3<sup>rd</sup> is weakly laminated, top 1/3<sup>rd</sup> rooting traces, peds, cutans, slickensides, blocky weathering texture

**4.85 m** Paleosol, 3 calcic beds, calcite nodules, manganese and iron staining, rooting traces, cutans, peds

**3.51 m** Silty mudstone, rooting traces, cutans, slickensides, blocky weathering texture

**11.6 m** Sandstone, fine-grained, dark red, gray/white laminae, ripple cross-lamination, dune cross-sets, sigmoidal dunes, planar bedding, channel-form, basal 6.4 m is amalgamated

**Paleocurrent measurements:**

Dunes and sigmoidal dunes: 263° 254° 259°, 54° 39° 63°

**10 m** Silty mudstone and fine-grained sandstone sheets. Mudstone is well-laminated. Sand bodies were observed from a distance due to inaccessibility—sheets and lobe geometries.

**7.53 m** Mudstone, high clay content, occasional discrete sandstone lenses, fine-grained

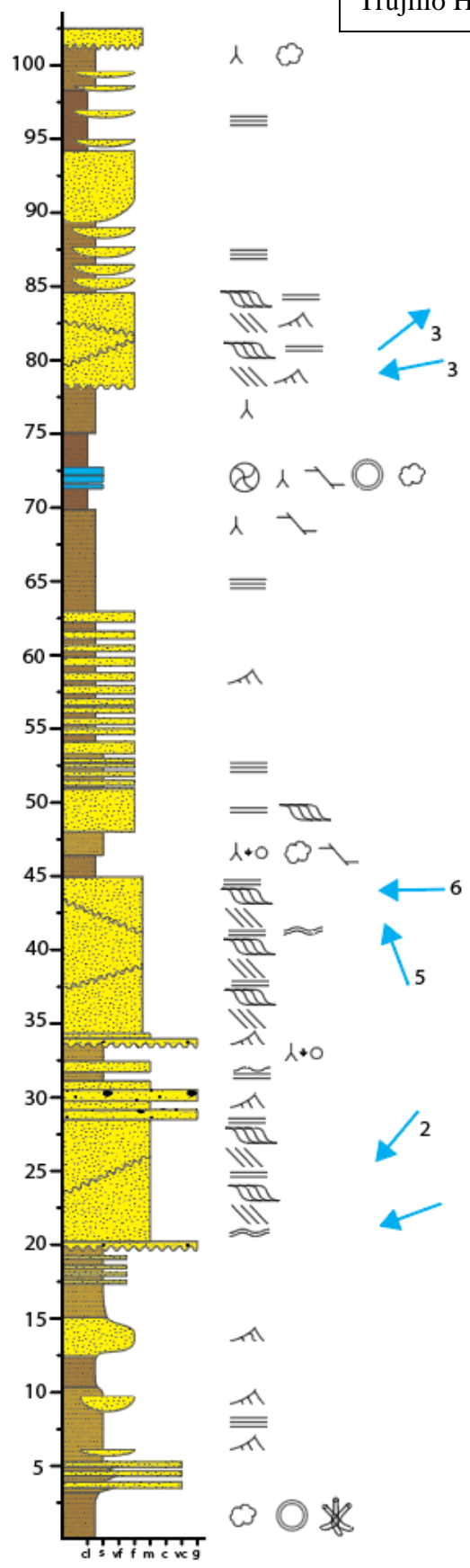
Base of this unit – mudstone is well-laminated

Top of this unit – silty mudstone, root traces, peds, blocky weathering texture

**Contact** – sharp, erosional with Jurassic Exeter

**Top of the section**

Trujillo Hill Composite







Tecovas Fm (bottom), Trujillo SS (middle), Cooper Canyon Fm (top)

## US Hwy 84

35° 30' 55" N

105° 14' 39" W

**Base of section:** Tecovas Fm.

**7.67 m** Siltstone, red, white fractures/laminae, peds, blocky weathering texture, clay content increases toward the top, discrete sandstone lenses, very fine-grained, ripple cross-lamination, occasionally sandstone lenses contain conglomerate interbeds

**3.2 m** Sandstone, fine-grained, red to purple, well-indurated, gray/white laminae, dune cross-sets, ripple cross-lamination, bars, channel-form geometry, bedding thins upwards and planar bedding at the top

**Paleocurrent measurements:**

Dunes: 24°, 356°, 32°, 355°, 349°

**0.66 m** Siltstone, discrete sandstone lenses, fine-grained

**1.58 m** Cover – vegetation and modern soil

**0.94 m** Sandstone, fine-grained, ripple cross-lamination, interbedded with conglomerate

**7.99 m** Silty mudstone, deep red and purple, peds, blocky weathering texture, occasional lenses of sandstone and conglomerate. At top, clay content increases and soil horizons develop

**Contact** – sharp, erosional with the Trujillo Ss.

**6.58 m** Sandstone, fine-grained, light tan, well-indurated, stack of amalgamated sandstones with channel-form geometry, sigmoidal dune cross-sets, discrete antidunes preserved as hummocks, planar bedding

**Paleocurrent measurements from bottom half of channel stack**

Sigmoidal dunes: 163°, 176°, 197°, 234° 175°

**7.68 m** Mudstone, clay-rich, purple, peds, blocky weathering texture, very occasional sand sheets, very fine-grained, ripple cross-lamination. At top of mudstone, paleosol horizons develop and a higher percentage of clay is present.

**9.2 m** Sandstone, fine to medium-grained, light tan, stack of amalgamated sandstones with channel-form geometry, dune cross-sets, sigmoidal dune cross-sets, planar bedding, discrete antidunes preserved as hummocks, gravel bar

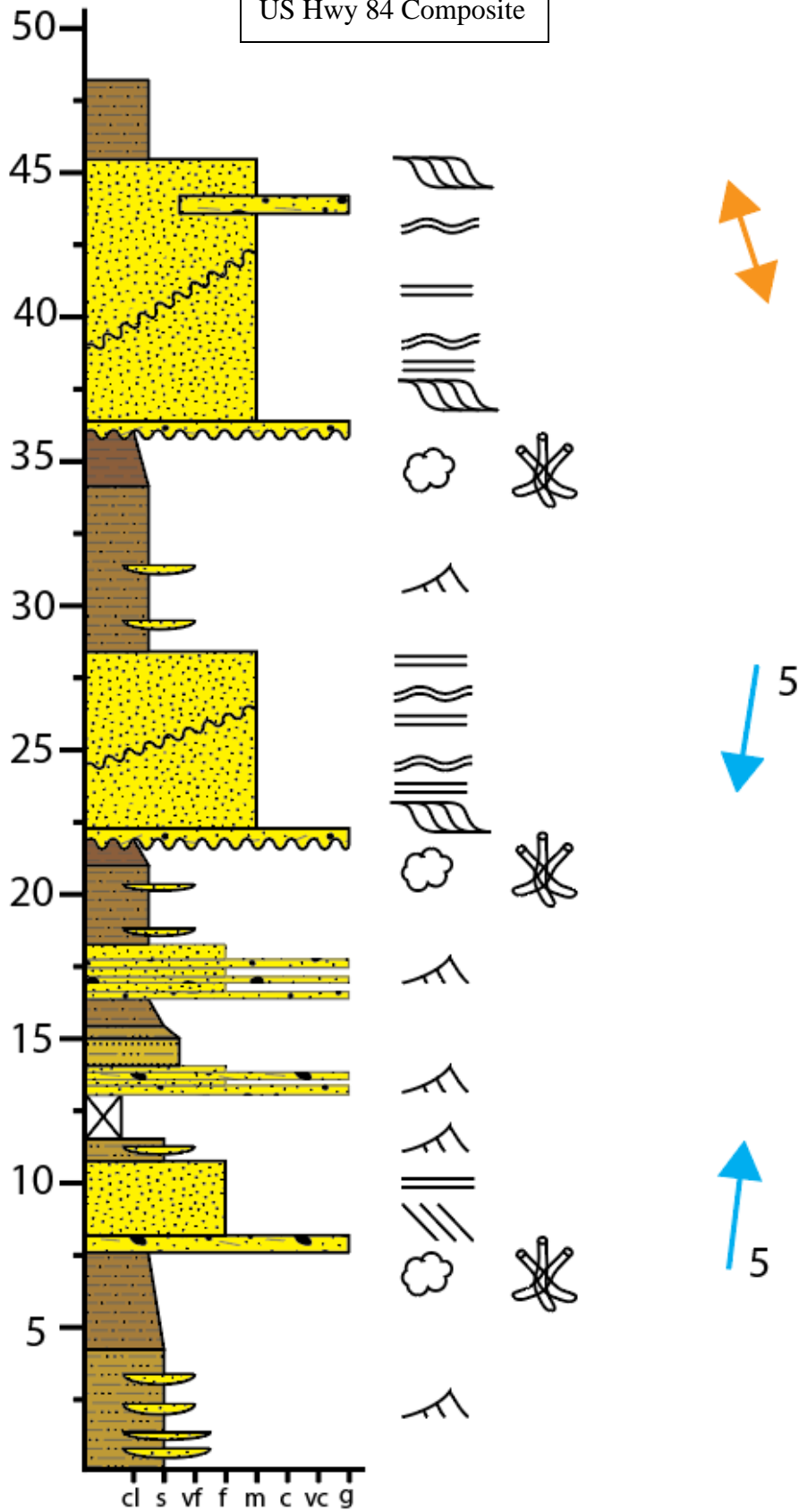
**Paleocurrent measurements:**

Antidune crests: 162°/342°

**2.5 m** muddy siltstone

Top of Section

US Hwy 84 Composite







Tecovas Fm (below), Trujillo SS (above)





## **I-25**

**35° 30' 44" N**

**105° 15' 22" W**

This section is not used for research purposes in this thesis because it lacks stratigraphic context other than being Triassic in age. The location where this section was measured is structurally complex, and all that is known stratigraphically is that it overlies the Permian-aged Bernal Formation. It is either a repeat section of the Trujillo Sandstone or it is stratigraphically below the Trujillo Sandstone.

**Base of the section:** Unknown

Beds dipping 30° NE, Strike: 341°

**0.91 m** Sandstone, fine-grained, ripple cross-lamination, tan and gray, occasional pebbles

**0.91 m** Mudstone, red

**2.4 m** Conglomerate, fossilized wood, boulder-sized clasts of: conglomerates, limestones, and other extraformational material—limestone boulders – brachiopods

**4.99 m** Sandstone, fine-grained, tan, occasional conglomerate lenses, planar bedding and lamination, antidunal hummocks

**2.4 m** Silty mudstone, beige

**2.23 m** Sandstone, fine-grained, tan with iron staining, fossilized tree and smaller wood, beds are on a 10's of cm scale, planar bedding and lamination, antidunal hummocks

**1.89 m** Sandstone, fine-grained, dark tan, planar bedding and lamination, antidunal hummocks, slicken sides

**4.57 m** Silty mudstone, beige

**3.2 m** Sandstone, fine-grained, tan and gray, planar bedding and lamination, antidunal hummocks

**48 cm** Silt, laminated

**2.26 m** Sandstone, fine-grained, dark tan to gray, occasionally interbedded with conglomerates – antidunes, fossilized wood

**1.83 m** Sandstone, coarse-grained, tan, thinly bedded, planar bedding and lamination

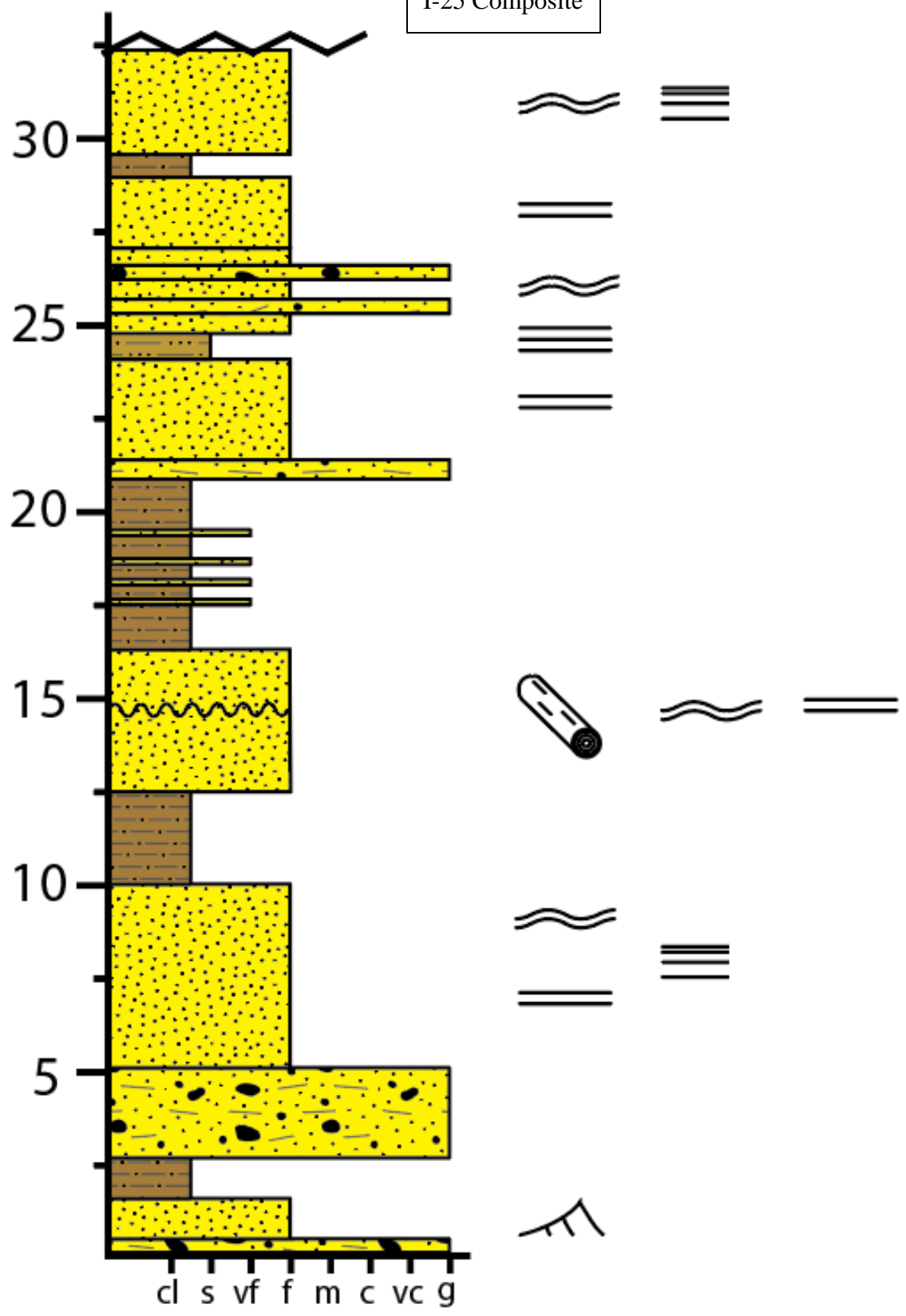
**0.67 m** Mudstone

**2.87 m** Sandstone, fine-grained, tan to gray, thinly bedded, planar bedding and lamination, antidunal hummocks

Cover – modern soil

**Top of section**

I-25 Composite





Trujillo SS

## **Red Rock Ranch**

**36° 58' 22" N**

**103° 24' 37" W**

This section is not used for correlation purposes in this thesis because it is off-trend from both the E-W cross-section as well as the N-S cross-section.

**Base of section:** Baldy Hill Fm.

**2.41 m** Sandstone, very fine-grained, planar, stacked sequences in bedding at **61 cm** thick each

**0.88 m** Cover – modern soil and rockfall

**0.91 m** Sandstone, fine-grained, ripple cross-lamination

**0.76 m** Conglomerate, thinly bedded towards top, normal grading, purple matrix – matrix reacts to HCl. 1.5cm wide clasts at most large, thin very fine-grained sandstone laminations/lenses throughout.

**2.13 m** Sandstone, very fine-grained, red/purple, ripple cross-lamination, planar lamination, very thinly bedded (1-5 cm) bioturbation at the top

**2.59 m** Sandstone, very fine-grained, purple and red, heavily bioturbated, tops of beds have filled in burrows, **61 cm** thick bed of burrows at the top of unit. Bedding size increases up section.

**3 m** Cover - rockfall and modern soil

**61 cm** Silty mudstone, purple, rooting traces

**46 cm** Sandstone, very fine-grained, linear staining – bioturbation/burrow trace fossils, occasionally there is wavy to p laminated, mostly lacks structure.

**7 cm** Sandstone, very coarse-grained, very poorly sorted, quartz and feldspars clasts

**61 cm** Sandstone, very fine-grained, red, heavily bioturbated – cicada burrows, lenses of underlying very coarse sandstone on a cm scale interval, planar lamination and ripple cross-lamination where bioturbation has not destroyed internal structure

**Contact** – Travesser Fm.

**3.66 m** Sandstone, very fine-grained, red, minor silt content, heavily bioturbated, occasional wavy lamination, calcite cement, organized network of burrows

**6.1 m** Cover – boulder field – rockfall

**30 cm** Silty mudstone

**30 cm** Conglomerate interbedded with sandstone, very fine-grained

**1.22 m** Silty mudstone interbedded with cm-scale sandstone, very fine-grained, planar lamination and ripple cross-lamination

**10 cm** Sandstone, very fine-grained, bioturbation

**2.44 m** Cover – rockfall

**1.98 m** Sandstone, fine to very fine-grained, bioturbated throughout – basal bioturbation has white infill, bedding size increases from cm scale to 10's of cm scale, areas without bioturbation have planar bedding and lamination, and antidunal hummocks

**38 cm** Sandstone, very fine-grained, red, thinly bedded, bioturbated, wavy lamination

**1.1 m** Sandstone, very fine-grained, red, planar lamination

**15 cm** Sandy silt, recessive, planar lamination

**0.61 m** Sandstone, very fine-grained, red, bioturbated rare planar lamination and ripple cross-lamination

**30 cm** Sandy silt, lacks organized internal structure

**1.22 m** Sandstone, fine-grained, red, planar lamination and wavy lamination, bioturbation increases upwards through the unit

**46 cm** Siltstone, thinly bedded, white stains

**1.83 m** Cover – rockfall

**0.61 m** Sandstone, very fine-grained, red, heavily bioturbated

**0.61 m** Sandstone, very fine-grained, red, minor silt content, recessive, pinch and thickening structures, antidunal hummocks

**4.57 m** Sandstone, very fine-grained, red, bedding size decreases upwards from 10's of cm scale to cm scale, slight bioturbation, antidunes and antidunal hummocks – thickest part of hummock is 1 cm

**1.83 m** Sandstone, very fine-grained, red, heavily bioturbated

**1.22 m** Cover – rockfall

**1.22 m** Sandstone, very fine-grained, red, minor silt, bedding is 10's of cm scale, abundant bioturbation,

**7 cm** Conglomerate

**6.1 m** Sandstone, very fine-grained, red, well-indurated, abundant bioturbation throughout – basal bioturbation is infilled with lighter colored sediment, antidunes and antidunal hummocks

**46 cm** Sandstone, very fine-grained, conglomerate lenses, bioturbated

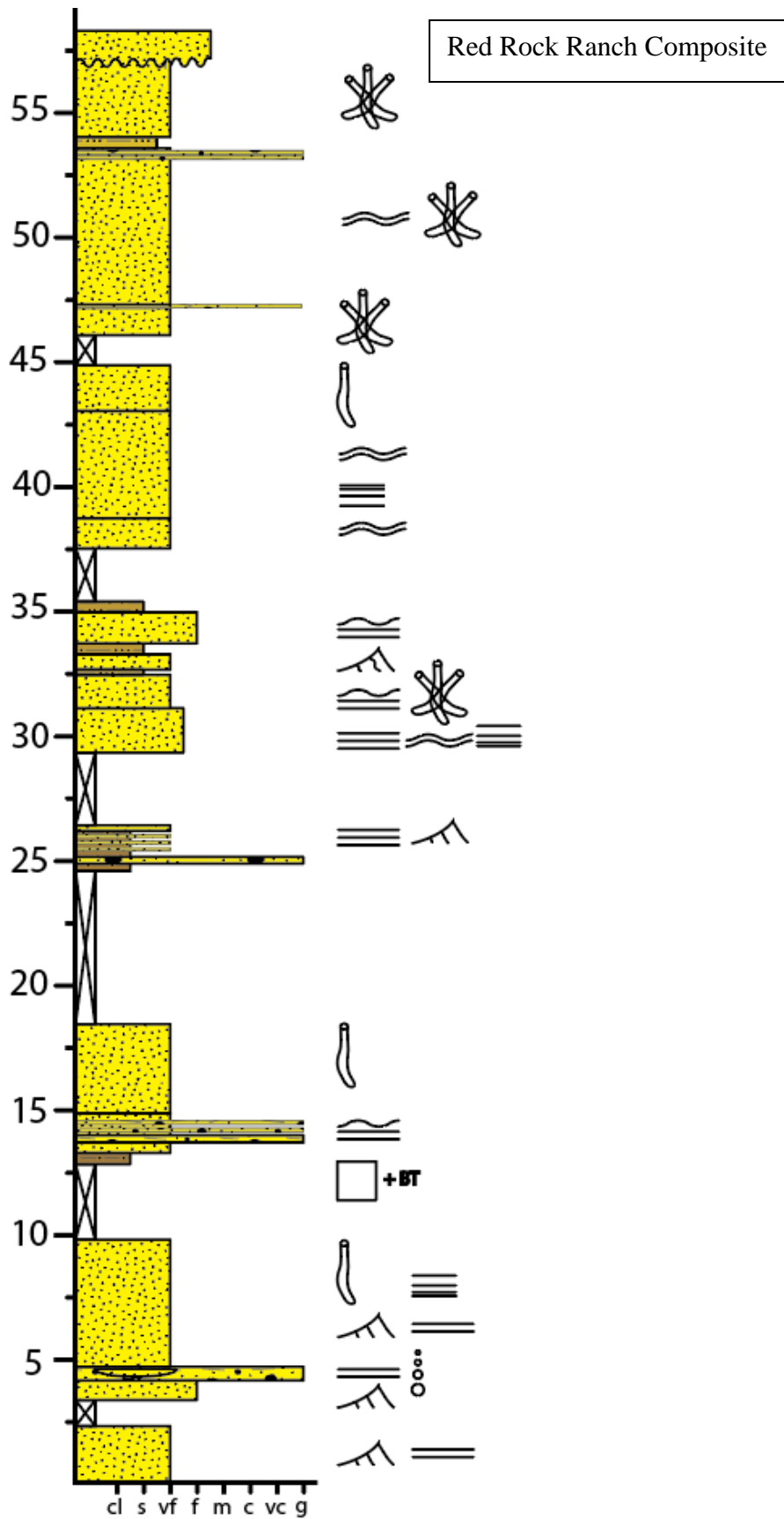
**46 cm** Siltstone, recessive but well-consolidated

**3.35 m** Sandstone, very fine-grained, red, well-indurated, heavily bioturbated, difficult to interpret internal structure due to the rind/desert varnish on the unit

**Contact** – sharp, erosional with the Jurassic Exeter

Jurassic Exeter Sandstone - fine-grained, white/tan, large cross-sets, this sandstone infills directly into burrows at the contact with the Triassic

**Top of section**







Travesser Fm (above) Baldy Hill Fm (below)





## References

- Adams, J.E., 1929, Triassic of West Texas: American Association of Petroleum Geologists Bulletin, v. 13, pp. 1045-1055.
- Alexander, J., and Fielding, C. R., 1997, Gravel Antidunes in the Tropical Burdekin River, Queensland, Australia. *Sedimentology*, vol. 44, no. 2, pp. 327 - 337
- Alexander, J., 2008, Bedforms in Froude-supercritical flow, in marine and river dune dynamics proceedings, pp. 1-5
- Alexander, J., et al., 2001, Bedforms and Associated Sedimentary Structures Formed under Supercritical Water Flows over Aggrading Sand Beds. *Sedimentology*, vol. 48, no. 1, pp. 133-152,
- Alexander, J., Fielding, C. R., and Pocock, G. D., 1999, Flood Behaviour of the Burdekin River, Tropical North Queensland, Australia. Geological Society, London, Special Publications 163.1, pp. 27-40.
- Allen, J.R.L., 1978, Studies in fluvial sedimentation: An exploratory quantitative model for the architecture of avulsion-controlled alluvial suites: *Sedimentary Geology*, v. 21, pp. 129-147
- Allen, J.R.L., 1984, Sedimentary structures: their character and physical basis. *Developments in Sedimentology*, 30. Elsevier, Amsterdam (663 pp.).
- Atanassov, M. N., 2002, Two new archosaur reptiles from the late Triassic of Texas. Ph.D dissertation, Texas Tech University, Lubbock, Texas, 352 p.
- Baines, E.R.C., Lague, D., and Kermarrec, J.J., 2018, Supercritical river terraces generated by hydraulic and geomorphic interactions. *Geology*, 46, 499-502.
- Baldwin, B., and Muehlberger, W. R., 1959, Geologic studies of Union County, New Mexico: New Mexico Bureau of Mines and Mineral Resources Bulletin 63, 171 p.
- Belmonte, A. M. C., and Beltran, F. S., 2001, Flood events in Mediterranean ephemeral streams (ramblas) in Valencia region. Spain. *Catena* 45, pp. 229-249.
- Bezucha, B. B., 2022, Geochronologic Connections between the Chinle Formation and Dockum Group [M.S. thesis]: Fort Worth, Texas Christian University, 110 p.
- Bolt, J. R., and Chatterjee, S., 2000, A new temnospondyl amphibian from the Late Triassic of Texas. *Journal of Paleontology* 74(4), pp. 670-683
- Bridge, J.S., and Leeder, M.R., 1979, A simulation model of alluvial stratigraphy: *Sedimentology*, v. 26, pp. 617-644
- Brown, A., 2016, Dockum Group Revisited: Deposition and Tectonic Significance: Search and Discovery. #51257
- Bryant, M., Falk, P., and Paola, C., 1995, Experimental study of avulsion frequency and rate of deposition: *Geology*, v. 23, pp. 365-368

- Bullard, F. M., 1928, Lower Cretaceous of western Oklahoma: Oklahoma Geological Survey Bulletin 47, 116 p.
- Carling, P.A. and Shvidchenko, A.B., 2002, A consideration of the dune-antidune transition in fine gravel. *Sedimentology* 49, 1269-1282.
- Cartigny, M.J.B., 2012, Morphodynamics of supercritical high-density turbidity currents. *Utrecht Studies in Earth Sciences*, 10, 153 pp.
- Cartigny, M.J.B., et al., 2011, "A Comparative Study of Sediment Waves and Cyclic Steps Based on Geometries, Internal Structures and Numerical Modeling." *Marine Geology*, vol. 280, no. 1-4, pp. 40-56.
- Cartigny, M. J.B., et al., 2013, "Morphodynamics and Sedimentary Structures of Bedforms under Supercritical-Flow Conditions: New Insights from Flume Experiments." *Sedimentology*, vol. 61, no. 3, pp. 712-748.
- Cather, S. M., Zeigler, K. E., Mack, G. H., & Kelley, S. A., 2013, Toward standardization of phanerozoic stratigraphic nomenclature in New Mexico: *Rocky Mountain Geology*, v. 48, iss. 2, p. 101-124.
- Chakraborty, C., Bose, P. K., 1992, Ripple/dune to upper stage plane bed transition: some observations from the ancient record. *Geol. J.* 27, 349-359
- Chatterjee, S., 1983, An ictidosaur fossil from North America. *Science* 220, pp. 1151-1153.
- Chatterjee, S., 1984, A new ornithischian dinosaur from the Triassic of North America. *Naturwissenschaften* 71, pp. 630-631.
- Chatterjee, S., 1985, Postosuchus, a new thecodontian reptile from the Triassic of Texas, and the origin of tyrannosaurs. *Philosophical Transactions of the Royal Society of London B* 309, pp. 395-460.
- Chatterjee, S., 1986, The Late Triassic Dockum vertebrates: Their stratigraphic and paleobiogeographic significance, *in* Padian, K., ed., *The beginning of the age of dinosaurs: Faunal change across the Triassic-Jurassic boundary*: Cambridge, United Kingdom, Cambridge University Press, pp. 139-150.
- Cigizoglu, H. K., Adamson, P. T., and Metcalfe, A. V., 2002, Bivariate stochastic modeling of ephemeral streamflow. *Hydrological Processes* 16, pp. 1451-1465.
- Colombera, L., Mountney, N.P., and McCaffrey, W.D., 2015, A meta-study of relationships between fluvial channel-body stacking pattern and aggradation rate: Implications for sequence stratigraphy: *Geology*, v. 43, pp. 283-286
- Cummins, W.F., 1890, The Permian of Texas and its overlying beds: *Geological Survey of Texas Annual Report*, v. 1, pp. 185-200.
- Cummins, W.F., 1892, Report on the geography, topography, and geology of the Llano Estacado or staked plains, with some notes on the geology of the country west of the plains, *in* *Third annual report of the Geological Survey of Texas: Geological Survey of Texas Annual Report*, v. 3, pp. 127-223.

- Davidow-Henry, B. 1987, New metoposaurs from the southwestern United States and their phylogenetic relationships. M.S. thesis, Texas Tech University, Lubbock, Texas, 75 p.
- Davidow-Henry, B., 1989, Small metoposaurid amphibians from the Triassic of western North America and their significance; pp. 278-292 in S. G. Lucas and A. P. Hunt (eds.), Dawn of the Age of Dinosaurs in the American Southwest. New Mexico Museum of Natural History, Albuquerque, New Mexico.
- Darton, N. H., 1928, "Red beds" and associated formations in New Mexico: United States Geological Survey Bulletin 794, 356 p.
- Dickinson, W. R., 1981, Plate tectonic evolution of the southern Cordillera: Arizona Geological Society Digest, v.14, p.113-135.
- Dickinson, W. R., and Gehrels, G. E., 2008, U-PB ages of detrital zircons in relation to paleogeography: Triassic paleodrainage networks and sediment dispersal across southwest Laurentia: *Journal of Sedimentary Research*, v. 78, pp. 745-764.
- Dick, G. S., Anderson, R. S., and Sampson, D. E., 1997, Controls on flash flood magnitude and hydrograph shape, Upper Blue Hills badlands, Utah. *Geology* 25, pp. 45-48.
- Dickinson, W. R., Gehrels, G. E., Stern, R. J., 2010, Late Triassic Texas uplift preceding Jurassic opening of the Gulf of Mexico: Evidence from U-Pb ages of detrital zircons: *Geosphere*, v. 6, no. 5, pp. 641-662.
- Dobrovolsky, R., Summerson, C. H., and Bates, R. L., 1946, Geology of northwestern Quay County, New Mexico: U.S. Geological Survey Oil and Gas Investigations Map OM-62, scale 1:63,360, 2 sheets.
- Drake, N. F., 1892, Stratigraphy of the Triassic formation of northwest Texas: Texas Geological Survey Annual Report 3, pp. 225-247.
- Edler, A., 1999, Late Triassic dicynodonts: their anatomy, relationships, and paleobiogeography. M.S. thesis, Texas Tech University, Lubbock, Texas, 91 pp.
- Elder R. L., 1978, Paleontology and paleoecology of the Dockum Group, Upper Triassic, Howard County, Texas; M.A. thesis, University of Texas, Austin
- Fielding, C. R., 2006, Upper Flow Regime Sheets, Lenses and Scour Fills: Extending the Range of Architectural Elements for Fluvial Sediment Bodies. *Sedimentary Geology*, vol. 190, no. 1-4, pp. 227-240.
- Fielding, C.R., Webb, J.A., 1996. Facies and cyclicity of the Late Permian Bainmedart Coal Measures in the Northern Prince Charles Mountains, MacRobertson Land, Antarctica. *Sedimentology* 43, pp. 295-322.
- Fielding, C. R., et al., 2009, Facies Model for Fluvial Systems in the Seasonal Tropics and Subtropics. *Geology*, vol. 37, no. 7, pp. 623-626.
- Fielding, C. R., et al., 2018, The Role of Discharge Variability in the Formation and Preservation of Alluvial Sediment Bodies. *Sedimentary Geology*, vol. 365, pp. 1-20.
- Frehler, A. P., 1987, Sedimentology, fluvial paleohydrology, and paleogeomorphology of the

- Dockum Formation (Triassic), West Texas. M. S. thesis, Texas Tech University, Lubbock, Texas, 198 p.
- Froude, M. J., et al., 2017, Interpreting Flash Flood Paleoflow Parameters from Antidunes and Gravel Lenses: An Example from Montserrat, West Indies, *Sedimentology*, vol. 64, no. 7, pp. 1817-1845.
- Gilbert, G.K., 1914, The transportation of debris by running water. U. S. Geol. Surv. Prof.Pap. 86, pp. 1–263.
- Gould, C. N., 1907, The geology and water resources of the eastern portion of the Panhandle of Texas: United States Geological Survey Water Supply Paper 191, pp. 1-70.
- Granata, G. E., 1981, Regional sedimentation of the Late Triassic Dockum Group, west Texas and eastern New Mexico [M.A. thesis]: Austin, University of Texas, 199 p.
- Green, F. E. 1954, The Triassic Dockum deposits of northwestern Texas. Ph.D dissertation, Texas Tech University, Lubbock, Texas, 196 p.
- Griggs, R. L., and Read, C. B., 1959, Revisions in stratigraphic nomenclature in Tucumcari–Sabinoso area, northeastern New Mexico: American Association of Petroleum Geologists Bulletin, v. 43, pp. 2003–2007.
- Hansford et al., 2020, Global quantitative analyses of river discharge variability and hydrograph shape with respect to climate types. *Earth-Science Reviews*, v. 200.
- Hassan, M. A., 1990, Observations of desert flood bores. *Earth Surface Processes and Landforms* 15, pp. 481-485.
- Heckert, A. B., and Lucas, S. G., 2015, Triassic vertebrate paleontology in New Mexico, *in* Lucas, S. G., and Sullivan, R. M., eds., *Fossil vertebrates in New Mexico*: New Mexico Museum of Natural History and Science, Bulletin 68, pp. 77-95.
- Heller, P.L., and Paola, C., 1996, Downstream changes in alluvial architecture: An exploration of controls of channel-stacking patterns: *Journal of Sedimentary Research*, v. 66, pp. 297-306
- Hester, P. M., 1988, Depositional environments of a Late Triassic lake, east-central New Mexico [M.S. thesis]: Albuquerque, University of New Mexico, 152 p.
- Hester, P. M., and Lucas, S. G., 2001, Lacustrine depositional environments of the Upper Triassic Redonda Formation, east-central New Mexico, *in* Lucas, S. G., Ulmer-Scholle, D., eds., *Geology of Llano Estacado: New Mexico Geological Society 52<sup>nd</sup> Annual Fall Field Conference Guidebook*, 340 p.
- Houle, M., and Mueller, B., 2004, A new occurrence of *Buettneria bakeri* (Temnospondyli: Metoposauridae) from the Norian (Cooper Canyon Formation, Dockum Group) of West Texas. *Journal of Vertebrate Paleontology* 24(3, supplement):73A.
- Hunt, A. P., 2001, The vertebrate fauna, biostratigraphy and biochronology of the type Revultian land vertebrate faunachron, Bull Canyon Formation (Upper Triassic), east-central New Mexico, *in* Lucas, S. G., and Ulmer-Scholle, D., eds., *Geology of Llano Estacado: New Mexico Geological Society, Guidebook 52*, pp. 123-151.

- Hunt, A. P., and Lucas, S. G., 1991a, A rhynchosaur from West Texas (USA) and the biochronology of Late Triassic rhynchosaurs; *Palaeont.* 34, pp. 191-198.
- Hunt, A. P., and Lucas, S. G., 1991b, The *Paleorhinus* biochron and the correlation of the nonmarine Upper Triassic of Pangea; *Palaeont.* 34, pp. 487-501.
- Hunt, A. P., and Lucas, S. G., 1992, The first occurrence of the *Paratypothorax andressi* (Reptilia, Aetosauria) in the western United States and its biochronological significance; *Paleont. Z.* 66, pp. 147-157.
- Hunt, A. P., and Lucas, S. G., 1993a, Triassic vertebrate paleontology and biochronology of New Mexico; *New Mexico Mus. Nat. Hist. Sci. Bull.* 2, pp. 49-62.
- Hunt, A. P., and Lucas, S. G., 1993b, A new phytosaur (Reptilia: Archosauria) genus from the uppermost Triassic of western United States and its biochronologic significance; *New Mexico Mus. Nat. Hist. Sci. Bull.* 3, pp. 193-196.
- Hunt, A. P., and Lucas, S. G., 1994, Ornithischian dinosaurs from the Upper Triassic of the United States; In: *In the shadow of the dinosaurs: early Mesozoic tetrapods* (eds) N C Fraser and H D Sues (Cambridge: Cambridge University Press), pp. 225-241.
- Hunt, A. P., and Lucas, S. G., 1995, Vertebrate paleontology and biochronology of the lower Chinle Group (Upper Triassic) Santa Fe County, north-central New Mexico; *New Mexico Geol. Soc. Guide Book* 46, pp. 243-246.
- Hunt, A. P., and Lucas, S. G., 1997, Stratigraphy, paleontology and biochronology of the Upper Triassic Chinle Group in east-central New Mexico; In: *Southwest Paleontological Symposium Proceedings* (eds) B Anderson, D Boaz and R D McCord (Mesa: Mesa Southwest Museum), 1, pp. 25-40.
- Izumi, N., Yokokawa, M., and Parker, G., 2017, Incisional cyclic steps of permanent form in mixed bedrock-alluvial rivers, *J. Geophys. Res.-Earth*, 122, pp. 130-152.
- Jacobson, P. J., Jacobson, K. M., and Seeley, M. K., 1995, Ephemeral rivers and their catchments: Sustaining people and development in western Namibia. Desert Research Foundation of Namibia, Windhoek.
- Kanhalangsy K., 1997, Petrography, geochemistry, and clay mineralogy of a paleosol in the Dockum Group (Triassic), Texas Panhandle unpub. M.S. Thesis, Texas Tech University
- Kelley, V. C., 1972, Triassic rocks of the Santa Rosa area: New Mexico Geological Society, 23<sup>rd</sup> Field Conference, Guidebook, pp. 84-90.
- Kennedy, J.F., 1961, Stationary waves and antidunes in alluvial channels. W.M. Keck Laboratory of Hydraulics and Water Research, California Institute of Technology, Report KH-R-2, 146 p.
- Kennedy, J.F., 1963, The mechanics of dunes and antidunes in erodible-bed channels. *Journal of Fluid Mechanics*, 16, pp. 521-544.
- Kennedy, J.F., 1969, The Formation of Sediment Ripples, Dunes, and Antidunes. *Annual Review of Fluid Mechanics*, vol. 1, no. 1, pp. 147-168.

- Kluth, C. F., and Coney, P. J., 1981, Plate tectonics of the Ancestral Rocky Mountains: *Geology*, v. 9, pp. 10-15.
- Knighton, A. D., and Nanson, G. C., 1997, Distinctiveness, diversity and uniqueness in arid zone river systems. in Thomas, D. S. G. (Ed.), *Arid zone geomorphology: Process, form, and Change in drylands*. Second ed. Wiley, Chichester, pp. 185-203.
- Kostic, S., Sequeiros, O., Spinewine, B. and Parker, G., 2010, Cyclic steps: a phenomenon of supercritical shallow flow from the high mountains to the bottom of the ocean. *J. Hydroenviron. Res.*, 3, 167-172.
- Marcou, J., 1853, *A geological map of the United States and British provinces of North America, with explanatory text, geological sections and plates of fossils which characterize the formations*: Boston, Gould and Lincoln, 92 p.
- Kues, Barry S., 1985, Stratigraphy of the Tucumcari area—A historical account, in Lucas S. G., and Zidek, J., *Santa Rosa-Tucumcari region: New Mexico Geological Society Guidebook, 36th Field Conference*, pp. 119-140.
- Latrubesse, E.M., Stevaux, J.C., Sinha, R., 2005, Tropical rivers. *Geomorphology* 70, pp. 187-206.
- Lamb, G. H., 2019, *An Architectural Analysis and Depositional Interpretation of the Dockum Group in the West Texas High Plains [M.S. thesis]*: Fort Worth, Texas Christian University, 94 p.
- Lang, J., and Winsemann, J., 2013, Lateral and Vertical Facies Relationships of Bedforms Deposited by Aggrading Supercritical Flows: From Cyclic Steps to Humpback Dunes. *Sedimentary Geology*, vol. 296, pp. 36-54.
- Langford, R., Bracken, B., 1987, Medano Creek, Colorado, a model for upper-flow-regime fluvial deposition. *J. Sediment. Petrol.* 57, pp. 863-870.
- Leeder, M. R., 1978, A quantitative stratigraphic model for alluvium, with special reference to channel deposit density and interconnectedness, in Miall, A. D., ed., *Fluvial Sedimentology: Canadian Society of Petroleum Geologists Memoir 5*, pp. 587-596.
- Lehane, J., 2006, *Anatomy and relationships of Shuvosaurus, a basal theropod from the Triassic of Texas*. M. S. thesis, Texas Tech University, Lubbock, Texas, 92 p.
- Lehman T.M., 1992, Stratigraphic nomenclature of the Triassic Dockum Group in West Texas and eastern New Mexico; *New Mexico Geol.* 1476.
- Lehman, T. M., 1994a, The saga of the Dockum Group and the case of the Texas-New Mexico boundary fault: *New Mexico Bureau of Mines and Mineral Resources Bulletin* 150, p. 37-52.
- Lehman, T. M., 1994b, Save the Dockum Group! *West Texas Geological Society Bulletin* 34(4), pp. 1-10.
- Lehman, T. M., and Chatterjee, S., 2005, Depositional setting and vertebrate biostratigraphy of the Triassic Dockum Group of Texas: *Journal of Earth System Science*, v. 114, pp. 325-351.

- Lighthill, J., 1978, *Waves in Fluids*. Cambridge University Press, Cambridge, 516 p.
- Long, R. A., and Murry, P. A., 1995, Late Triassic (Carnian and Norian) tetrapods from the southwestern United States: New Mexico Museum of Natural History and Science Bulletin 4. New Mexico Museum of Natural History and Science, Albuquerque, New Mexico, 254 p.
- Lucas, S. G., 1991, Triassic stratigraphy, paleontology and correlation, south-central New Mexico, *in* Barker, J. M., and three others, eds., *Geology of the Sierra Blanca, Sacramento and Capitan ranges, New Mexico*, New Mexico Geological Society, 42nd Annual Field Conference, Guidebook, pp. 243–259.
- Lucas, S.G., 1993, The Chinle Group: Revised stratigraphy and biochronology of Upper Triassic nonmarine strata in the western United States: *Museum of Northern Arizona Bulletin* 59, pp. 27–50.
- Lucas, S. G., and Anderson, O. J., 1992, Triassic stratigraphy and correlation, west Texas and eastern New Mexico, *in* Cromwell, D. W., Moussa, M. I., and Mazzullo, L. J., eds., *Transactions Southwest Section AAPG*, pp. 201–207.
- Lucas, S. G., and Anderson, O. J., 1993, Triassic stratigraphy in southeastern New Mexico and southwestern Texas, *in* Love, D. W., and four others, eds., *Carlsbad region, New Mexico and West Texas: New Mexico Geological Society, 44th Annual Field Conference Guidebook*, pp. 231–235.
- Lucas, S. G., and Hunt, A. P., 1987, Stratigraphy of the Anton Chico and Santa Rosa Formations, Triassic of east-central New Mexico: *Journal of the Arizona-Nevada Academy of Science*, v. 22, pp. 21–33.
- Lucas, S. G., and Hunt, A. P., 1989, Revised Triassic stratigraphy in the Tucumcari Basin, east-central New Mexico, *in* Lucas, S. G., and Hunt, A. P., eds., *Dawn of the age of the dinosaurs in the American Southwest: Albuquerque, New Mexico*, New Mexico Museum of Natural History, pp. 150–170.
- Lucas, S. G., and Spielmann, J., 2012, Tetrapod fauna of the Upper Triassic Redonda Formation, east-central New Mexico: the characteristic assemblage of the Apachean Land-vertebrate Faunachron: *New Mexico Museum of Natural History and Science Bulletin*. 55, 119 p.
- Lucas, S. G., Anderson, O. J., and Hunt, A. P., 1994, Triassic stratigraphy and correlations, southern High Plains of New Mexico-Texas: *New Mexico Bureau of Mines and Mineral Resources Bulletin* 150, pp. 105–126.
- Lucas, S. G., Hunt, A. P., and Morales, M., 1985, Stratigraphic nomenclature and correlation of Triassic rocks of east-central New Mexico: A preliminary report, *in* Lucas, S. G., and Zidek, J., eds., *Santa Rosa – Tucumcari Region: New Mexico Geological Society, 36th Annual Field Conference Guidebook*, p. 171–184.
- Lucas, S. G., Hunt, A. P., and Hayden, S. N., 1987, The Triassic system in the Dry Cimarron Valley, New Mexico, Colorado and Oklahoma, *in* Lucas, S. G., and Hunt, A. P., eds., *Northeastern New Mexico: New Mexico Geological Society, 38th Annual Field Conference Guidebook*, pp. 97–117.



- Marcou, J., 1855, Resume of a geological reconnaissance extending from Napoleon, at the junction of the Arkansas with the Mississippi, to the Pueblo de Los Angeles, in California, in Whipple, A. W., Report of the explorations for a railway route near the thirty-fifth parallel of latitude from the Mississippi River to the Pacific Ocean: 33<sup>rd</sup> Congress, 1<sup>st</sup> Session, House Executive Document 129, pp. 40-48.
- Marcou, J., 1858, Geology of North America, with two reports on the prairies of Arkansas and Texas, the Rocky Mountains of New Mexico, and the Sierra Nevada of California, originally made for the United States government: Zurich, Zurcher and Furrer, 144 p.
- Riggs, N. R., Lehman, T. M., Gehrels, G. E., and Dickinson, W. R., 1996, Detrital zircon link between headwaters and terminus of the Upper Triassic Chinle-Dockum paleo-river system: *Science*, v. 223, pp. 93-100.
- Martz, J. W., 2002, The morphology and ontogeny of *Typhothorax coccinarum* (Archosauria, Stagonolepididae) from the Upper Triassic of the American southwest. M.S. thesis, Texas Tech University, Lubbock, Texas, 279 p.
- Martz, J. W., 2008, Lithostratigraphy, chemostratigraphy, and vertebrate biostratigraphy of the Dockum Group (Upper Triassic), of southern Garza County, West Texas [Ph.D. dissert.]: Lubbock, Texas, Texas Tech University, 504 p.
- Martz, J. W., Mueller, B., Nesbitt, S., Stocker, M. R., Parker, W. G., Atanassov, M., Fraser, N. C., Weinbaum, J., and Lehane, J., 2013, A taxonomic and biostratigraphic re-evaluation of the Post Quarry vertebrate assemblage from the Cooper Canyon Formation (Dockum Group, Upper Triassic) of southern Garza County, western Texas: *Earth and Environmental Science Transactions of the Royal Society of Edinburgh*, v. 103, iss. 3-4, pp. 339-364.
- May, B. A., 1988, Depositional environments, sedimentology, and stratigraphy of the Dockum Group (Triassic) in the Texas Panhandle [M. S. thesis]: Lubbock, TX, Texas Tech University, 180 p.
- McGowen, J. H., G. E. Granata, and S. J. Seni., 1979, Depositional framework of the lower Dockum Group (Triassic), Texas Panhandle. University of Texas Bureau of Economic Geology Report of Investigations 97, pp. 1-60.
- McGowen, J. H., Granata, G. E., and Seni, S. J., 1983, Depositional Setting of the Triassic Dockum Group, Texas Panhandle and Eastern New Mexico; *Rocky Mountain Sec., Soc. Econ. Paleont. Min., Rocky Mountain Paleogeog. Symp.* 213-38.
- McQuilkin, K., 1998, An articulated phytosaur skeleton: preparation techniques from field to exhibit; MA thesis, Texas Tech University, Lubbock
- Mueller, B. D., and Parker, W. G., 2006, A new species of *Trilophosaurus* (Diapsida: Archosauromorpha) from the Sonsela Member (Chinle Formation) of Petrified Forest National Park, Arizona; pp. 119-125 in W. G. Parker, S. R. Ash, and R. B. Irmis (eds.), *A Century of Research at Petrified Forest National Park 1906-2006: Museum of Northern Arizona Bulletin 62*. Museum of Northern Arizona, Flagstaff, Arizona



- Muto, T., Yamagishi, C., Sekiguchi, T., Yokokawa, M., Parker, G., 2012, The hydraulic autogenesis of distinct cyclicity in delta foreset bedding: flume experiments. *J. Sediment. Res.* 82, pp. 545–558.
- Parrish, J. T., 1993, Climate of the supercontinent pangea. *The Journal of Geology* 101.2, pp. 215-233.
- Parrish, J. T., and Peterson, F., 1988, Wind Directions Predicted from Global Circulation Models and Wind Directions Determined from Eolian Sandstones of the Western United States—A Comparison. *Sedimentary Geology* 56.1-4 pp. 261-282.
- Plink-Bjorklund, P., 2015, Morphodynamics of Rivers Strongly Affected by Monsoon Precipitation: Review of Depositional Style and Forcing Factors. *Sedimentary Geology*, vol. 323, pp. 110-147.
- Powell, D. M., Brazier, R., Parsons, A. J., Wainwright, J. W., and Nichols, M., 2007, Sediment transfer and storage in dryland headwater streams. *Geomorphology* 88, pp. 152-166.
- Reid, I., Powell, D. M., Laronne, J. B., and Garcia, C., 1994, Flash floods in desert rivers: studying the unexpected. *Eos (Transactions of the American Geophysical Union)* 75, p. 452.
- Retallack, G.J., 1992, *Weathering Soils and Paleosols*, P.I. Martini and W. Chesworth, Eds. (Elsevier, Amsterdam), pp. 543-564.
- Rhoads, B. L., 1990, Hydrologic characteristics of a small desert mountain stream: implications for short-term magnitude and frequency of bedload transport. *Journal of Arid Environments* 18, pp. 151-163.
- Russell, H.A.J., Arnott, R.W.C., Sharpe, D.R., 2003, Evidence for rapid sedimentation in a tunnel channel, Oak Ridges Moraine, southern Ontario, Canada. *Sediment. Geol.* 160, pp. 33–55.
- Salvador, A., 1987, Late Triassic-Jurassic paleogeography and origin of the Gulf of Mexico Basin: The American Association of Petroleum Geologists, Bulletin 71, v. 4, pp. 419-451.
- Salvador, A., 1991, Triassic-Jurassic, *in* Salvador, A., ed., *The Gulf of Mexico: The Geology of North America: Boulder, CO, Geological Society of America*, v. J, pp. 131-180.
- Saunderson, H.C., Lockett, F.P.J., 1983, Flume experiments on bedforms and structures at the dune-plane bed transition. In: Collinson, J.D., Lewin, L. (Eds.), *Modern and ancient fluvial systems*. Spec. International Association of Sedimentologists Special Publication, vol. 6. Blackwell Science, Oxford, pp. 49-58.
- Seni, S. J., 1978, Genetic stratigraphy of the Dockum Group (Triassic), Palo Duro Canyon, Panhandle, Texas. M. S. thesis, University of Texas, Austin, 157 p.
- Simpson, E. O., 1998, The phylogeny and biostratigraphic utility of parasuchids from the Dockum Group of West Texas. M. S. thesis, Texas Tech University, Lubbock, Texas, 140 p.

- Sloutman, A., and Cartigny, M.J.B., 2018, Cyclic Steps: Review and aggradation based classification, *Earth-Science Reviews*
- Small, B. J., 1985, The Triassic thecodontian reptile *Desmatosuchus*: osteology and relationships. M. S. thesis, Texas Tech University, Lubbock, Texas, 83 p.
- Small, B. J., 1989a, Post Quarry; pp. 145-148 in S. G. Lucas, and A. P. Hunt (eds.), *Dawn of the Age of Dinosaurs in the American Southwest*. New Mexico Museum of Natural History and Science, Albuquerque, New Mexico.
- Small, B. J., 1989b, Aetosaurs from the Upper Triassic Dockum Formation, Post Quarry, West Texas; pp. 301-308 in S. G. Lucas and A.P. Hunt (eds.), *Dawn of the Age of Dinosaurs in the American Southwest*. New Mexico of Natural History and Science, Albuquerque, New Mexico.
- Small, B. J., 1997, A new procolophonid from the Upper Triassic of Texas, with a description of tooth replacement and implantation. *Journal of Vertebrate Paleontology* 17(4), pp. 674-678.
- Small, B. J., 2002, Cranial anatomy of *Desmatosuchus haploceros* (Reptilia: Archosauria: Stagonolepididae); pp. 97-111 in D. B. Norman and D. J. Gower (eds.), *Archosaurian Anatomy and Paleontology: Essays in Memory of Alick D. Walker*. *Zoological Journal of the Linnean Society*, vol. 136.
- Syvitski, J. P. M., Brakenridge, G. R., 2013. Causation and avoidance of catastrophic flooding along the Indus River, Pakistan. *GSA Today* 23, pp. 4-10.
- Tooth, S., 2013, Dryland fluvial environments: Assessing distinctiveness and diversity from a global perspective. *Treatise on Geomorphology*, vol. 9, pp. 612-644.
- Viele, G. W., and Thomas, W. A., 1989, Tectonic synthesis of the Ouachita orogenic belt, in Hatcher, R. D., Thomas, W. A., and Viele, G. W., eds., *The Appalachian-Ouachita Orogen in the United States: The Geology of North America: Boulder Colorado*, Geological Society of America, v. F-2, pp. 695-728.
- Van den Berg, J.H. and Van Gelder, A., 1993, A new bedform stability diagram, with emphasis on the transition of ripples to plane bed in flows over fine sands and silt. In: *Alluvial Sedimentation* (Eds M. Marzo and C. Puigdefabregas), *Int. Ass. Sed. Spec. Publ.*, 17, pp. 11-21
- Van der Voo, R. F., Mauk, F. J., and French, R. B., 1976, Permian-Triassic continental configurations and the origin of the Gulf of Mexico: *Geology*, v. 4, pp. 177-180.
- Walker, S. P., 2020, Profiles and paleohydrology of supercritical rivers, the Triassic Dockum Group of West Texas [M.S. thesis]: Fort Worth, Texas Christian University, 90 p.
- Walker, S., Holbrook, J., 2022. Structures, architecture, vertical profiles, palaeohydrology and taphonomy of an upper-flow-regime-dominated fluvial system, the Triassic Dockum Group of the Palo Duro Canyon, Texas. *Sedimentology*, v. 70, iss. 3, pp. 645-684.
- Walper, J. L., 1977, Paleozoic tectonics of the southern margin of North America: *Gulf Coast Association of Geological Societies Transactions*, v. 27, pp. 230-241.

- Walters, M. O., 1989, A unique flood event in an arid zone. *Hydrological Processes* 3, pp. 15-24.
- Weinbaum, J. C., 2002, Osteology and relationships of *Postosuchus kirkpatricki* (Archosauria, Crurotarsi). M. S. thesis, Texas Tech University, Lubbock, Texas, 78 p.
- Weinbaum, J. C., 2007, Review of the Triassic reptiles *Poposaurus gracilis* and *Postosuchus kirkpatricki* (Reptilia: Archosauria). Ph.D. dissertation, Texas Tech University, Lubbock, Texas, 183 pp.
- Yokokawa, Miwa, et al., 2010, Formative Conditions and Sedimentary Structures of Sandy 3D Antidunes: an Application of the Gravel Step-Pool Model to Fine-Grained Sand in an Experimental Flume. *Earth Surface Processes and Landforms*, vol. 35, no. 14, pp. 1720-1729.
- Yokokawa, M., Izumi, N., Naito, K., Parker, G., Yamada, T. and Greve, R., 2016, Cyclic steps on ice. *J. Geophys. Res.-Earth*, 121, pp. 1023-1048.
- Zeigler, K. E., Ramos, F. C., Zimmerer, M. J., 2019, Geology of northeastern New Mexico, Union and Colfax Counties, New Mexico: A geologic summary, *in* Ramos, F. C., Zimmerer, M. J., Zeigler, K. E., Ulmer-Scholle, D., eds., *Geology of the Raton-Clayton area: New Mexico Geological Society 70<sup>th</sup> Annual Fall Conference Guidebook*, pp. 47-54.

## Vita

### Personal Background

Anthony Skaleski  
Salt Lake City, Utah  
Son of Stephen Skaleski and Monika McLaughlin  
Married Andrea Skaleski nee Lottman, 8 October 2022

### Education

Diploma, Saint Thomas More High School  
Rapid City, South Dakota

Bachelor of Science, Geology & English,  
University of Nebraska

### Experience

Teaching Assistant, Texas Christian University  
2018 – 2020

Geology and Geophysics Intern, TEP Barnett,  
Fort Worth, Texas, 2019

Environmental Scientist I, Utah DNR,  
Division of Water Rights, Salt Lake City, Utah  
2022 – present

## ABSTRACT

### LONGITUDINAL TRENDS IN THE DOCKUM GROUP: VARIATIONS IN THE LATE TRIASSIC MEGAMONSOON

by Anthony Skaleski  
Department of Geological Sciences  
Texas Christian University

Thesis Advisor: Dr. John Holbrook, Professor of Geology

Recent work has identified the Late Triassic Dockum Group of West Texas and New Mexico as a fluvial system which records abundant supercritical flow in upper-flow-regime channels fed by megamonsoons. Lithofacies and fluvial architectural elements were recently characterized in this system, yet the scope of the field area for this study was geographically limited.

This field study extends the field area to a reach of 425 kilometers to assess how the fluvial system varies longitudinally. Using paleocurrent data and lithosomes—groupings of lithofacies and architectural elements—this study characterizes the trends in flow rates of Dockum Group channels from the headwaters to locations down dip. The cyclic nature of the Late Triassic megamonsoon climate pattern is noted through observations of alternating dying and strengthening of flow strength down dip.